

Stony Brook University



OFFICIAL COPY

The official electronic file of this thesis or dissertation is maintained by the University Libraries on behalf of The Graduate School at Stony Brook University.

© All Rights Reserved by Author.

**The Study of XPG Domains that Regulate the Late Steps of
Nucleotide Excision Repair**

A Dissertation Presented

By

Adebanke Fidelia Fagbemi

to

The Graduate School

In Partial Fulfillment of the

Requirements

for the Degree of

Doctor of Philosophy

in

Molecular and Cellular Biology

(Immunology and Pathology)

Stony Brook University

May 2011

Stony Brook University

The Graduate School

Adebanke Fidelia Fagbemi

We, the dissertation committee for the above candidate for the
Doctor of Philosophy degree, hereby recommend acceptance of this
dissertation.

Orlando D. Schärer, Ph.D. – Dissertation Advisor

Professor, Departments of Pharmacological Sciences and Chemistry

Arthur P. Grollman , M.D. – Chairman of Defense

Distinguished Professor, Department of Pharmacological Sciences

Daniel Bogenhagen, M.D.

Professor, Department of Pharmacological Sciences

Dale Deutsch, Ph.D.

Professor, Department of Biochemistry and Cell Biology

Carlos de los Santos, Ph.D.

Professor, Department of Pharmacological Sciences

This dissertation is accepted by the Graduate School

Lawrence Martin

Dean of the Graduate School

Abstract of the Dissertation

**The Study of XPG Domains that Regulate the Late Steps of
Nucleotide Excision Repair**

by

Adebanke Fidelia Fagbemi

Doctor of Philosophy

In

Molecular and Cellular Biology

(Immunology and Pathology)

Stony Brook University

2011

The human nucleotide excision repair (NER) pathway resolves a range of lesions in DNA including those caused by harmful UV light, environmental mutagens, and agents of chemotherapy. The pathway involves the concerted action of over 30 proteins that recognize the damage, excise it within an oligonucleotide, and fill in the resulting gap, restoring the DNA to its original form. The importance of NER is evident in impaired patients who suffer from a range of diseases with symptoms such as high predisposition to skin cancer, extreme sensitivity to sunlight, and neurological and developmental abnormalities. While the early steps in NER involving the damage recognition and incision steps are well understood, a lot remains to be learned about the later steps including the transition from dual incision to repair synthesis, and finally ligation of the DNA.

XPG is the endonuclease that makes the 3' cut on the damaged DNA strand during dual incision. The protein has been suggested to play an important role in regulating the late steps of NER, as it interacts with the replication and repair synthesis factor PCNA. In this thesis the roles of four domains of XPG in the late steps of NER were analyzed. These domains include a previously identified PCNA-interacting domain (PIP-C), a new putative PCNA-interacting domain (PIP-N), a ubiquitin-binding motif (UBM), and the nuclease active site. The nuclease active site mutant (E791A) supported uncoupled incisions as well as partial repair synthesis, suggesting that the incisions could be ordered with the 5' incision occurring before the 3' incision, and that XPG itself is involved in regulating the transition from dual incision to repair synthesis. Additionally, the PIP-N and UBM domains were found to be important for damage removal, as well as assembly and disassembly of late factors of NER. The UBM mutant displayed a phenotype similar to the E791A mutant, suggesting that an interaction of XPG with ubiquitin is important to trigger its nuclease activity. This work reveals that the timing of the XPG incision plays an important role in regulating the late steps of NER, and that interactions with PCNA and ubiquitin are important elements of this regulation.

TABLE OF CONTENTS

List of Tables	vii
List of Figures	viii
List of Abbreviations	x
Acknowledgements	xi
Chapter 1	1
Introduction	
Abstract	2
Introduction	3
Nucleotide Excision Repair	4
Damage recognition and preincision complex formation primes the endonucleases for incision	7
XPG is a latent endonuclease with structural and catalytic roles in NER	9
ERCC1-XPF, the last factor arriving in the preincision complex, initiates dual incision	14
Is there a defined order of the two incisions in NER?	19
Factors contributing to the coordination of dual incision and repair synthesis	21
Conclusions	23
Preview	24
Chapter 2	25
Coordination of Dual Incision and Repair Synthesis in Human Nucleotide Excision Repair	
Abstract	26
Introduction	27
Results	29
Discussion	47
Materials and Methods	54

Chapter 3	60
A UBM and new PIP domain in XPG Regulate the Late Steps in Nucleotide Excision Repair.	
Introduction	61
Results	65
Discussion	82
Materials and Methods	90
Conclusions and Future Directions	94
References	99
Appendix	114

LIST OF TABLES

Table 1: Known functions of the XPG protein	13
Table 2: Known functions of the ERCC1-XPF protein	19

LIST OF FIGURES

Figure 1: Images of two Xeroderma pigmentosum patients	5
Figure 2: Model for the nucleotide excision repair (NER) pathway.	6
Figure 3: The structure-specific endonuclease XPG	10
Figure 4: The structure-specific endonuclease ERCC1-XPF	15
Figure 5: The ERCC1-XPA interaction is required for NER	17
Figure 6: XPF Active Site Mutants Deficient in NER in vitro.	31
Figure 7: Efficient XPG cleavage is dependent on the catalytic activity of XPF	34
Figure 8: XPG E791A Supports Partial DNA Repair Synthesis in vitro	35
Figure 9: Recruitment of XPF to Sites of Local UV Damage in Different XP-F Cell Lines	39
Figure 10: XPF- and XPG-Dependent Co-localization of PCNA and CAF-1 with XPC	41
Figure 11: Catalytically active XPF is required for pol δ recruitment to damage regions	43
Figure 12: UDS in XP-F and XP-G Cells transduced with wild-type and mutant XPF and XPG, respectively.	46
Figure 13: Model for the Coordination of Dual Incision and Repair Synthesis Steps in NER.	49
Figure 14: Schematic of proposed similarities between TLS synthesis and NER dual incision and repair synthesis	64
Figure 15: XPG structure and domains	65
Figure 16: UBM and PIP-N domain alignments	66
Figure 17: The UBM domain in XPG mediates its binding to ubiquitin.	67
Figure 18: Removal of (6-4)PPs is impaired in the E791A, UBM and PIP-N mutants	71
Figure 19: IF images of (6-4)PP foci in mutants at all time-points analyzed	72
Figure 20: PCNA recruitment in the PIP mutants	74
Figure 21: PCNA association with damaged regions is impaired in PIP-N mutants, while its dissociation is impaired in UBM and E791A mutants	76
Figure 22: ERCC1 remains associated with damaged regions in E791A and UBM mutants up to 24h	77
Figure 23: XPG remains associated with damaged regions for longer periods in the E791A, UBM and PIP-N mutants than the wildtype	78

Figure 24: IF images of cells showing co-localization of XPG with (6-4)pp foci at 0.5h and 3h after UV irradiation	79
Figure 25: The damage recognition factor XPC-RAD23B behaves with similar kinetics in XPG-WT and all mutants tested	81
Figure 26: IF images of (6-4)PPs colocalized with ERCC1 foci in XPG cell-lines at 0.5h following UV irradiation	115
Figure 27: IF images of PCNA foci colocalized with ERCC1 foci in XPG cell-lines at 0.5h following UV irradiation	116
Figure 28: IF images of PCNA foci colocalized with ERCC1 foci in XPG cell-lines at 6h following UV irradiation	117
Figure 29: IF images of PCNA foci colocalized with ERCC1 foci in XPG cell-lines at 9h following UV irradiation	118
Figure 30: IF images of PCNA foci colocalized with ERCC1 foci in XPG cell-lines at 15h following UV irradiation	119
Figure 31: IF images of PCNA foci colocalized with ERCC1 foci in XPG cell-lines at 24h following UV irradiation	120
Figure 32: IF images of XPC foci colocalized with ERCC1 foci in XPG cell-lines at 0.5h following UV irradiation	121
Figure 33: IF images of XPC foci colocalized with ERCC1 foci in XPG cell-lines at 1h following UV irradiation	122
Figure 34: IF images of XPC foci colocalized with ERCC1 foci in XPG cell-lines at 3h following UV irradiation	123
Figure 35: IF images of XPC foci colocalized with ERCC1 foci in XPG cell-lines at 16h following UV irradiation	124
Figure 36: IF images of XPC foci colocalized with ERCC1 foci in XPG cell-lines at 24h following UV irradiation	125

LIST OF ABBREVIATIONS

(6-4)PP:	(6-4)photo-products
BER:	base excision repair
CAF-1:	chromatin assembly factor 1
CS:	Cockayne Syndrome
DAPI:	(4'-6'-diamino-2-phenylindole)
ERCC:	excision repair cross complementing
FEN1:	flap endonuclease 1
IF:	immunofluorescence
LUD:	local UV damage
NER:	nucleotide excision repair
PCNA:	proliferating cell nuclear antigen
PIP:	PCNA-interacting peptide
RFC:	replication factor C
RPA:	replication protein A
ssDNA:	single-stranded DNA
TFIIH:	transcription factor IIH
TLS:	translesion synthesis
TTD:	trichothiodystrophy
UBM:	ubiquitin-binding motif
UDS:	unscheduled DNA synthesis
UV:	ultraviolet
XAB2:	XPA binding protein 2
XP:	Xeroderma pigmentosum

ACKNOWLEDGEMENTS

The work I have accomplished over the past few years would not have been possible without the help and support of a number of people in my life. I would first like to thank my advisor Dr. Orlando Schärer for giving me the opportunity to work in his lab, do some very interesting and exciting research, and meet new people. He has been very supportive, encouraging, and patient during all the highs and lows that come with research, and I am very grateful for this, and for everything I have learned from him. I would also like to thank my Thesis committee for their time, support, advice, and constructive criticism over the last few years. They have helped me to focus on the relevant work, and this has saved me a lot of time and effort.

During my years in the Schärer lab, I have met many people, some I will forever consider friends, as we've shared laughter, tears, frustrations, and joys, both within and outside lab. The first lab members I met were Vinh, Jerome, Barbara and Angelo, who all made me feel comfortable, and right at home the very first day I met them. Over the years we spent time together talking about everything from science to politics and religion, and I can say it was all time well spent, so I have to thank them all for being a great support system. I met Lidija a short while later, and she began the work discussed in this dissertation, a lot of the work in Chapter 2 was performed by her. We had discussions just before she left (and even after) about my project, and I would like to thank her for always having the time to answer my questions. Other lab members who have become my friends as well as colleagues, and have never complained about my constant talking, singing (and oftentimes complaining!) in lab are Ilana, AJ, Jung-Eun, Yan, Burak, Shivam, Andy, and Alejandra. Thank you for our conversations, and discussions over the years.

In graduate school I made friends who got me through the tough times. In my first year here, Ada, Tracy, and Catherine were my support

system. We took classes together, studied together, and shared the tribulations of rotations and finding a lab together, and I truly appreciate those moments with them. In later years my times hanging out with Ilaria, Dumaine, Erika and Bennett made it all worthwhile, and I'm grateful for our friendship.

My family and friends far and wide have been my anchor during these years of my life. Zeina and Oye, friends from way, way back, (more like family) were always there for me, and I thank them for their support. My in-laws who are much closer geographically than my own family, have done so much for me and I have to thank them all. Big thanks especially to Tobi for helping me settle in the US, and in so many ways that I can't even list! My parents-in-law have given me love and support, a big thank you to them, and a sad goodbye to Dad Fagbemi whom we have just lost – I know you were very proud of my educational achievements, and could not have been more proud if I were your daughter – thank you, and rest in peace.

My parents who gave me not only life, but all the love and support over the last – years! My dear mother who never hesitates to come to my side (across oceans in the last 9 years) whenever I need her, just like I have the past few months – thank you Mummy – I love you and appreciate you! A big thank you to my Dad, whom I know is beaming with pride at this time. My sister, Maryam – I couldn't do it without you, my brother Ade, and all my siblings. Finally, my wonderful family; my patient, supportive and very proud husband Bankole – thank you love, and our wonderful little son, Ayotunde – you're the light of my life. I couldn't have made it through the last few years without you two by my side!

Thanks to everyone – I did it!!!!

CHAPTER 1

Introduction

Adapted from the review titled “Regulation of endonuclease activity in human nucleotide excision repair” by Adebanke F. Fagbemi, Barbara Orelli and Orlando D. Schärer, accepted in the DNA Repair special issue (in press).

Abstract

Nucleotide excision repair (NER) is a DNA repair pathway that is responsible for removing a variety of lesions caused by harmful UV light, chemical carcinogens, and environmental mutagens from DNA. The NER pathway involves the concerted action of over 30 proteins that sequentially recognize a lesion, excise it in the form of an oligonucleotide, and fill in the resulting gap by repair synthesis. ERCC1-XPF and XPG are structure-specific endonucleases responsible for carrying out the incisions 5' and 3' to the damage respectively, culminating in the release of the damaged oligonucleotide. The introductory chapter of the thesis reviews the recent work that led to a greater understanding of how the activities of ERCC1-XPF and XPG are regulated in NER to prevent unwanted cuts in DNA or the persistence of gaps after incision that could result in harmful, cytotoxic DNA structures.

Introduction

Maintenance of the integrity of the genetic material or deoxyribonucleic acid (DNA) within living organisms is vital for the survival and evolution of all living species. The DNA is involved in the control of every aspect of the physiology of an organism and codes for the proteins that run all processes within it. DNA in living organisms, however, is under constant attack from both endogenous agents produced as a result of metabolic activities within the cell, such as reactive oxygen species [1, 2], as well as exogenous agents of damage such as UV from sunlight, ionizing radiation, or environmental mutagens [3, 4]. Damage to the DNA, if left unrepaired, interferes with normal cellular processes such as replication and transcription, and can lead to cell death by apoptosis, or, in the long run, introduce mutations in the genome that ultimately result in carcinogenesis [3].

Five main DNA repair pathways have evolved to deal with the different types of lesions: direct repair, base excision repair, nucleotide excision repair, mismatch repair and double-strand break repair by non-homologous end joining or homologous recombination [1, 4, 5]. Most of these repair processes involve removal of a lesion within the DNA by excision, often carried out by endonucleases that incise the DNA near a lesion. This thesis is focused on the nucleotide excision repair (NER) pathway, and specifically on the structure-specific endonuclease XPG, which makes the 3' incision in NER. Regulation of the function of the

structure-specific endonucleases in NER is important to prevent unwanted cuts within the genome. Furthermore coordination of transition from one step of the pathway to the next is also of significance to prevent the occurrence of dangerous intermediates and will be addressed in this thesis.

Nucleotide Excision Repair

The pathway responsible for resolving bulky modifications of the DNA resulting from ultraviolet (UV) light or a variety of environmental chemicals is nucleotide excision repair (NER) [6, 7]. A number of genetic disorders resulting from mutations in NER genes, xeroderma pigmentosum (XP), Cockayne syndrome (CS), and trichothiodystrophy (TTD), underscore the biological importance of this pathway [8]. Among these, XP is the prototypical DNA repair disorder and XP patients are extremely photosensitive due to their inability to repair UV-induced lesions and have a high predisposition to tumors in the skin, and, in severe cases, develop neurological disabilities (Figure 1) [8, 9]. These patients are classified into eight complementation groups (XP-A through XP-G, so named for the respective mutated gene, and XP-V for the variant form). The phenotypic manifestations of CS and TTD are more complex and involve severe developmental and neurological abnormalities [8], which are not caused by defects in NER, but are likely due to a mild impairment of transcription.



Figure 1: Images of two Xeroderma pigmentosum patients displaying skin abnormalities resulting from sun exposure. Xeroderma pigmentosum, a disease resulting from impaired NER, is characterized by extreme sensitivity to sunlight and subsequent high susceptibility to tumors in the skin and other exposed organs such as the eyes and tongue, as shown in the pictures [10, 11].

The NER pathway is highly versatile and complex and has the ability to process a myriad of different lesions [6]. Versatility in substrate recognition is accomplished by over 30 different proteins that sequentially assemble at sites of damage to recognize the lesion, excise it in the form of a 24-32-nucleotide-long stretch of ssDNA, fill in the gap using the non-damaged strand as a template and ligate the nick (Figure 2) [6, 12].

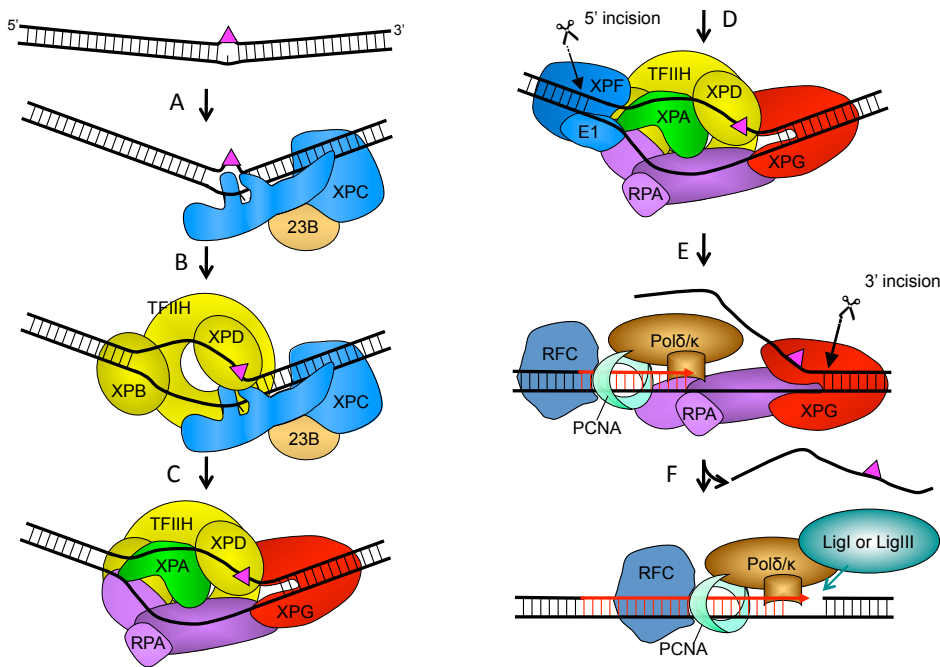


Figure 2: Model for the nucleotide excision repair (NER) pathway. (A) A bulky DNA lesion is recognized by XPC-RAD23B, which binds to the undamaged strand of DNA, allowing for the recruitment of TFIIH (B). The lesion is verified by XPD resulting in the recruitment of XPA, RPA, and XPG leading to formation of the preincision complex (C). ERCC1-XPF is recruited to the preincision complex through interaction with XPA leading to DNA incision 5' to the damage (D), which produces a free 3'-OH group available for initiation of repair synthesis by the replication machinery, and in turn triggers 3' incision by XPG (E). Repair synthesis is completed and DNA ligase III α or ligase I seals the nick to complete the process (F).

This chapter focuses on a key step in NER, the excision of the damaged oligonucleotide by two incisions made 5' and 3' to the lesion by the two structure-specific endonucleases ERCC1-XPF and XPG, respectively. This dual incision represents the first irreversible step in the pathway, formally resulting in the formation of a ssDNA gap of about 30 nucleotides. Since persistence of a 30-nucleotide gap or an incision in the absence of DNA damage is a possible deleterious side effect of this dual

incision reaction, it is crucial that the activity of ERCC1-XPF and XPG is tightly regulated. We will discuss emerging evidence that the timing and order of the incisions and the careful synchronization with repair synthesis is a built in feature of the NER pathway to prevent unwanted cuts within the genome.

Damage recognition and preincision complex formation primes the endonucleases for incision

Two sub-pathways of NER lead up to damage excision and they make use of pathway-specific factors and differ in their mode of damage recognition. Transcription-coupled NER (TC-NER) functions on actively transcribed strands, involves recognition of the lesion through stalling of RNA-Polymerase II, and additionally involves the recruitment of CSA, CSB and XAB2 factors to the damage prior to recruitment of core NER factors [13]. The second pathway, global genome NER (GG-NER) removes lesions throughout the genome, and is better understood at a mechanistic level. GG-NER is initiated by XPC-RAD23B, which recognizes the thermodynamic destabilization of a DNA duplex induced by a lesion. To achieve this, XPC-RAD23B does not interact with the lesion itself, but rather binds to DNA with single-stranded character opposite the lesion (Figure 2A) [14-16]. XPC then recruits the ten-subunit complex TFIIH, which contains two helicase subunits. It is thought that XPB pries apart the two DNA strands [17], while XPD tracks along the DNA with a 5'-3' polarity

stalling as it encounters the lesion ensuring the presence of a chemical alteration in the DNA (Figure 2B) [18, 19].

The result of TFIIH activity is an opened DNA structure [20, 21] that leads to the recruitment of the next three factors, XPA, RPA, and XPG, and formation of a stable preincision complex (Figure 2C). XPA is a small 273 amino acid protein originally thought to be the damage recognition factor. It was later found to have high affinity to kinked rather than damaged DNA, leading to the hypothesis that it interacts with an intermediate DNA structure in NER subsequent to damage recognition [22, 23]. XPA additionally interacts with several NER factors, including RPA [24], TFIIH [25, 26] and ERCC1 [27, 28]. It is therefore thought that XPA helps in positioning the different factors in the complex to allow dual incision to occur accurately. RPA is a trimeric protein that binds single-stranded DNA and has essential functions in replication and recombination [29]. Each RPA trimer has a preferred binding site of 30 nucleotides, which is strikingly similar to the size of the excised fragment in NER. Current models therefore place RPA on the non-damaged strand of DNA (Figure 2C-E), where it helps to position the two endonucleases, while protecting the non-damaged strand following incision [12]. At the same time, XPG is recruited to the damage region by interaction with TFIIH independently of XPA and RPA, to complete the formation of a stable preincision complex, resulting in the simultaneous release of XPC-RAD23B [30-32]. As we will discuss in more detail below, recent studies

suggest that the catalytic activity of XPG is not revealed at this point [21, 33] and XPG fulfills a structural role in stabilizing the pre-incision complex generating an open-stable complex [34].

The last factor to join the preincision complex is the second endonuclease, ERCC1-XPF, which is recruited through interaction with XPA [28, 35]. Following its arrival, a number of catalytic steps are triggered (Figure 2D-F): dual incisions 5' and 3' to the lesion by XPF and XPG, respectively [33]; repair synthesis filling in the gap by DNA polymerases δ , ϵ , or κ and associated factors [36] and finally, sealing of the nick by DNA ligase I or III α [37], restoring the DNA to its original undamaged state. The order and regulation of these catalytic steps, with an emphasis on the role of ERCC1-XPF and XPG is discussed below.

XPG is a latent endonuclease with structural and catalytic roles in NER

XPG is a FEN1 family nuclease member with a unique spacer region that regulates its function in NER

XPG belongs to the FEN1/XPG family of endonucleases, possessing the N- and I-nuclease domains that are highly conserved within the family (Figure 3A). Crystal structures of the family-members, T4 RNase H [38], T5 5'-exonuclease [39] and FEN1 [40, 41] suggested that

the N- and I-domains together form the nuclease core. In XPG, mutation of several conserved acidic active site residues, including D77, E791, and D812 abolished catalytic activity of the protein [42, 43]. However, XPG differs from FEN1 in that it contains a much larger (600 amino acid) spacer region that separates the N and I domains (Figure 3A) [44]. The spacer region is predicted to be highly disordered, has no known structural motifs, and is highly acidic. The spacer region mediates multiple protein-protein interactions, including with TFIIH [31, 45, 46], and RPA [47] and is therefore required for the recruitment of XPG to sites of NER [48].

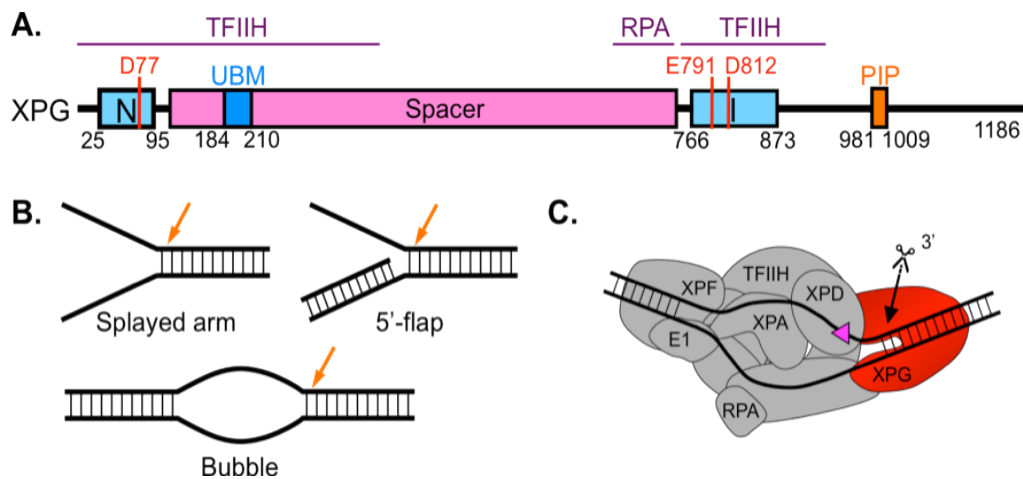


Figure 3: The structure-specific endonuclease XPG. (A) The primary structure of XPG shows the 1186 amino acid protein with its active site made up of the N and I regions (light blue) separated by the 600 amino acid spacer region (pink). Active site residues that were functionally analyzed (D77, E791, and D812) are shown in red. Regions for interaction with TFIIH, RPA, and PCNA (PIP) and the ubiquitin-binding motif (UBM) are indicated. (B) XPG cleaves 5' flap, splayed-arm and bubble substrates at ss/dsDNA junctions with 5' overhangs (orange arrows), and (C) makes the 3' incision in NER.

The spacer region of FEN1 is only about 70 amino acids long and forms a flexible helical loop. Biochemical and structural studies have suggested that the DNA threads through the loop and that the loop needs to undergo a structural rearrangement for FEN1 to become catalytically active [40, 49, 50]. It is likely that the XPG spacer region undergoes a similar rearrangement as it has been shown that XPG has distinct requirements for binding and cleaving DNA substrates [51]. Interestingly, replacing the spacer region of FEN1 with that of XPG generated a FEN1-XPG hybrid protein with biochemical characteristics of both proteins, able to cleave bubble substrates which are not processed by FEN1, while also showing a preference for double-flap over single-flap substrates, typical of FEN1 and not XPG [52]. Intriguingly, the FEN1-XPG hybrid protein was able to partially complement the NER activity in XPG-deficient cell lines, demonstrating that the spacer region has important roles in mediating substrate specificity and protein-protein interactions in NER. Other studies have attributed this effect of a contribution of the spacer region to the binding of bubble structures [53].

XPG is recruited to NER complexes through interaction with TFIIH

In the course of NER, XPG makes dynamic interactions with several other proteins in the NER pathway including RPA [47, 54], PCNA [55] and TFIIH [31, 45, 46, 48, 56]. The strongest interaction is the one with TFIIH [31], and is required for the recruitment of XPG to NER complexes [57]. The interaction between XPG and TFIIH seems to occur

through at least two different domains, located in the N-terminal/spacer region as well the C-terminal region of XPG [45]. Interestingly, the interaction of XPG and TFIIH does not only seem to be necessary to localize XPG to sites of repair, but also to complete NER, likely by ensuring that XPG is properly positioned to catalyze the 3' incision reaction. In line with this thinking, a protein corresponding to the patient allele of XPG with deletion of residues 225-231 (found in XP/CS patient XPCS1BD) had reduced affinity for TFIIH and was unable to restore UV sensitivity to XP-G cells, despite having normal nuclease activity [46]. Nonetheless, the XPG Δ 225-231 protein colocalized with sites of UV damage initially, but its association within the NER preincision complex was unstable, not allowing for proficient NER. Observations that certain patient mutations in XPB and XPD subunits of TFIIH that result in NER deficiencies lead to a delayed recruitment of XPG to sites of UV damage underscore the complexity of the interaction between XPG and TFIIH [56].

Possible roles of XPG in TC-NER, transcription and the repair of oxidative damage

The biological complexity of XPG function is evidenced by the fact that patients with XPG deficiency may suffer from XP or combined XP/CS phenotype. Point mutations that primarily affect the nuclease of XPG result in an XP phenotype, while truncation mutations lead to an XP/CS phenotype, indicative of important protein-protein interactions at the C-terminus of the protein [58, 59]. The other factors that are also associated

with the XP/CS phenotype are the XPB and XPD subunits of TFIIH [8]. In line with this observation, a fraction of XPG appears to be stably associated with TFIIH, where it appears to support a role of TFIIH in receptor-mediated transcription (Table 1) [60, 61]. Furthermore, a role of the *S. cerevisiae* XPG homolog Rad2 in RNA polymerase II-mediated transcription has been demonstrated more directly [62]. Significantly, these transcription-related functions of XPG and Rad2 are independent of its nuclease function. The mechanisms by which XPG functions in TC-NER are the subject of active research and discussion and remain to be fully elucidated [53, 63-65]. Additionally, XPG is thought to have other roles in maintaining genome stability, including the modulation of removal of oxidative damage by base excision repair (BER) and possibly other pathways (Table 1) [66-68].

Pathway	Function(s)	Interacting Partners	References
GG-NER	Preincision complex formation; 3' incision	RPA, TFIIH, PCNA	[31, 45-47, 55, 69]
TC-NER	TC-NER complex assembly; 3' incision	TFIIH, PCNA, RNA Pol II, CSB	[53, 63, 64]
Transcription	?	RNA Pol II, TFIIH	[53, 60, 62]
BER	Stimulation of DNA glycosylase, other roles (?)	NTH1	[66, 67]

Table 1. Known functions of the XPG protein

ERCC1-XPF, the last factor arriving in the preincision complex, initiates dual incision

Properties, functional domains and structures of ERCC1-XPF

ERCC1-XPF forms an obligate heterodimer in mammalian cells [70] and *in vitro*, and the two proteins are unstable in the absence of each other [71, 72]. Both ERCC1 and XPF were originally cloned by complementation of UV sensitive rodent cell lines [73, 74] and by sequence homology to the yeast Rad1 gene [70]. ERCC1 and XPF dimerization occurs through two helix-hairpin-helix (HhH) motifs found at the C-termini of both proteins (Figure 4) [75, 76]. The HhH motifs are structurally similar to those found in other DNA binding proteins and also contribute to DNA binding in ERCC1-XPF [77-80]. Another important DNA binding region is believed to be the N-terminus of XPF, which bears the same structure as the helicase domain of the archeal superfamily 2 (SF2) helicases, but lacks the residues necessary for ATP hydrolysis [81, 82].

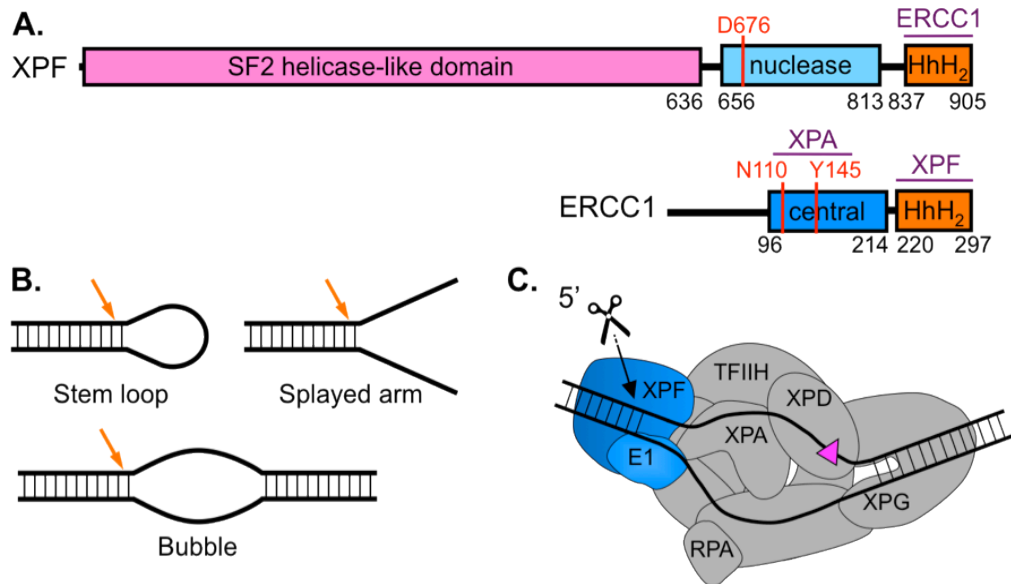


Figure 4. The structure-specific endonuclease ERCC1-XPF. (A) The primary structure of ERCC1-XPF shows the two members of the heterodimer that interact through their helix-hairpin-helix regions (orange). The nuclease active site XPF is indicated in light blue and the active site residue D676 in red. The central domain of ERCC1 (blue) interacts with XPA with the residues that mediate this interaction highlighted in red. The helicase-like domain of XPF (pink) belongs to the SF2 family of helicases, but has a defective ATP binding site. Interaction regions for heterodimer formation and with XPA are shown. (B) ERCC1-XPF cleaves stem-loop, splayed-arm and bubble substrates at ss/dsDNA junctions with 3' ssDNA overhangs (red arrows), and (C) makes the 5' incision in NER.

The first indication that ERCC1-XPF carries out the 5' incision in NER was provided by studies of the yeast homologs Rad1-Rad10, which were found to cleave ss/dsDNA junctions with 3' ssDNA overhangs [83]. An equivalent role was subsequently shown for the human ERCC1-XPF protein [70, 74, 84]. Subsequently, work from our laboratory revealed that the nuclease active site of the heterodimer resides within the XPF subunit of the complex, and contains the highly conserved V/IERKX₃D signature motif [85, 86]. The cluster of acidic residues allows the coordination with

metal ions necessary to catalyze the incision in the DNA strand, and mutations of key residues affect nuclease, but not DNA binding activity.

Intriguingly, it was suggested that ERCC1 has evolved through gene duplication from the XPF gene in lower eukaryotes, as XPF forms a homodimer in archaea [75]. Indeed, the crystal structure of the ERCC1 central domain revealed a high structural homology with the nuclease domain found in archeal orthologs of XPF [77, 87]. However, the groove that harbors the catalytic residues in XPF is rich in aromatic and basic amino acids in ERCC1 implicating a role in DNA or protein binding.

An Interaction with XPA is essential for recruitment of ERCC1-XPF to NER complexes

The ERCC1-XPF heterodimer interacts specifically with XPA, and this interaction is necessary for functional NER. The first evidence of this interaction came from yeast two-hybrid and pull-down assays [27, 88], which revealed that amino acid residues 91-119 of ERCC1, and 75-114 of XPA are necessary for the interaction and for NER to take place [27]. Three highly conserved glycine residues, G72, G73, and G74 of XPA were found to be necessary for the interaction and deletion of these residues resulted in loss of the ability of the XPA protein to restore UV resistance to XP-A cells [88]. More recent studies revealed that a small peptide of XPA (residues 67-80) is necessary and sufficient for mediating the interaction with ERCC1 [28]. Structural studies revealed that this peptide, which is

unstructured in solution, undergoes a transition to assume a turn made up of G72-74 and F75 upon binding to a cleft lined by residues N110, Y145, and Y152 in the central domain of ERCC1 (Figure 5A) [28]. Importantly, this 14 residue XPA peptide acts as a specific inhibitor of NER in cell-free extracts by blocking access of endogenous XPA to the ERCC1 binding pocket. This inhibitory effect was found to be highly specific as the mutant XPA-F75A peptide does not interfere with the NER reaction highlighting the importance of the F75 residue in mediating the XPA-ERCC1 interaction (Figure 5B) [28].

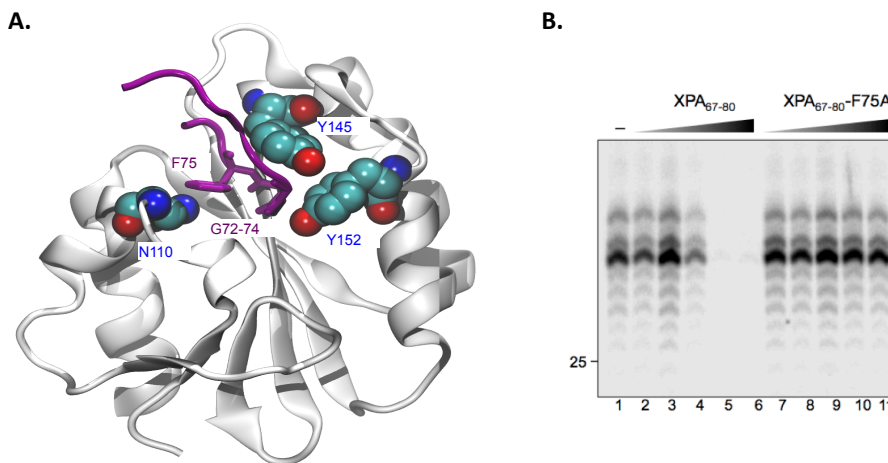


Figure 5. The ERCC1-XPA interaction is required for NER. (A) The structure of an XPA peptide (residues 67-80 shown in purple) bound to the central domain of ERCC1 (gray). The peptide undergoes a disorder to order transition upon binding ERCC1. The residues in XPA and ERCC1 that are important for this interaction are highlighted in pink and atom color, respectively. Figure adapted from [28, 35] (B) The XPA₆₇₋₈₀ peptide inhibits the *in vitro* NER reaction. Addition of increasing concentration of the XPA₆₇₋₈₀ peptide to a cell-free extract inhibits the excision of the cisplatin-containing oligonucleotide from a plasmid by NER. The XPA peptide containing the F75A mutation has no effects on the NER reaction, indicating the importance of the F75 residue in the ERCC1-XPA interaction. The NER reaction is visualized by radiolabeling excised DNA fragments, resulting in a characteristic pattern of 28-34mer oligonucleotides, which are separated on a DNA sequencing gel and visualized by autoradiography. Figures adapted from [28] and [35].

Conversely, mutation of the ERCC1 residues N110, Y145, and Y152, located within the XPA-binding pocket in the central domain of ERCC1, resulted in reduced NER activity of the ERCC1-XPF complex *in vitro* [35]. The most severely affected mutant ERCC1-N110A/Y145A, failed to colocalize with other NER proteins at sites of UV damage in cells, indicating a deficiency in the interaction with XPA under physiological conditions. Significantly, ERCC1-deficient UV20 CHO cells transduced with ERCC1-N110A/Y145A displayed significant sensitivity to UV, consistent with a defect in NER [35]. An intriguing question was whether these mutations would also affect other roles of ERCC1-XPF in ICL repair and homologous recombination, which are believed to be at least partially responsible for the severe phenotypes observed in some ERCC1- and XPF-deficient mice and patients that are not just due to defects in NER (Table 2) [89, 90]. ERCC1-N110A/Y145A expressing cells were not sensitive to other types of damage including mitomycin C- and cisplatin-induced interstrand crosslinks (ICLs) and ionizing radiation-induced double-strand breaks (DSBs), indicating that the XPA interaction and the XPA binding pocket are not required for these functions of ERCC1-XPF. Therefore, NER-specific functions of ERCC1-XPF can be separated by mutation of the XPA binding pocket.

Pathway	Function	Interacting Partners	References
NER	5' incision	XPA	[27, 28, 70]
Interstrand Crosslink Repair	ICL unhooking, homologous recombination (?)	SLX4	[91-94]
DSB Repair/ ssDNA annealing	Flap cutting (?)	SAW1, SLX4	[95-97]
Telomere maintenance	?, Nuclease-independent	TRF2	[98-100]

Table 2. Known functions of the ERCC1-XPF protein

Is there a defined order of the two incisions in NER?

Once all the preincision factors are in place in the NER complex, the question arises whether the two incisions occur simultaneously or consecutively in a defined order. There are two main arguments why it would be advantageous for the two incisions to occur in an ordered fashion; first, simultaneous incisions could result in the instantaneous release of the damaged oligonucleotide, exposing a ssDNA gap in the non-damaged strand. ssDNA patches may activate DNA damage responses [101] and are considered to be more unstable than bulky DNA lesions in intact DNA. Secondly, consecutive incisions would allow a tighter regulation of the transition from the incision to repair synthesis steps. If the 5' incision occurred first, this would provide a free 3'-OH tail

for the polymerase to initiate replication, while still protecting the DNA from exposure until the 3' incision is made. By contrast, making the cut 3' to the lesion would not set the system up for repair synthesis.

As will be described in Chapter 2 of this thesis, a recent study by our group using catalytically inactive forms of XPG and XPF showed that the incisions may indeed be ordered. In agreement with earlier studies [42, 43], using nuclease-dead XPG-E791A in an *in vitro* repair assay resulted in the formation of 5' uncoupled incision products (Figure 7). By contrast, the use of nuclease-dead XPF-D676A resulted in negligible 3' incision products [21, 33]. Interestingly, when XPG-E791A was used in an *in vitro* repair synthesis assay, formation of products of partial repair synthesis were observed, suggesting that after 5' incision the replication machinery had extended the incised DNA strand by 18-20 nucleotides from the 5' incision, even in the absence of the 3' incision (Figure 8). Furthermore, *in vivo* immunofluorescence experiments utilizing XP-F and XP-G cell-lines stably expressing the respective mutants, revealed that XPG-E791A supported recruitment of replication factors PCNA and Pol δ and chromatin remodeler CAF-1 to sites of local UV lesions, whereas neither were visible in XPF-D676A cells (Figures 10 and 11) [33]. These findings suggest a model for the late steps in NER in which the 5' cut by XPF is made first, repair synthesis is initiated, followed by the 3' cut by XPG, and completion of repair synthesis, with ligase finally sealing the nick.

In contrast with these findings, 3' uncoupled incisions by XPG in the absence of ERCC1-XPF have been observed using a variety of substrates [20, 34, 102, 103]. While this discrepancy has not yet been resolved, one possible explanation could be that ERCC1-XPF and XPG can incise NER intermediates *in vitro* under conditions that do not reflect the *in vivo* situation. It is known that both endonucleases are able to cleave model NER intermediates *in vitro* in the absence of additional proteins [51, 69, 70]. It is therefore possible that excess amounts of XPG, or the absence of ERCC1-XPF in a cell extract could allow the 3' incision by XPG in the absence of a properly assembled complex.

Factors contributing to the coordination of dual incision and repair synthesis

The fact that repair synthesis can occur prior to XPG incision, suggests that there might be a trigger that renders XPG catalytically active. Consistent with this notion, XPG has distinct requirements for binding and cleaving its substrates, which are mediated by its spacer region [48, 51] and it has also been shown that the XPG family member FEN1 undergoes a conformational change to become catalytically active [49]. What are potential factors that could facilitate this transition? In principle the transition could be due to a simple structural rearrangement caused by the approaching DNA polymerase, but there is increasing evidence that additional protein factors may contribute to and facilitate the transition.

One of the factors that has a key role in dual incision and repair synthesis is RPA. Studies have shown that RPA remains bound to sites of NER after dual incision and that it can stimulate the XPG incision on model substrates and is therefore a strong candidate for the regulation of XPG incision activity [104, 105]. Perhaps an even more attractive candidate is PCNA. PCNA has been shown to interact with XPG [55], and has been established to play a key role in triggering incision of DNA by FEN1 during the resolution of Okazaki fragments during replication [106, 107]. In NER, such an interaction between XPG and PCNA could be involved in triggering 3' incision by XPG. Our data showing that repair synthesis proceeds a little more than half way through the repair patch in the presence of catalytically inactive XPG [33] suggests that there is an obstacle that blocks the DNA polymerase. This situation is reminiscent of replicative polymerases stalling at DNA lesions. This is known to result in PCNA ubiquitylation, which results in the recruitment of translesion synthesis (TLS) polymerases [108]. Two observations suggest that a related mechanism could apply during NER. First, a recent study by Ogi *et al.* showed that three different polymerases, pol δ , pol κ , and pol ϵ are responsible for repair synthesis in NER, and that selective recruitment of at least pol κ is dependent on functional Rad18 and PCNA ubiquitylation [36]. Second, sequence analysis of XPG shows that, like TLS polymerases [109], it contains a ubiquitin-binding motif (UBM) [110] in addition to its PIP domain for PCNA interaction [55], raising the possibility

that an interaction between ubiquitylated PCNA and XPG could be involved in triggering 3' incision in NER. To what extent such protein-protein interactions among PCNA, XPG, Pol κ and other factors contribute to the completion of repair synthesis and possibly to the triggering of UV induced DNA damage signaling are intriguing areas for future investigations [111]. The focus of this thesis is the relevance of the interaction of XPG with ubiquitin (via its UBM domain) [110], and with PCNA via the previously identified C-terminal PIP domain (PIP-C) [55] and a new putative N-terminal PIP domain (PIP-N) that we have identified.

Conclusions

Structure-specific endonucleases are important for maintaining the integrity of DNA in many DNA repair pathways. ERCC1-XPF and XPG are two such endonucleases and make the incisions 5' and 3' to a lesion in the NER pathway, respectively. The work discussed in this chapter has helped to understand how the function of these two proteins is tightly regulated such that the inadvertent incision of DNA is avoided and that nicks or gaps formed as reaction intermediates are promptly subjected to an appropriate repair synthesis process to avoid the formation of deleterious intermediates. Much remains to be done to understand exactly how the dual incision and repair synthesis processes are coordinated to complete the NER process.

Preview

This thesis addresses the role of the structure-specific endonuclease XPG, which performs the 3' incision in NER in coordinating the late steps in NER, the transition from dual incision to repair synthesis. Chapter 2 describes studies showing that the presence of XPG, but not its catalytic function, is necessary for XPF to perform the 5' incision, and importantly that the replication machinery is recruited prior to the 3' incision by XPG. These findings strongly support the hypothesis that XPG somehow mediates the transition from dual incision to repair synthesis. Chapter 3 describes studies investigating the role of different domains in XPG that may mediate this function of the protein. Analysis of three different domains of XPG, two PCNA-interacting domains, and one ubiquitin-binding motif, reveals that the interaction between XPG and PCNA, and between XPG and ubiquitin is indeed important for the transition from dual incision to repair synthesis, possibly in the context of ubiquitylated PCNA. Conclusions and future directions are discussed at the end of the thesis.

CHAPTER 2

Coordination of Dual Incision and Repair Synthesis in Human Nucleotide Excision Repair

Adapted from the manuscript by Lidija Staresincic, Adebanke F. Fagbemi, Jacqueline H Enzlin, Audrey M. Gourdin, Nils Wijgers, Isabelle Dunand-Sauthier, Giuseppina Giglia-Mari, Stuart G. Clarkson, Wim Vermeulen, and Orlando D. Schärer, published in The EMBO Journal in 2009, Vol 28, pages 1111-1120

Abstract

Nucleotide excision repair (NER) requires the coordinated sequential assembly and actions of the involved proteins at sites of DNA damage. Following damage recognition, dual incision 5' to the lesion by ERCC1-XPF and 3' to the lesion by XPG leads to the removal of a lesion-containing oligonucleotide of about 30 nucleotides. The resulting single-stranded DNA gap on the undamaged strand is filled in by DNA repair synthesis. Here, we have asked how dual incision and repair synthesis are coordinated in human cells to avoid the exposure of potentially harmful single-stranded DNA intermediates. Using catalytically inactive mutants of ERCC1-XPF and XPG, we show that the 5' incision by ERCC1-XPF precedes the 3' incision by XPG and that the initiation of repair synthesis does not require the catalytic activity of XPG. We propose that a defined order of dual incision and repair synthesis exists in human cells in the form of a "cut-patch-cut-patch" mechanism. This mechanism may aid the smooth progression through the NER pathway and contribute to genome integrity.

Introduction

Nucleotide excision repair (NER) is a versatile DNA repair pathway that enables cells to eliminate a plethora of helix-distorting lesions caused by different environmental agents. Versatility and specificity in NER are achieved through the sequential and highly coordinated actions of at least 30 polypeptides that detect the lesion and excise a damage-containing oligonucleotide followed by repair synthesis and ligation events to restore the DNA sequence to its original state [6, 7, 12]. A subpathway of NER, transcription-coupled NER (TC-NER), preferentially removes damage from the transcribed strand of active genes and is initiated through stalling of an elongating RNA polymerase at DNA lesions [112, 113]. In bulk DNA, XPC-RAD23B appears to be the initial sensor of DNA damage and is essential for the assembly of all subsequent NER factors in the process known as global genome NER (GG-NER) [14, 57, 114, 115]. TFIIH, the next factor to be recruited, is responsible for strand separation around the lesion [20, 30, 116], enabling XPA, RPA and XPG to join the complex. ERCC1-XPF is then engaged [21, 28, 117] to perform the incision 5' to the damage [70, 83] while XPG cleaves 3' to the lesion [69]. An oligonucleotide of 24-32 nucleotides in length containing the lesion is then released and the resulting gap is filled by DNA polymerase δ/ϵ (and/or possibly κ) [118], replication factor C (RFC), PCNA, RPA and the nick is sealed by DNA ligase I or DNA ligase III/XRCC1 [37, 119] to restore the original DNA sequence. At a higher level of organization, chromatin assembly factor 1

(CAF-1) has been implicated in the restoration of chromatin following the repair reaction [120].

While many recent studies have been concerned with the mechanisms of damage recognition [15], less is known about the coordination of the two incision and the repair synthesis steps. For repair synthesis to occur, the 5' incision by ERCC1-XPF is required to generate a free 3'-OH group, the substrate for the DNA polymerase. By contrast, the 3' incision by XPG may not necessarily be needed to initiate polymerization. If both incisions occurred without any DNA repair synthesis, simple release of the oligonucleotide containing the damaged residue could result in the formation of a single-stranded DNA (ssDNA) gap, another deleterious DNA lesion with a key role in activating DNA damage signaling pathways [121]. Furthermore, the occurrence of aberrant DNA breaks is associated with inadvertent NER activity at non-damaged sites in XP/CS cells, underscoring the importance of avoiding the formation of unwanted NER incision reactions [122, 123]. It therefore appears likely that a mechanism ensuring the smooth transition between the dual incision and repair synthesis steps would have evolved.

The similar kinetics of the damage removal and repair synthesis indeed suggests a coordination of these two events [32]. Analysis of the literature, however, reveals that there is no consensus concerning the order of the two incisions. Although there is agreement that the 5' and 3' incisions are made in a near-synchronous manner [124], both 5'

uncoupled [103, 124] and 3' uncoupled [20, 34, 102] incisions have been observed in different experimental contexts *in vitro*. Using catalytically inactive forms of XPG it has been shown that the presence of XPG, but not its catalytic activity, is required for the generation of the 5' incision by ERCC1-XPF [42, 43]. Another study showed that the efficient 3' incision by XPG required the presence and catalytic activity of ERCC1-XPF [21].

Here we report the use of catalytically inactive mutants of XPF and XPG to establish the relative temporal order of the two incision reactions and DNA repair synthesis in human cell-free extracts and cells. The results suggest a novel “cut-patch-cut-patch” mechanism whereby the dual incision and repair synthesis events of NER are highly coordinated. In turn, this mechanism can explain how the potentially dangerous effects of ssDNA intermediates are minimized or even prevented.

Results

Active site mutants of XPG and XPF do not support dual incision

To try to determine if there is a strict temporal order to the 5' and 3' incisions in human NER, we made use of mutants of ERCC1-XPF and XPG that are catalytically inactive, but retain full DNA binding ability, with the hope of trapping NER intermediates. Three useful active site mutants of XPG have previously been reported. These D77A, E791A and D812A proteins do not display 3' nuclease activity and prevent dual incision in NER *in vitro*, but allow 5' incision by ERCC1-XPF to occur [42, 43]. We

have recently characterized the active site of human XPF and constructed several mutants with severely impaired endonuclease activity while retaining full DNA binding activity [86]. Here, we further characterized these mutants to select a catalytically inactive mutant devoid of NER dual incision activity analogous to the previously characterized XPG mutants. Hence, we tested the ability of these purified recombinant proteins, expressed as heterodimers with ERCC1, to restore NER activity in XP-F deficient cell extracts [124].

The wild-type, R678A, R681A, E701A and R715A XPF proteins fully restored the excision of a lesion-oligonucleotide from a plasmid containing a site-specific 1,3-intrastrand d(GpTpG) cisplatin DNA crosslink (Figure 6, lanes 1, 3, 5, 6 and 9, respectively), whereas E679A displayed residual activity (Figure 6, lane 4). By contrast, the D676A, D704A, E714A, K716A and D720A XPF mutants (Figure 6, lanes 2, 7, 8, 10 and 11, respectively) failed to restore any NER activity. An earlier study using a fully reconstituted system showed that XPF-D676A was devoid of any NER activity, whereas D720A had some residual activity [21].

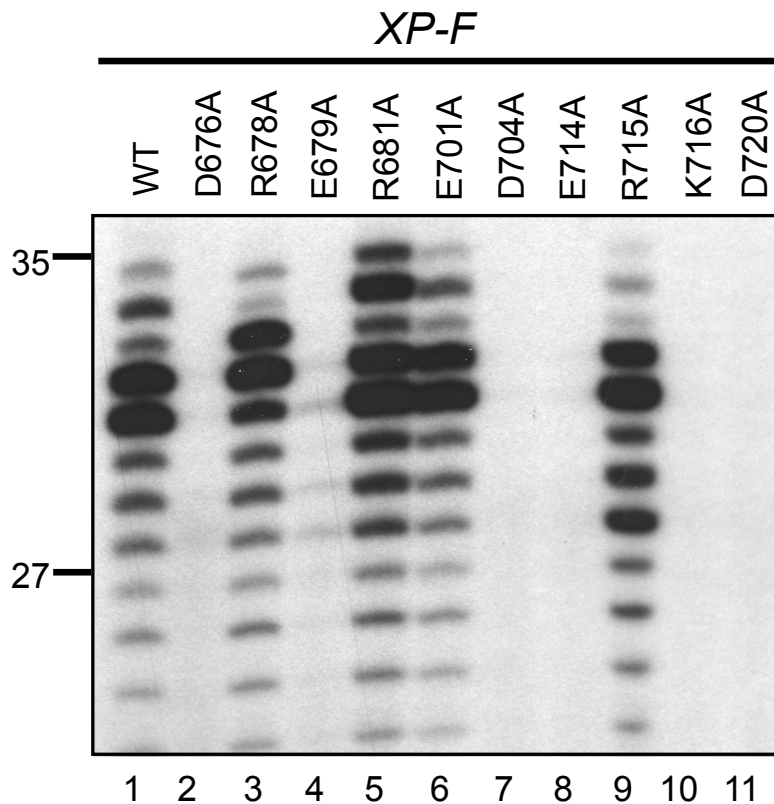


Figure 6. XPF Active Site Mutants Deficient in NER *in vitro*. Cell extracts prepared from XPF-deficient XP2YO cells were incubated with a plasmid containing a single 1,3 cisplatin intrastrand crosslink in presence of 200 fmol purified recombinant wild-type ERCC1-XPF (lane 1) or ERCC1-XPF proteins with different point mutations in XPF (lanes 2-11). The excision products containing the cisplatin adduct were labeled by the annealing of an oligonucleotide complementary to the excised oligonucleotides with a G₄ overhang and filling in with Sequenase 2.0 and [α -³²P] dCTP. The products were separated on a 14% denaturing polyacrylamide gel and visualized by autoradiography. The positions of size markers are indicated on the left.

Efficient 3' incision by XPG is dependent on prior 5' incision by ERCC1-XPF

We used ERCC1-XPF-D676A and XPG-E791A for further studies to discern any possible interdependency of the 5' and 3' incision steps. Covalently closed circular DNA containing a single 1,3-intrastrand cisplatin

DNA crosslink was incubated with an XPF- or XPG-deficient cell-free extract complemented with wild-type or nuclease-deficient ERCC1-XPF and XPG proteins. The reaction products were purified and cleaved with *Bss*III to excise a 190 bp fragment from the plasmid DNA. Incision products were detected by annealing an oligonucleotide complementary to the *Bss*III incision site 3' to the lesion followed by a fill-in reaction to generate a fragment of approximately 130 nt for the 5' uncoupled incision by XPF and a 100 nt fragment for incision by XPG, in the presence or absence of the 5' incision (Figure 7A).

Incubation of the plasmid with XP-G or XP-F cell extract did not yield any incision products (Figure 7B, lanes 2 and 5, respectively). When the extracts were complemented with wild-type XPG or XPF proteins (lanes 3 and 6, respectively), products specific for 3' incision by XPG (3 bands around 100 nt) were visible. Addition of XPF-D676A to the XP-F cell extract only yielded marginal amounts of 3' incision products (lane 7), suggesting that 3' uncoupled incision by XPG does not occur efficiently in the presence of catalytically inactive XPF. By contrast, addition of XPG-E791A to the XP-G cell extract resulted in the appearance of two intense specific bands (of around 130 nt in length) corresponding to the product of XPF 5'-uncoupled incision (lane 4). These results indicate that efficient 3' incision by XPG is dependent on the presence and catalytic activity of ERCC1-XPF, while the presence, but not the catalytic activity of XPG is

required for the 5' incision by ERCC1-XPF. Hence, the 5' incision might precede the 3' incision.

DNA Repair Synthesis can be initiated *in vitro* without the 3' incision by XPG

To determine if both 5' and 3' incisions need to occur before DNA repair synthesis can be initiated, we investigated the nature of the repair synthesis products in XP-G cell extracts complemented with wild-type XPG and XPG-E791A, by incubating a plasmid containing a single defined cisplatin lesion in the extracts together with [α - 32 P]-dCTP and [α - 32 P]-TTP. After the reaction, DNA was purified and digested with *KpnI* and/or *SacI* or *XhoI* and/or *BsrBI* (Figure 8A).

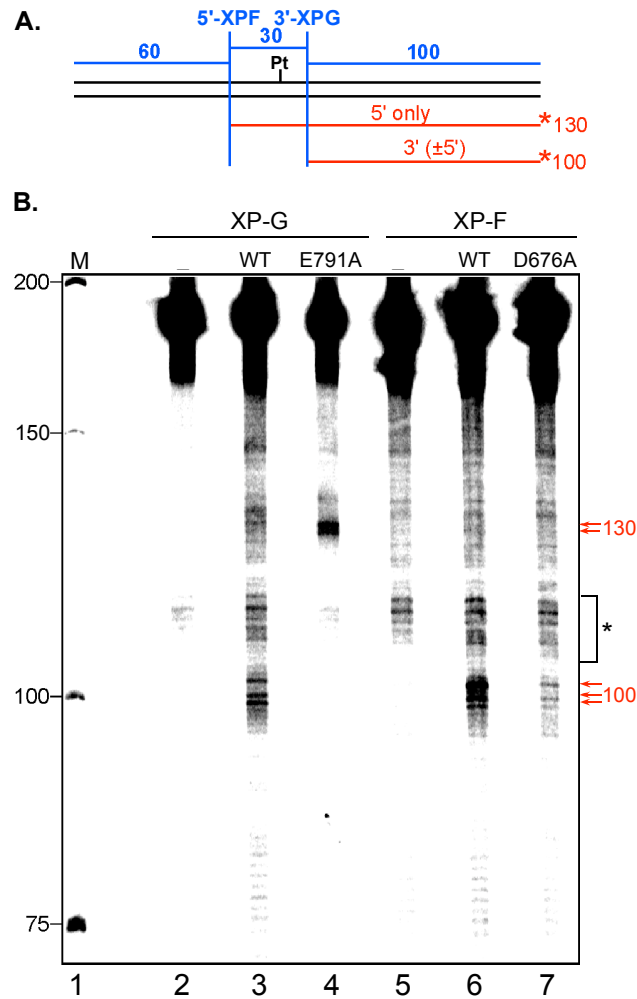


Figure 7. Efficient XPG cleavage is dependent on the catalytic activity of XPF. (A) Schematic representation of a 190bp *BssHII* fragment with a single defined cisplatin lesion. Incision sites by ERCC1-XPF and XPG are indicated. Incisions were detected using fill-in reactions with Sequenase 2.0 and [α - 32 P] dCTP by annealing an oligonucleotide complementary to a *BssHII* cleavage site containing a G₄ overhang allowing for the visualization of the 130 and 100 mer products for 5' and 3' incision respectively. Possible excision products are indicated in red and the position of the [α - 32 P] label is indicated by an asterisk. **(B)** cccDNA with a single defined cisplatin lesion was incubated with cell extracts lacking XPG- (XPCS1RO, lanes 2-4) or XPF-deficient (XP2YO, lanes 5-7), either alone (lanes 2 and 5) or complemented with wild-type XPG (lane 3), XPG E791A (lane 4), wild-type XPF (lane 6), XPF D676A (lane 7), purified, digested with *BssHII*, radioactively labeled and analyzed on a denaturing PAGE gel. The positions of size markers are indicated on the left, and the position of the reaction products on the right of the gel. Unspecific bands present in all the lanes are marked by asterisk.

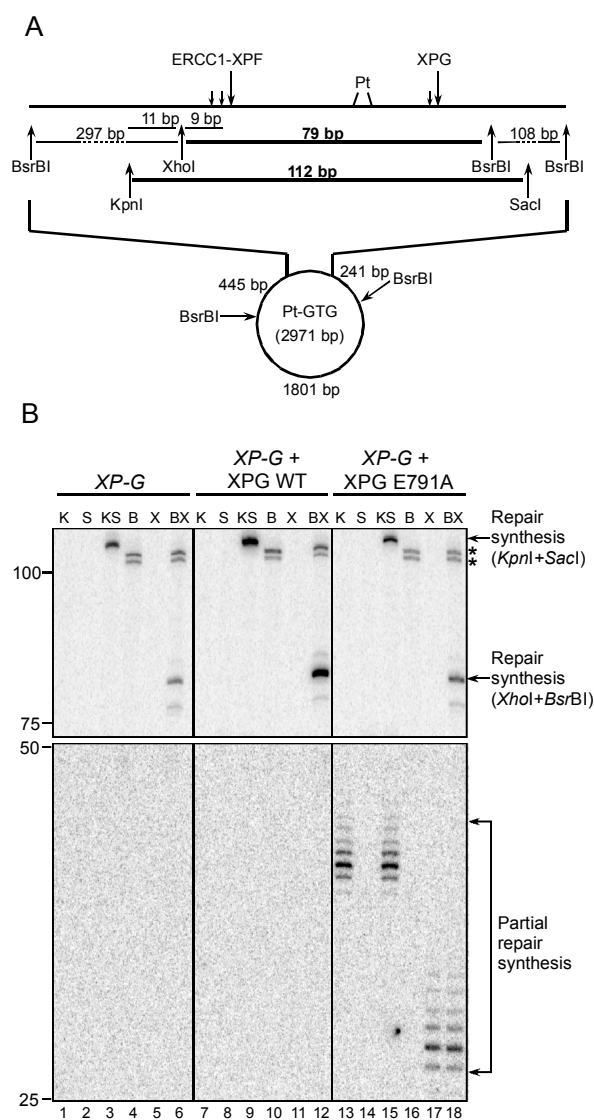


Figure 8. XPG E791A Supports Partial DNA Repair Synthesis *in vitro*. (A) Schematic representation of the lesion-containing plasmid used in the assay. Incision sites by ERCC1-XPF and XPG and the sizes of restriction fragments are indicated. The fragments containing the repair synthesis products are shown in bold (79 bp and 112 bp). (B) cccDNA with a single defined cisplatin lesion was incubated with a XP-G cell extract, either alone (lanes 1-6) or in the presence of 600 fmol of wild-type XPG (lanes 7-12) or XPG E791A (lanes 13-18) as well as 10 μ Ci of [α - 32 P]dCTP and 10 μ Ci [α - 32 P]TTP. DNA was further purified, digested with *KpnI* (lanes 1, 7, 13), *SacI* (lanes 2, 8, 14), *KpnI*+*SacI* (lanes 3, 9, 15), *BsrBI* (lanes 4, 10, 16), *XhoI* (lanes 5, 11, 17), *BsrBI*+*XhoI* (lanes 6, 12, 18) and analyzed on a denaturing PAGE gel. The positions of size markers are indicated on the left, the nature of the observed products on the right of the gel. Two unspecific bands are marked by asterisk. Abbreviations: K= *KpnI*, S= *SacI*, KS= *KpnI*+*SacI*, B= *BsrBI*, X= *XhoI*, BX= *BsrBI*+*XhoI*.

When DNA was incubated with the XP-G deficient cell extract alone, products of nonspecific DNA synthesis were observed with signal intensities roughly proportional to the length of the DNA fragments (Figure 8B, lanes 1-6). These signals are likely due to random nicks produced by topoisomerases and/or nucleases present in the cell-free extracts [125]. Addition of wild-type XPG to the mixture led to a significant increase in the intensity of the bands of 112 nt (*KpnI* and *SacI*) and 79 nt (*BsrBI* and *XhoI*), corresponding to newly synthesized and ligated DNA at the site of the cisplatin lesion (lanes 9 and 12, respectively). Note that the 79 nt signal of the *BsrBI/XhoI* digestion in lane 12 is much more intense than the non-specific signal at 108 nt, strongly suggesting that the 79 bp band results from XPG-induced repair synthesis. The specificity of the signal for repair synthesis was further supported by the observation that no increase of the specific band at 79bp was seen if the reaction was carried out with the parental non-damaged plasmid (data not shown). Addition of nuclease deficient XPG-E791A, which permits incision by ERCC1-XPF, to the XP-G cell extracts, did not result in a change in the intensity of the full-length repair synthesis products of 112 bp and 79 bp. However, two new products with the most intensive bands of 39 nt (*KpnI* and *SacI*) and 28 nt (*BsrBI* and *XhoI*) were visible after a longer exposure of the gel (lanes 15 and 18, respectively). These bands were also present after the cleavage with only one restriction enzyme 5' to the damaged site (lanes 13 and 17), while no products were visible after cutting with restriction enzymes 3' to

the incision sites (lanes 14 and 16). The appearance of these bands is therefore consistent with their being partial repair synthesis products, in which the polymerase extended the 3'-OH group generated by ERCC1-XPF about 18-20 nt in the absence of XPG incision. These observations indicate that initiation of repair synthesis is dependent on cleavage by ERCC1-XPF and that it can occur prior to 3' cleavage by XPG. No partial repair synthesis products were observed when an extract made from XP-F cells was complemented with wild-type XPF or XPF-D676A (data not shown). These results demonstrate that repair synthesis can be initiated *in vitro* prior to the 3' incision by XPG.

Catalytically inactive XPF persists at sites of UV damage

Having observed partial repair synthesis without XPG cleavage *in vitro*, we wished to test whether repair synthesis could also be initiated *in vivo* prior to 3' incision by XPG. For repair synthesis to take place, the DNA replication machinery has to be recruited to the sites of DNA damage. Therefore, we examined the localization of PCNA, a component of the DNA replication machinery, after local UV irradiation of a XP-G cell line expressing wild-type XPG or XPG-E791A and a XP-F cell line expressing wild-type XPF or XPF-D676A. We have previously described the generation and characterization of XP-G cell lines expressing wild-type XPG and XPG-E791A using lentiviral transduction. Both XPG proteins were localized to UV-damaged spots in cell nuclei shortly after damage infliction, but only XPG-E791A persisted in these spots, suggesting that

completion of NER is required for the dissociation of XPG [46]. XP-F cell lines expressing wild-type XPF and XPF-D676A were generated in an analogous fashion by transducing XPF-deficient XP2YO cells with lentiviral recombinants encoding HA-tagged wild-type XPF and XPF-D676A. The resulting cells were subjected to local UV irradiation and the recruitment of XPC, the initial damage recognition factor, and XPF to sites of UV damage was analyzed [57].

At 0.5 hrs after irradiation, we observed co-localization of XPC with both HA-tagged wild-type XPF and XPF-D676A (Figure 9A). 3 hours after local UV irradiation, XPC and XPF were no longer present at the damaged sites in the cells expressing wild-type XPF. However, in the mutant XPF transductants XPC remained co-localized with the catalytically deficient XPF-D676A (Figure 9B). Hence, cleavage by ERCC1-XPF and XPG is needed for both nucleases to dissociate from the damaged site and for the completion of NER.

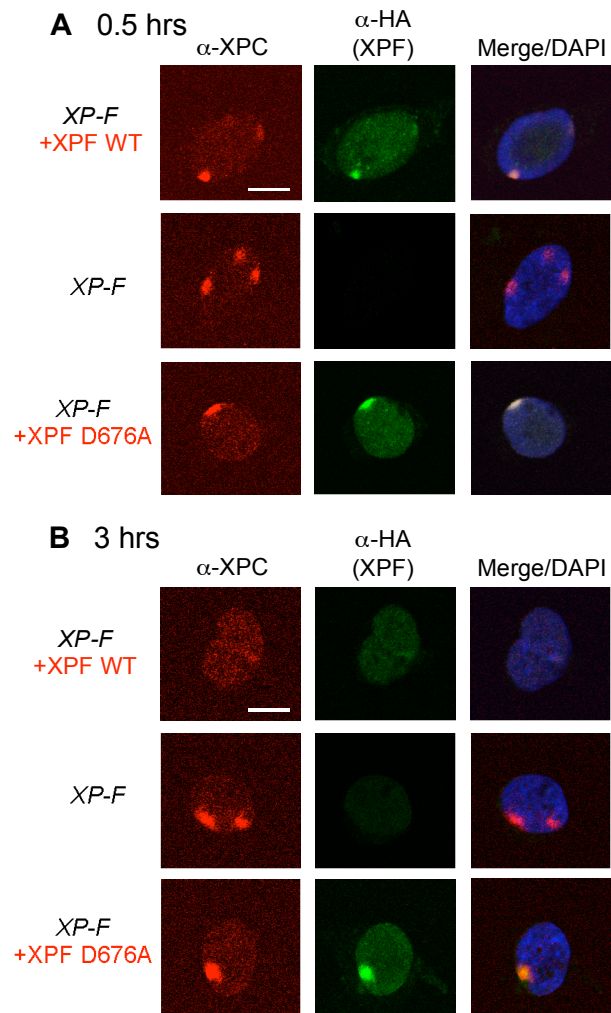


Figure 9. Recruitment of XPF to Sites of Local UV Damage in Different XP-F Cell Lines. XP2YO (XP-F) cells, untransduced or transduced with XPF-WT or XPF-D676A, were grown on coverslips and locally irradiated with a UV dose of 150 J/m² through filters with 5 μ m pores and fixed 0.5 hours (**A**) or 3 hours (**B**) after irradiation. The cells were immunolabeled with antibodies against XPC (red) or the HA tag present on the C-terminus of XPF (green). Merged images indicate the overlay of XPC, XPF and DAPI staining. Scale bars, 10 μ m.

Recruitment of PCNA and CAF-1 to sites of local UV damage depends on the presence, but not the catalytic activity of XPG

Using the transduced XP-G and XP-F cell lines, we studied how the catalytic activity of the two nucleases correlates with the recruitment of repair synthesis factors to NER sites. It has been shown before that recruitment of PCNA to the sites of local UV damage is severely affected in XPG-deficient cells [126]. In agreement with this report, we did not observe any co-localization of PCNA with XPC in XP-G cells 0.5 hrs after UV irradiation (Figure 10A, middle row). However, as expected, XPC and PCNA co-localized at sites of UV damage in XP-G cells expressing wild-type XPG (Figure 10A, top row). PCNA also co-localized with XPC in the XPG-E791A transductants (Figure 10A, bottom row). In principle, the recruitment of PCNA to sites of UV damage in the presence of catalytically inactive XPG could reflect partial DNA repair synthesis or be due to the recruitment of PCNA prior to incision, possibly by direct interaction with XPG [55]. To distinguish between these possibilities, we investigated the recruitment of PCNA in various XP-F cells. While PCNA was found at sites of UV damage in XP-F cells expressing wild-type XPF, PCNA did not colocalize with XPC in untransduced XP-F cells or in the XPF-D676A transductants (Figure 10B). These observations demonstrate that the recruitment of PCNA to sites of UV damage is dependent on the catalytic activity of XPF and therefore likely on active DNA repair synthesis. Consistent with this notion, the presence of Pol δ at sites of UV damage

also required catalytically active XPF (Figure 11).

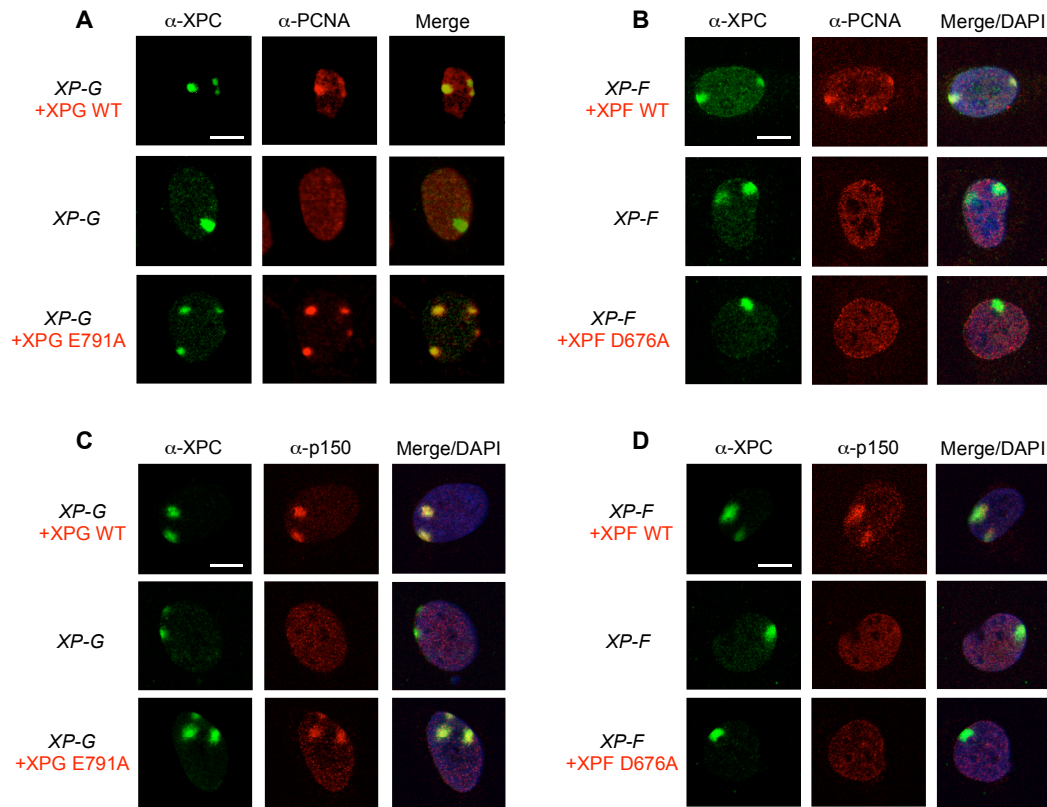


Figure 10. XPF- and XPG-Dependent Co-localization of PCNA and CAF-1 with XPC. XPCS1RO (XP-G) cells, untransduced or transduced with XPG-WT or XPG-E791A (**A** and **C**) and XP2YO (XP-F) cells, untransduced or transduced with XPF-WT or XPF-D676A (**B** and **D**), were grown on coverslips and locally irradiated with a UV dose of 150 J/m² through filters with 5 μm pores and fixed 0.5 hours after irradiation. The cells were immunolabeled with antibodies against XPC (green), PCNA (red) and CHAF150, the largest subunit of CAF-1 (red). Merged images indicate the overlay of XPC, PCNA or CHAF150 and DAPI staining. Scale bars, 10 μm.

Having established that the recruitment of the replication machinery required the catalytic activity of XPF, but not that of XPG, we asked if factors acting even later in NER could be recruited to sites of UV damage in the absence of XPG incision. We examined the recruitment of

CHAF150, a subunit of the chromatin assembly factor 1 (CAF-1) that is involved in the restoration of chromatin after a NER reaction [120]. CHAF150 behaved like PCNA in that its recruitment was dependent on the catalytic activity of XPF, but not on that of XPG (Figure 10D and 10C). These results are consistent with an earlier observation that CAF-1 is recruited to the sites of DNA damage in a PCNA-dependent manner [120]. The important novel conclusion is that even factors acting downstream of DNA repair synthesis can be recruited to sites of UV damage before the second incision 3' to the lesion has occurred.

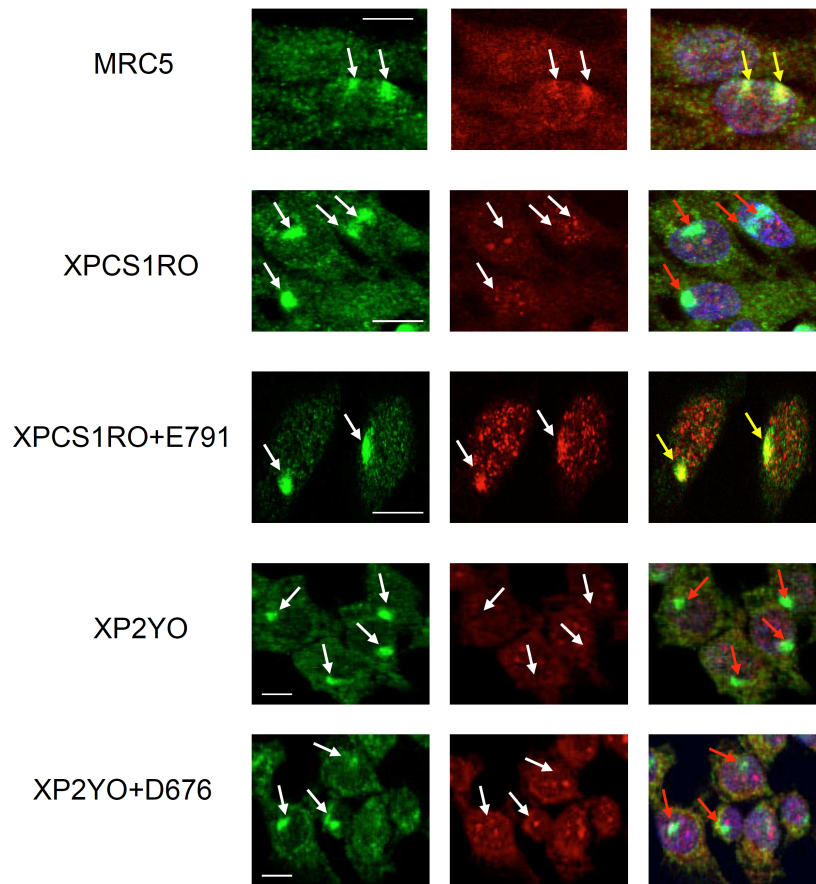


Figure 11: Catalytically active XPF is required for pol δ recruitment to damage regions. MRC5 cells, XPCS1RO (XP-G) cells untransduced or transduced with XPG-E791A, and XP2YO (XP-F) cells, untransduced or transduced with XPF-D676A, were grown on coverslips, cultured in the presence of HU-AraC for 30 mins, locally irradiated with a UV dose of 150 J/m^2 through filters with $5 \mu\text{m}$ pores and fixed 1 hour after irradiation. The cells were immunolabeled with antibodies against XPB (green) used as a marker to locate UV-damaged spot (white arrows) and polymerase δ (red). Merge indicates the overlay of XPB, polymerase δ and DAPI stainings. Scale bars, $10 \mu\text{m}$, yellow arrows indicate co-localization between XPB and polymerase δ , whereas red arrows indicate absence of this co-localization.

Partial unscheduled DNA synthesis (UDS) occurs in the absence of 3' incision by XPG

To test whether loading of PCNA to NER sites is able to stimulate DNA repair synthesis in the absence of 3' incision *in vivo*, we examined DNA repair by unscheduled DNA synthesis (UDS) after UV-irradiation of XP-G transductants expressing wild-type XPG or XPG-E791A. Wild-type XPG complemented the severe UDS defect of untransduced XP-G cells (102 % versus 7%, with NER-proficient cells assayed in parallel set at 100%, Figure 12A). In line with the observed partial DNA repair synthesis *in vitro* and recruitment of PCNA, the very low UDS level of untransduced XP-G cells was significantly increased upon expression of the catalytically inactive XPG (from 7 to 49 % UDS, Figure 12A). To try to ensure that this UV-induced DNA synthesis occurs at sites of NER rather than being a non-specific artifact, we monitored repair synthesis at locally UV-damaged areas (Figure 12B). Although quantification is difficult, significant numbers of autoradiographic grains were found clustered together over non-S phase nuclei in NER-proficient cells and XP-G transductants expressing wild-type XPG (Figure 12B, upper panels). Very few grains were found over comparable nuclear areas of untransduced XP-G cells but the nuclei of the XPG-E791A transductants exhibited a significant amount of grain clustering, roughly mid-way between the wild-type and XP-G levels (Figure 12B, lower panels). In contrast, the levels of UDS in XP-F cells expressing XPF-D676A (8% of wild-type, Figure 12A) was at the same

background level as untransduced XP-F cells, whereas UDS was restored to normal levels in cells expressing wild-type XPF (104%, Figure 12A). Local UDS experiments confirmed these findings; while UDS sites were clearly observed for XP-F transductants expressing wild-type XPF, they were not evident in XPF-D676A transductants (Figure 12C). Together, these results strongly suggest that the observed UDS is linked to sites of local UV damage, and that partial repair synthesis can occur in living cells in the absence of the catalytic activity of XPG, whereas it does require the catalytic activity of XPF.

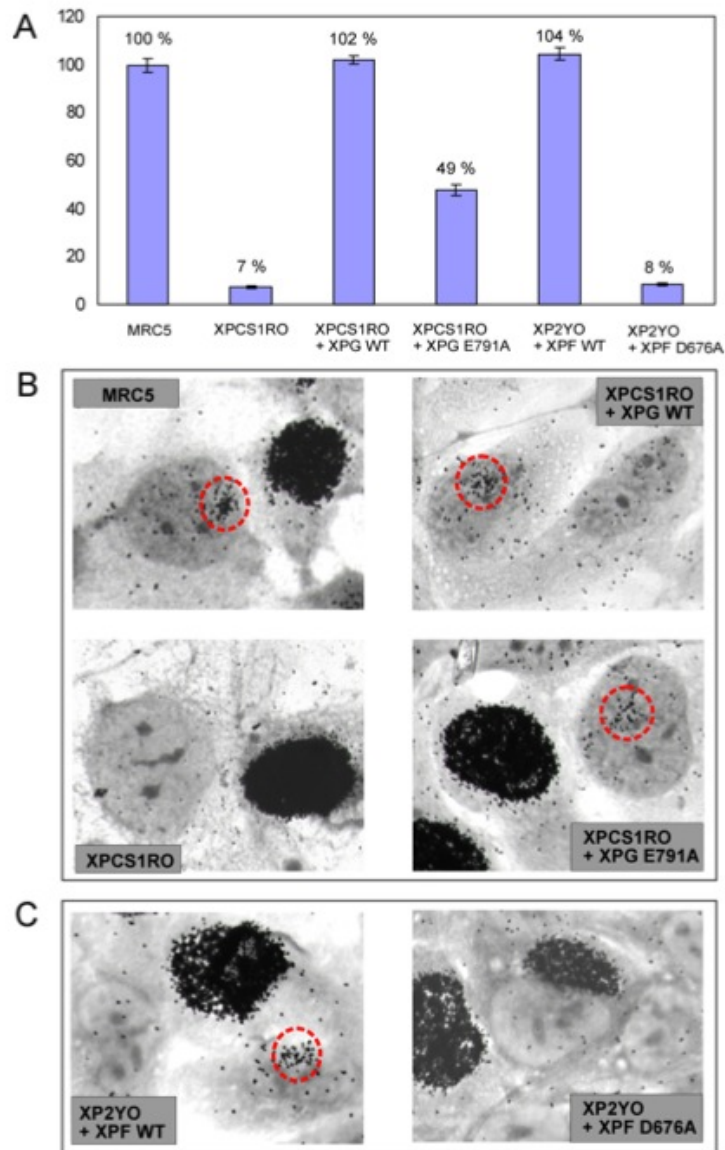


Figure 12. UDS in XP-F and XP-G Cells transduced with wild-type and mutant *XPF* and *XPG*, respectively. (A) DNA repair synthesis or UV-induced UDS levels of different, as indicated, XP-F and XP-G cells, expressed as percentage of the UDS of a NER-proficient cell line (MRC5) assayed in parallel. (B and C) UDS in cells locally irradiated through a 5 μm microporous filter (60 J/m^2), NER-proficient MRC, XPCS1RO, XPCS1RO transduced with wild type XPG and XPG-E791A (B) and XP2YO transduced with wild-type XPF or XPF-D676A (C). Heavily labeled cells were cells in S-phase, incorporating large amounts of tritiated thymidine by replicative DNA synthesis. Dotted circles indicate the position of pores in which UV damage has been induced and UDS has been observed.

Discussion

An unresolved longstanding issue for human NER is whether the 5' and 3' incisions, by ERCC1-XPF and XPG, respectively, occur in a strict temporal order and, if so, which one occurs first. A related issue is how these incisions are coordinated with DNA repair synthesis to prevent the exposure of potentially extremely damaging ssDNA gaps. We believe that the following observations described here provide novel and important insight into these issues.

First, the 5' incision by ERCC1-XPF depends on the presence, but not catalytic activity, of XPG whereas efficient 3' incision by XPG requires the catalytic activity of ERCC1-XPF (Figure 7), extending previous findings [21, 42, 43]. Second, and most important, partial DNA synthesis is detectable *in vitro* in the presence of catalytically inactive XPG (Figure 8), thereby demonstrating that the incision 5' to the lesion by ERCC1-XPF is both necessary and sufficient for the initiation of repair synthesis, whereas 3' incision by XPG is needed for the completion, but not the initiation of repair synthesis. Third, some late NER factors, including the replication factors PCNA and Polymerase δ as well as the chromatin assembly factor CAF-1, are recruited to sites of local UV damage in cells expressing catalytically inactive XPG, but not in cells expressing catalytically inactive XPF (Figure 10). Fourth, cells expressing catalytically inactive XPG, but not those expressing catalytically inactive XPF, are capable of undergoing intermediate levels of unscheduled DNA repair synthesis (Figure 12).

A defined temporal order for human NER incision and DNA repair synthesis events

Based on these observations we suggest that the human NER pathway does indeed have a defined temporal order for the 5' and 3' incisions and for DNA repair synthesis. Specifically, we propose the following model for the coordination of the dual incision and repair synthesis steps (Figure 13). After assembly of all the factors of the preincision complex, 5' cleavage by ERCC1-XPF takes place, generating a free 3'-OH group. The repair synthesis machinery consisting minimally of polymerase δ , the clamp loader RFC and the processivity factor PCNA are recruited and repair synthesis is initiated. Which factors and interactions may facilitate this recruitment remains to be established, but it is possible that RPA has an important role in this transition [32]. DNA synthesis is then initiated and proceeds about half way through the repair patch. The stalling of the polymerase at this point might trigger the XPG endonuclease activity, allowing the repair synthesis to be completed. We have previously shown that XPG has distinct requirements for binding and cleaving DNA [51] raising the possibility that a conformational change in the NER complex brought about by the polymerase activity triggers the catalytic activity of XPG.

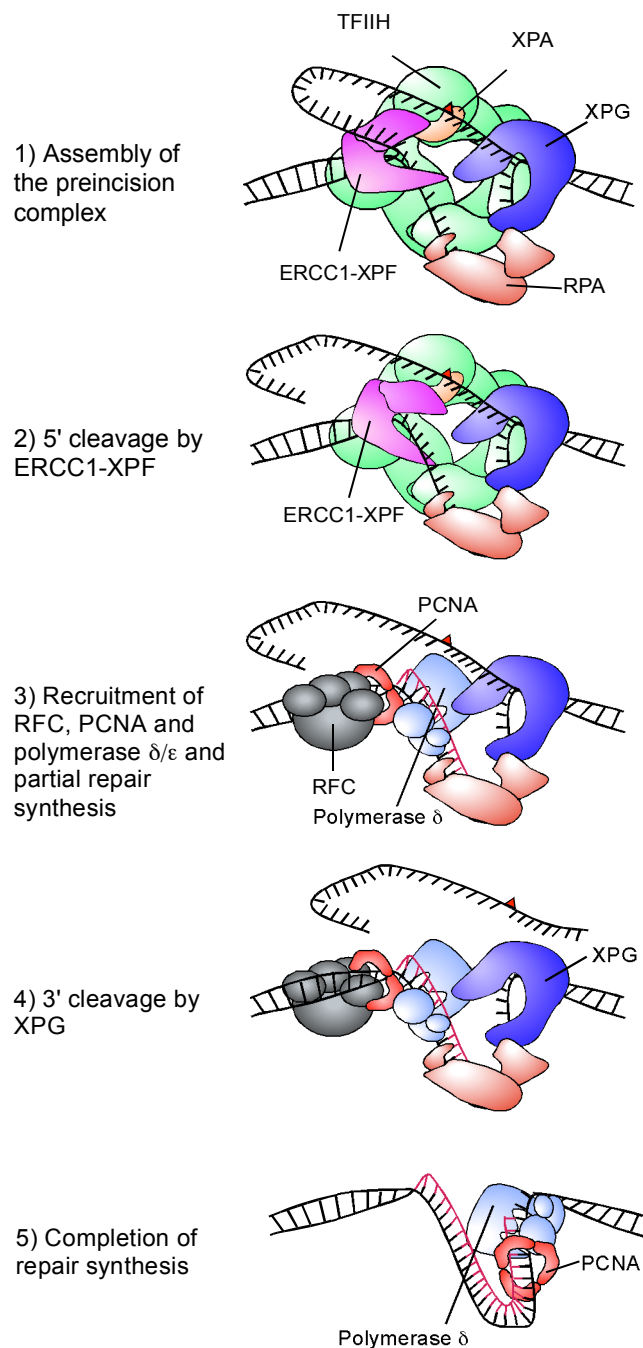


Figure 13. Model for the Coordination of Dual Incision and Repair Synthesis Steps in NER. Schematic representation of the proposed sequence of events following the assembly of the preincision complex. The red triangle stands for the DNA lesion. Individual proteins involved in each step are indicated.

Due to the near simultaneous occurrence of the two incision reactions, we have not yet been able to prove that this reaction sequence is also favored in a situation where wild-type XPF and XPG proteins are present. However, indirect support for our model comes from a recent study that considered the sequence of arrival and release of various NER factors during the dual incision and repair synthesis steps in NER using a fully reconstituted system [104]. This study showed that ERCC1-XPF is released from repair complexes with the arrival of RFC, while XPG (and RPA) are only fully displaced once the entire repair synthesis machinery (RFC, PCNA and Pol δ) has been recruited.

One prediction of our model is that the addition of DNA polymerase inhibitors might inhibit 3' incision by XPG. We observed that addition of the Pol δ inhibitor aphidicolin to an *in vitro* NER reaction did not show a significant inhibition of the 5' or 3' incision (data not shown), consistent with an earlier study [124]. While further studies will be necessary to fully delineate the biochemical relationship of repair synthesis and the 3' incision by XPG, it is interesting to note that a recent study found that treatment of cells with HU and AraC inhibited the removal of 6-4PPs [37]. Although the molecular basis for this observation is currently unknown, it is consistent with our model and the notion that inhibition of repair synthesis blocks at least one of the incisions (presumably by XPG).

The model proposed here does not exclude an involvement of additional protein-protein interactions or protein modifications in the

various steps. For example, it is known that XPG has a PIP box and that it can interact with PCNA [55]. Although it has not yet been shown convincingly that the interaction between PCNA and XPG is required for NER, an interaction between the two proteins may contribute to the activation of the XPG incision. A recent study has implicated polk in the repair synthesis step of NER [118]. It is possible that two polymerases, pol δ and polk, act at different steps of repair synthesis, for example before and after incision by XPG has taken place. Further studies will be required to determine how the various phases of repair synthesis in NER are regulated by protein-protein interactions and possibly post-translational modifications.

Apparent contradictions

One set of experimental observations appears to be in contrast with our results. Under very similar experimental conditions and using a variety of substrates either 5' uncoupled [103, 124] or 3' uncoupled [20, 34, 102, 103] incisions have been observed. Our model would predict that 3' uncoupled incision by XPG should not occur at any appreciable frequency. One possible explanation is that ERCC1-XPF and XPG, can incise NER intermediates under certain conditions *in vitro* that would be disfavored *in vivo*. It is known, for example, that the intrinsic structure-specific endonuclease activity of both ERCC1-XPF and XPG can be readily detected *in vitro* without the need for additional proteins [69, 70]. Similarly, high relative concentration of XPG or the absence of ERCC1-XPF in a cell

extract or reconstituted system may allow incision by XPG 3' to the lesion in the absence of a properly assembled NER complex. We have previously shown that XPG has distinct requirements for binding and cleaving DNA substrates and that the XPG spacer region has a critical role in mediating this substrate preference [48, 51, 52]. We suggest that XPG is present in a catalytically inactive conformation prior to 5' incision and partial repair synthesis and that its catalytic activity is revealed by a change in the complex brought about by partial repair synthesis. The barrier for XPG to cleave certain substrates does not occur at the level of substrate binding, but likely involves a subsequent rearrangement of an XPG-substrate complex [51]. We propose that a lowering of this activation barrier under certain experimental conditions leads to 3' uncoupled incisions.

A “Cut-patch-cut-patch” mechanism

Early investigations of excision repair in bacteria focused on the discrimination between two models: “patch and cut”, involving a first incision close to the damage, followed by repair synthesis and second incision, and “cut and patch”, invoking excision of the damaged base/s prior to repair synthesis [127, 128]. Subsequently, in particular with the ability to reconstitute NER *in vitro*, and the ability to observe dual incision on NER substrates in the absence of repair synthesis, the “cut and patch” model became accepted as the way by which NER operates [124, 129, 130].

The present work suggests that the human NER machinery operates via a “cut-patch-cut-patch” mechanism that includes features of both previous models. Interestingly, long-patch base excision repair (BER) has been shown to proceed in a similar way. In long-patch BER, polymerase δ/ϵ , supported by the replication accessory factors RFC and PCNA or polymerase β , carries out repair synthesis past the abasic site and introduces 2-6 nucleotides. The short oligonucleotide overhang generated in this way is excised by the Flap endonuclease FEN1, and the nick is sealed by DNA ligase I [131, 132]. In line with this model, it was demonstrated that PCNA facilitates excision in long-patch BER [133]. Stimulation of the dual incision by PCNA has also been observed in NER, leading to the proposal that PCNA may promote the turnover of the early NER factors [134] linking the excision and repair synthesis steps. Although many aspects of these important DNA repair processes remain to be discovered, it is interesting and unexpected that both NER and long-patch BER have operational similarities.

Materials and Methods

Protein Purification

Wild type XPF, XPF D676A, XPF R678A, XPF E679A, XPF 681A, XPF E701A, XPF D704A, XPF E714A, XPF R715A, XPF K716A, XPF D720A, wild type XPG and XPG E791A proteins were expressed in Sf9 insect cells and purified as described previously [51, 86]. The purity of the enzyme preparations was very similar to the ones previously reported and 0.2-0.5 mg of proteins were obtained at concentrations of 0.2-0.3 mg/ml.

***In vitro* NER Dual Incision Assay**

Covalently closed circular DNA (pBluescript) containing a single 1,3-intrastrand d(GpTpG) cisplatin-DNA crosslink was prepared as described previously [124] and additionally purified over two consecutive sucrose gradients. Reactions were carried out in a buffer containing 40 mM HEPES-KOH (pH 7.8), 70 mM KCl, 5 mM MgCl₂, 0.5 mM DTT, 2 mM ATP, 0.36 mg/ml BSA, 22 mM phosphocreatine (di-Tris salt) and 50 ng/μl creatine phosphokinase. Each reaction contained 200 ng DNA and 30 μg of cell-free extract prepared from XPG- or XPF-deficient fibroblast cells (XPCS1RO and XP2YO, respectively). Complementation was assayed upon addition of 730 fmol wild-type or mutant protein (XPG or XPF). Reactions were incubated at 30°C for 45 minutes. 50 nM of an oligonucleotide complementary to the excision product with a G₄ 5'-overhang (5'-GGGGGAAGAGTGACACAGAAGAAGACCTGGTCGACC)

was added, followed by heat inactivation at 95°C for 5 minutes. Alternatively, for detection of individual incisions, the incision reaction was inactivated by addition of 1M EDTA, pH 8.0, 3% SDS and 12µg proteinase K. DNA was extracted with phenol:chloroform and ethanol precipitated as described previously [135], then 50nM of an oligonucleotide complementary to the BssHII restriction site with a G₅ 5'-overhang was added (5'-GGGGGCAATTAACCCTCACTAAAGGGGAACAAAAGCTGG) followed by heat inactivation at 95°C for 5 minutes. After cooling down the reactions for 15 minutes at room temperature, 0.5 units of Sequenase and 3.5 µCi of [α -³²P]-dCTP (both from Amersham-Pharmacia, diluted in Sequenase dilution buffer) were added. Reactions were incubated for 3 minutes at 37°C prior the addition of 1.2 µl dNTP mix (100 µM of each dATP, dGTP, TTP and 50 µM dCTP) and incubation for another 12 minutes at 37°C. This fill-in reaction labeled the product using the G₄ overhang provided by the respective complementary oligonucleotides as a template. Reactions were stopped by addition of formamide loading buffer, heated at 95°C for 5 minutes and analyzed on a 12% or 8% denaturing polyacrylamide sequencing gel. The gel was exposed on a phosphor screen and scanned on a PhosphorImager.

***In vitro* NER Repair Synthesis Assay**

The assay was performed using the same substrate, cell extracts and proteins as described for the excision assay. The reaction mixtures

additionally contained 10 μ M dATP, 10 μ M dGTP, 5 μ M dCTP, 5 μ M TTP, 10 μ Ci of [α -³²P]-dCTP and 10 μ Ci [α -³²P]-TTP. Complementation was assayed upon addition of 600 fmol of wild-type or mutant protein (XPG or XPF). Reactions were incubated at 30°C for 3 hours. DNA was purified using MinElute PCR Purification Kit (Qiagen), cleaved with *KpnI* and *SacI* or *BsrBI* and *XhoI* and analyzed on a 10% denaturing polyacrylamide sequencing gel.

Cell Culture Conditions and Preparation of Whole Cell Extracts

For the generation of whole cell extracts, SV40-transformed fibroblast cells XPCS1RO (XPG-deficient, [136] and XP2YO (XPF-deficient, GM08437) were cultured in Dulbecco's Modified Eagle's Medium (DMEM, Invitrogen) supplemented with 10% fetal calf serum and 2 mM L-glutamine, 100 U/ml penicillin, and 0.1 mg/ml streptomycin at 37 °C in the presence of 5% CO₂. Cells were grown to near confluency, and whole cell extract was prepared accordingly to a published procedure [137].

Cell Transduction with Lentiviral Recombinants

XPG wild type cDNA, XPG-E791A cDNA were cloned into the pLOX/EWGFP lentiviral vector and XPF wild type (with a C-terminal HA tag) and XPF-D676A (with a C-terminal HA tag) cDNAs were cloned into the pWPXL lentiviral vector by replacing the GFP cDNA. Lentiviruses containing the different constructs under the control of the EF1 α promoter were produced by co-transfecting 293T cells with the following 3 plasmids:

the packaging plasmid psPAX2, the envelope plasmid pMD2G and the lentiviral vector containing the different XPG and XPF cDNAs. Details of the vectors and protocols are described on the following web site <http://www.lentiweb.com>. XP-G/CS (94RD27, patient XPCS1RO) and XP-F (XP2YO) SV40 immortalized fibroblasts at 50% confluency were infected with viral particles containing the different XPG and XPF recombinants. Transduced cells were then cultured in DMEM supplemented with 10% FBS, 2 mM L-glutamine, 100 U/ml penicillin and 0.1 mg/ml streptomycin in a 5% CO₂ humidified incubator. The transduction efficiency was further assessed by immunofluorescence.

Local UV Irradiation and Immunofluorescence

Local DNA damage infliction within cultured cells was performed as described previously [138]. Briefly, cells cultured on coverslips were rinsed with PBS and covered with a micro-porous polycarbonate filter containing 5µm pores (Millipore). Cells were irradiated through the filter with a Philips TUV lamp (254 nm) with a dose of 150 J/m². After UV-irradiation cells were cultured for 0.5 hrs, washed first with PBS and then with PBS containing 0.05% Triton X-100 for 30 seconds prior to fixation with 3% paraformaldehyde for 15 minutes at room temperature or with ice-cold methanol for 20 min (for PCNA staining). Subsequently, cells were permeabilized by a 2 times 10 min. incubation in PBS containing 0.1% Triton X-100, and washed with PBS⁺ (PBS containing 0.15% glycine and 0.5% bovine serum albumin). For the experiments with Polδ, cells were

incubated with Hu-AraC (10mM HU, 0.1mM AraC) from 30 minutes prior to irradiation until fixation and cells were fixed with MeOH rather than formaldehyde. Cells were incubated at room temperature with the primary antibody (diluted in PBS⁺) for 2 hours in a moist chamber. Subsequently cells were washed 5 times for 10 min. with PBS Triton X-100, washed with PBS⁺, and incubated at room temperature with the secondary antibody (diluted in PBS⁺) for 1 hour in a moist chamber. Cells were washed 5 times for 10 mins in PBS Triton X-100, washed in PBS, and embedded in Vectashield mounting medium (Vector) containing 0.1 mg of DAPI (4'-6'-diamidino-2- phenylindole)/ml.

Primary antibodies were as follows: mouse monoclonal anti-PCNA (Dako, clone PC10), 1:1000, rabbit polyclonal affinity purified anti-XPC [139], 1:300, rabbit polyclonal anti-XPB (TFIIH p89, S-19m Santa Cruz), 1:1000, mouse monoclonal anti-Pol δ (A-9, Santa Cruz), 1:25, mouse monoclonal anti-CHAF150 (CAF-1) (abcam, ab7655), 1:2000, and mouse monoclonal FITC-conjugated anti-HA (Roche, clone 3F10) Secondary antibodies were as follows: Cy3-conjugated goat anti-mouse (Jackson ImmunoResearch Laboratories), 1:1000, Cy3-conjugated goat anti-rabbit (Jackson ImmunoResearch Laboratories), 1:1000, and Alexa-488 conjugated goat anti-rabbit (Molecular Probes), 1:800.

Confocal Microscopy

Confocal images of the cells were obtained using a Zeiss LSM 510 microscope equipped with a 25mW Ar laser at 488 nm, a He/Ne 543 nm

laser, and a 40 X 1.3 NA oil immersion lens. Alexa-488 was detected using a dichroic beam splitter (HFT 488), and an additional 505- to 530-nm bandpass emission filter. Cy3 was detected using a dichroic beam splitter (HFT 488/543) and a 560- to 615-nm bandpass emission filter.

Unscheduled DNA Synthesis (UDS)

To determine global genome NER activity in cultured cells, UV-induced DNA repair synthesis or unscheduled DNA synthesis (UDS) was measured. Coverslip cultures were rinsed with PBS, UV-irradiated (16 J/m², Philips 254 nm TUV lamp) and subsequently incubated for 2 hours in culture medium supplemented with 20 μ Ci/ml [³H-1',2']-thymidine (120 Ci/mmol, Amersham TRK565). After fixation coverslips were dipped in Ilford K2 photographic emulsion, exposed for three days and after development stained with Giemsa. Autoradiographic grains above the nuclei of 50 cells were counted and compared to the number of grains above nuclei of NER-proficient fibroblasts (MRC5, set at 100% UDS), assayed in parallel. UDS in locally damaged cells (local UDS) with 60 J/m² was performed in a similar fashion with the exception of an extended exposure time to six days.

Acknowledgements

Jacqueline Enzlin is the author of Figure 6, Nils Wijgers is the author of Figure 12, Lidija Staresincic is the author of Figures 8, 9, 10 and 11, and Isabelle Dunand-Sauthier generated XPG cell-lines used.

CHAPTER 3

A UBM and new PIP domain in XPG Regulate the Late Steps in Nucleotide Excision Repair

Introduction

Nucleotide excision repair (NER) is a highly versatile DNA repair pathway capable of eliminating a variety of lesions within DNA [6]. The pathway involves the concerted action of more than 30 proteins that sequentially recognize a lesion, excise it in the form of a 24-32-nucleotide long stretch of DNA containing the damage, fill in the ensuing gap by repair synthesis and finally ligate the DNA to seal the nick, restoring it to its original context [6, 12]. Two subpathways of NER exist that differ primarily in their mode of damage recognition. Transcription-coupled NER removes damage in the actively transcribed regions of the genome, and is triggered by stalling of the transcribing RNA polymerase at a lesion [112, 113]. Alternatively, lesions within the bulk DNA are recognized by XPC-RAD23B, which is essential for recruitment of all other NER factors [57, 114]. XPC-RAD23B recruits the multi-subunit transcription and repair factor TFIIH, which is responsible for opening up the DNA around the lesion [17, 18, 34], allowing recruitment of XPA, RPA and XPG to the complex, with simultaneous release of XPC [32]. ERCC1-XPF joins the complex [28, 32] and positions itself via its interactions with XPA [28, 35] and RPA to perform the 5' incision [140]. ERCC1-XPF performs the incision 5' to the damage while XPG makes the 3' incision [33, 69, 70] releasing a 24-32 nucleotide stretch of ssDNA containing the lesion. The resulting gap is filled in by polymerase δ , ϵ , or κ [36] and associated

factors and the nick sealed by ligase I or III α [37] restoring the DNA to its original state.

While the early steps of NER, starting with damage recognition by XPC-RAD23B [15, 18], and leading up to the dual incisions by ERCC1-XPF and XPG [32, 33, 57] have been studied extensively, less is known about how dual incision and repair synthesis are linked [6, 33]. We have recently shown that the 5' incision by ERCC1-XPF and partial repair synthesis can occur in the absence of 3' incision by XPG (Chapter 2) [33]. This observation suggests that the dual incision events may be ordered, with the 5' incision occurring first, releasing a free 3'-OH group which serves as a substrate for initiation of repair synthesis. This order of events likely represents a regulatory mechanism, preventing unwanted cuts within the DNA and avoiding deleterious ssDNA regions that could occur if the dual incisions are uncoupled from repair synthesis. Furthermore, XPG has been shown to interact with PCNA [55] and more recent evidence suggests that XPG has a role in the transition from dual incision to repair synthesis via its interaction with PCNA [104].

In light of these observations, we were interested in exploring whether an interaction between XPG and PCNA (and possibly other factors) has a role triggering the 3' incision by XPG, providing an additional layer of regulation. Precedent for such a mechanism exists in resolution of Okazaki fragments by the flap endonuclease-1 (FEN1), a member of the same nuclease family as XPG [141]. FEN1 remains bound

to the DNA in an inactive conformation until it interacts with PCNA from the approaching replication fork [106, 107], upon which it undergoes a conformational change to become catalytically active [49].

We considered whether the XPG incision might be similarly regulated. We were intrigued by a possible analogy between a polymerase carrying out repair synthesis blocked by the presence of XPG and a replicative polymerase blocked at a DNA lesion (Figure 14). Stalling of a polymerase at a lesion results in the ubiquitylation of PCNA, which serves as a signal for recruitment of TLS polymerases that have the ability to bypass DNA lesions [108]. In addition to their PIP domain, TLS polymerases contain a ubiquitin-binding motif, and the PIP and UBM domains act synergistically in recruiting TLS polymerases [109]. Intriguingly, sequence analysis reveals that XPG, like the translesion synthesis (TLS) polymerases, also possesses a ubiquitin-binding motif (UBM) in addition to its PIP domain for PCNA interaction [110], raising the possibility that XPG activity might also be regulated by interaction with ubiquitylated PCNA. Indeed, it has recently been shown that ubiquitylation of PCNA occurs during NER, and that this ubiquitylation was required for the recruitment of polk, one of three polymerases involved in NER repair synthesis (the other ones being pol δ and pol ϵ) [36]. A possible scenario during NER could therefore be that XPG initially binds DNA in an inactive conformation, and the approaching replication machinery collides with XPG allowing interaction with PCNA and stimulation activity of XPG. It is

conceivable that such collision could lead to ubiquitylation of PCNA, which could further stimulate XPG activity (Figure 14).

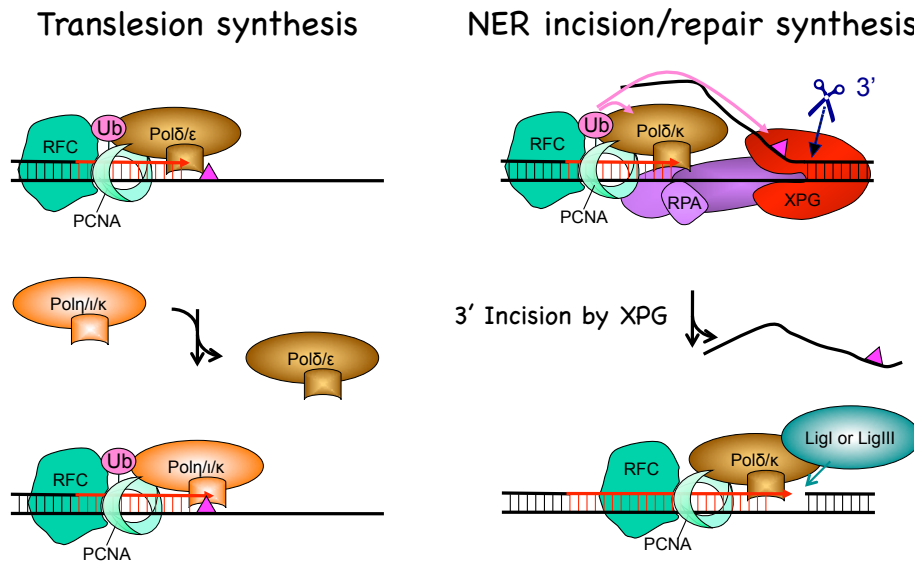


Figure 14: Schematic of proposed similarities between TLS synthesis and NER dual incision and repair synthesis. Left panel shows a stalled replication fork at a DNA lesion that leads to ubiquitylation of PCNA, which serves as a signal to switch from replicative polymerase to TLS polymerase allowing bypass of the lesion. The right panel is our proposed model whereby replication machinery stalls during repair synthesis, triggering PCNA ubiquitylation which could in turn trigger 3' incision by XPG.

To test these hypotheses we made mutations in the PIP (PIP-C) and UBM domains of XPG. We report here an additional putative PIP domain (PIP-N) in the protein, and observed the effects of these mutations on recruitment and departure of NER factors from regions of damage. We observed that mutations in the UBM and PIP-N domains impair damage repair, and the late steps of NER, but see no effects of PIP-C on XPG activity. Intriguingly, the UBM mutants exhibit a phenotype similar to the E791A mutant with regards to damage repair, and PCNA localization. Our

findings suggest that the role of XPG in coordinating dual incision with repair synthesis is multifaceted, and that it maintains several subtle interactions with PCNA to carry out this role.

Results

XPG contains a UBM that interacts specifically with ubiquitin.

An alignment of the XPG sequence with those of the TLS polymerases revealed the presence of a conserved ubiquitin-binding motif (UBM) in XPG [110] which, like the UBMs in the TLS polymerases [109] spans ~30 residues and is comprised of two predicted helical segments separated by a “Leucine-Proline” motif (Figures 15 and 16A).

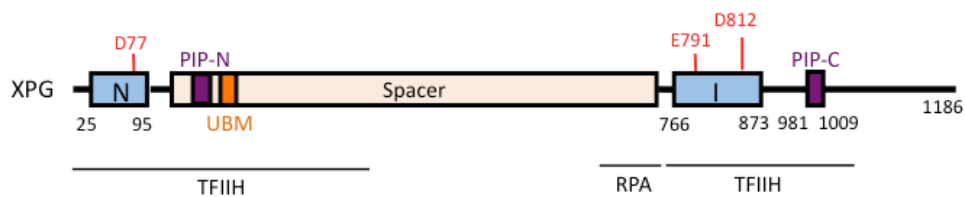


Figure 15: XPG structure and domains: The primary structure of XPG shows the 1186 amino acid protein with its active site made up of the N and I domains (light blue) separated by the 600 amino acid spacer region. The active site residues within the N and I domains are shown in red. Regions for interaction with TFIIH, and RPA are shown, and the PCNA-interaction domains (PIP-C and PIP-N) are indicated in purple, while the ubiquitin-binding motif (UBM) is shown in orange. Mutants used in this study include E791 (mutated to A) shown in red.

A.

XPG Hs UBM	184	-	Q	A	I	D	I	E	S	E	D	F	S	S	L	P	E	V	K	H	E	I	L	T	D	M	K	E	-	-	
Rev1 Sp UBM1	692	-	S	S	S	Q	I	S	S	S	A	L	A	Q	L	P	P	S	M	Q	S	D	I	Q	Q	Q	L	R	L	Q	K
Rev1 Sp UBM2	726	-	Y	P	S	Q	L	D	P	L	F	M	V	E	L	P	T	P	T	R	N	E	V	N	D	N	H	E	I	A	M
Rev1 Sp UBM3	796	-	N	K	P	N	V	D	Y	L	T	L	K	E	L	P	K	D	L	Q	K	Q	I	L	K	E	S	N	L	Q	K
Rev1 Sc UBM1	751	E	K	T	I	-	V	T	N	R	A	F	E	A	L	P	E	D	V	K	N	D	I	N	N	E	F	E	K	R	N
Rev1 Sc UBM2	809	-	L	P	S	T	M	E	E	Q	F	M	N	E	L	P	T	Q	I	R	A	E	V	R	H	D	L	R	I	Q	K
Rev1 Mm UBM1	934	-	S	P	S	Q	I	D	Q	S	V	L	E	A	L	P	L	D	L	R	E	Q	I	E	Q	V	C	A	A	Q	Q
Rev1 Mm UBM2	1012	-	A	F	S	Q	V	D	P	D	V	F	A	A	L	P	A	E	L	Q	K	E	L	K	A	A	Y	D	Q	R	Q
Rev1 Hs UBM1	934	-	S	P	S	Q	L	D	Q	S	V	L	E	A	L	P	P	D	L	R	E	Q	V	E	Q	V	C	A	V	Q	Q
Rev1 Hs UBM2	1012	-	A	F	S	Q	V	D	P	E	V	F	A	A	L	P	A	E	L	Q	R	E	L	K	A	A	Y	D	Q	R	Q
Rev1 Dm UBM	770	-	L	V	P	K	L	D	E	D	V	L	A	Q	L	P	E	D	I	R	L	E	V	I	A	N	R	E	E	H	L
Poli Mm UBM1	496	-	L	P	E	G	V	D	Q	E	V	F	K	Q	L	P	A	D	I	Q	E	E	I	L	Y	G	K	S	R	E	N
Poli Mm UBM2	681	-	F	P	P	D	I	D	P	Q	V	F	Y	E	L	P	E	E	V	Q	K	E	L	M	A	E	W	A	R	A	G
Poli Hs UBM1	498	-	L	P	E	G	V	D	Q	E	V	F	K	Q	L	P	V	D	I	Q	E	E	I	L	S	G	K	S	R	E	K
Poli Hs UBM2	679	-	F	P	S	D	I	D	P	Q	V	F	Y	E	L	P	E	A	V	Q	K	E	L	L	A	E	W	K	R	T	G
Poli Dm UBM	665	-	C	P	A	G	V	D	A	E	V	F	K	E	L	P	V	E	L	Q	T	E	L	I	A	S	W	R	S	S	L
			F	P			D		V	F		L	P			Q															

B.

			↓		★		↓	↓			
XPG Hs	-	-	K	Q	A	L	Q	E	E	F	F
XPG XI	-	-	K	Q	R	L	Q	E	D	F	F
XPG Mm	-	-	K	Q	A	L	Q	E	E	F	F
XPG Gg	-	-	K	K	L	L	Q	E	Q	L	F

Figure 16: UBM and PIP-N domain alignments. (A) Alignment of the XPG UBM domain with UBM domains of the TLS polymerases is shown with conserved residues highlighted. The numbers indicate the position of the first amino acid of each UBM in the sequence. For the Δ UBM mutant the conserved LP residues were mutated to AA. (B) Alignment of the PIP-N domain of XPG in different species. The canonical PIP residues conserved in humans are indicated by the arrows, while the non-canonical residue is indicated by a star. The conserved FF residues were mutated to AA to generate the Δ PIP-N mutant. Species abbreviations used: Hs, *Homo sapiens*; Sp, *Schizosaccharomyces pombe*; Sc, *Saccharomyces cerevisiae*; Mm, *Mus musculus*; Dm, *Drosophila melanogaster*; XI, *Xenopus laevis*; Gg, *Gallus gallus*.

We generated XPG mutants by site-directed mutagenesis of the critical Leu-Pro residues thought to be important for ubiquitin-binding, L196A, P197A (Δ UBM mutant) or deletion of the entire UBM domain (Δ UBM^{domain} mutant) [48]. Purified recombinant XPG^{WT}, XPG ^{Δ UBM} and XPG ^{Δ UBM-domain} were incubated with GST-Ub₄, pulled down with GST beads. Analysis of the GST-bound and supernatant fractions revealed that XPG^{WT} bound

specifically to ubiquitin, whereas XPG^{ΔUBM} and XPG^{ΔUBM-domain} lost the ability to bind ubiquitin (Figure 17, lanes 5-7). *In vitro* nuclease and NER assays revealed that the ΔUBM mutant retained normal nuclease activity (data not shown). These data show that XPG binds ubiquitin via its UBM domain but that the UBM domain is not essential for the activity of XPG *in vitro*.

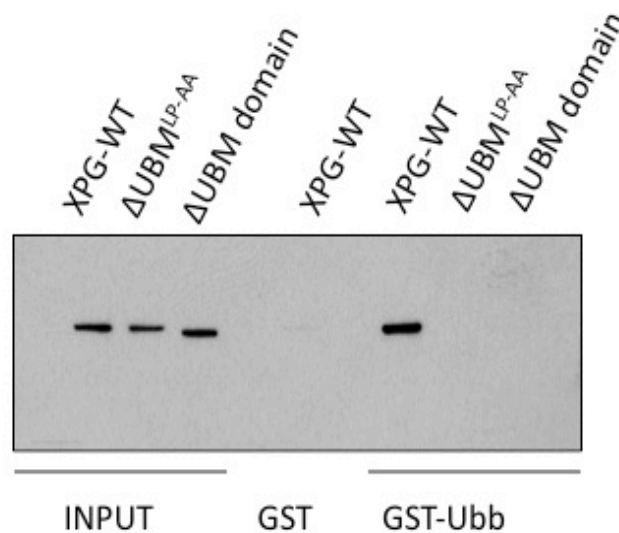


Figure 17: The UBM domain in XPG mediates its binding to ubiquitin. *In vitro* binding of GST-Ubb (GST fused to four ubiquitin residues) to the indicated XPG constructs, XPG-WT, XPG^{ΔUBM^{LP-AA}}, and XPG^{ΔUBM domain}. XPG-WT bound to GST-Ubb but not to GST alone (compare lanes 4 and 5), whereas mutation of the LP residues to AA as well as deletion of the UBM domain in XPG inhibited binding of the protein (compare lane 5 to lanes 6 and 7).

A putative PIP in the spacer region of XPG.

It has previously been shown that XPG contains a C-terminal PIP domain by which it specifically interacts with PCNA (PIP-C) (Figure 15) [55]. Mutation of the R992 residue in the PIP-C domain had minimal effect

on NER activity of XPG, although the PCNA interaction was specifically abolished [55]. Interestingly, the related endonuclease FEN1 also interacts specifically with PCNA via a PIP domain, and requires this interaction to activate nuclease activity of FEN1 for resolution of Okazaki fragments during replication [106, 107]. Although the XPG nuclease activity clearly does not require an interaction with PCNA, we were interested in determining whether the C-terminal PIP domain of XPG might contribute to NER in conjunction with other protein interaction domains. It has been reported that a number of TLS polymerases contain both PIP and UBM domains, and that mutations in both domains were required for TLS activity in cells [109]. These findings suggest a similar mechanism of action in XPG whereby it interacts with PCNA via both of these domains, possibly in a manner whereby it maintains subtle interactions with PCNA via these domains. It has also been reported that several PCNA-interacting proteins such as CAF-1 [142] contain more than one PIP. We searched for additional PIPs in XPG, and found another possible PIP domain in its spacer region (PIP-N), located immediately N-terminal to the UBM domain (Figures 15 and 16B). The newly found PIP-N domain lacks a critical residue that is conserved amongst most PIP domains, as canonical PIPs conform to the sequence QXXhXXaa, where Q is a glutamine, h is a hydrophobic residue (valine, methionine, leucine, or isoleucine), a is an aromatic residue (phenylalanine, tyrosine, tryptophan, or occasionally histidine), and X is any amino acid (see Figure 16B –

Q175 in XPG Hs instead of “h” indicated by a star). Yet alignment of XPG sequences in various organisms revealed conservation of this putative PIP in the higher order vertebrates *M. musculus*, and *X. laevis* (Figure 16B).

To better understand whether the PIPs and UBM domains in XPG have a role in NER, we generated mutations in the PIP-C domain, F996A, F997A (XPG^{ΔPIP-C}), the PIP-N domain, F179A, F180A (XPG^{ΔPIP-N}), and the UBM (XPG^{ΔUBM}), separately and in combination (XPG^{ΔUBMΔPIP-C}, and XPG^{ΔUBMΔPIP-N}). We used the lentiviral vector transduction system to stably transduce the XPG-deficient cell-line XPCS1RO with either of these mutants as well as the previously generated active site mutant XPG^{E791A} [33] and analyzed how these mutations affected the repair of DNA lesions and the recruitment of NER factors to the sites of local UV damage [57].

Damage removal is impaired in ΔUBM, and ΔPIP-N mutants but not in ΔPIP-C mutants.

We analyzed *in vivo* damage repair kinetics of the cell-lines by UV-irradiating them with 150J/m² of UV through a micro-pore filter generating sites of local UV damage (LUD). Following irradiation cells were fixed either immediately, or following incubation for various time-periods, and then washed and probed with antibodies to (6-4)PPs, and the NER factor ERCC1 (for images of cells with co-localized (6-4)PP and ERCC1 foci at 0.5h see Figure 26 in the Appendix). Cells containing damage foci were counted and graphed as illustrated in Figure 18. As expected, damage foci

levels persisted in the untransduced XP-G cells, with greater than 50% damage foci persisting to 24h, while in XPG^{WT} cells (6-4)PPs disappeared completely between 3h and 6h. The catalytically inactive XPG^{E791A} mutant, which we have previously shown to be severely impaired in NER (Chapter 2 and [33]), exhibited much reduced damage-removal ability with ~30% damage foci persisting up to 24h (Figures 18 and 19). Intriguingly, the Δ UBM mutant showed levels of damage foci very similar to those in XPG^{E791A} despite having normal nuclease and NER activity *in vitro* (Figure 18 and data not shown). Of the two PIP domains, PIP-N appeared to play a more important role in NER, as XPG ^{Δ PIP-N} cells, but not XPG ^{Δ PIP-C} cells exhibited a moderately reduced rate of damage removal (Figures 18 and 19). Importantly, incorporation of the UBM mutation into any other mutant resulted in phenotypes similar to that of XPG ^{Δ UBM} alone, suggesting that the UBM domain is of particular importance for damage removal *in vivo*.

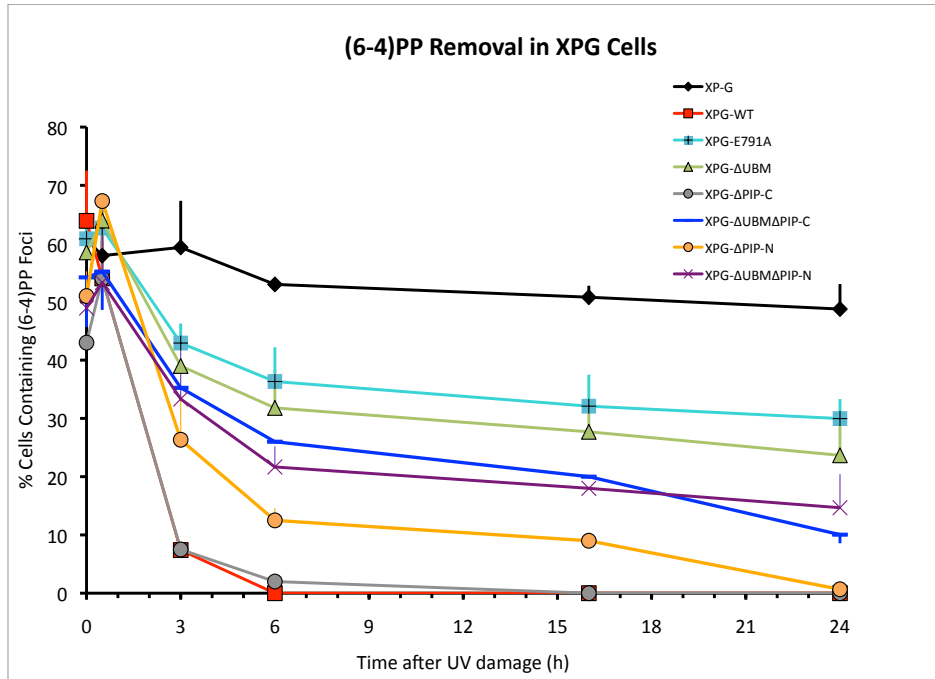


Figure 18: Removal of (6-4)PPs is impaired in the E791A, UBM and PIP-N mutants. XP-G deficient cells (XPCS1RO) were transduced with wild-type or mutant XPG and irradiated with UV light (150 J/m^2) through a polycarbonate filter with $5\mu\text{m}$ pores and fixed and stained for (6-4)PP (red) and the nuclear marker DAPI (4'-6'-diamino-2-phenylindole) in blue at the indicated time-points after irradiation. This is a graphical representation of the percentage of cells with persistent (6-4)PP foci at various time-points. Data represent the average of three independent experiments \pm S.D. (error bars).

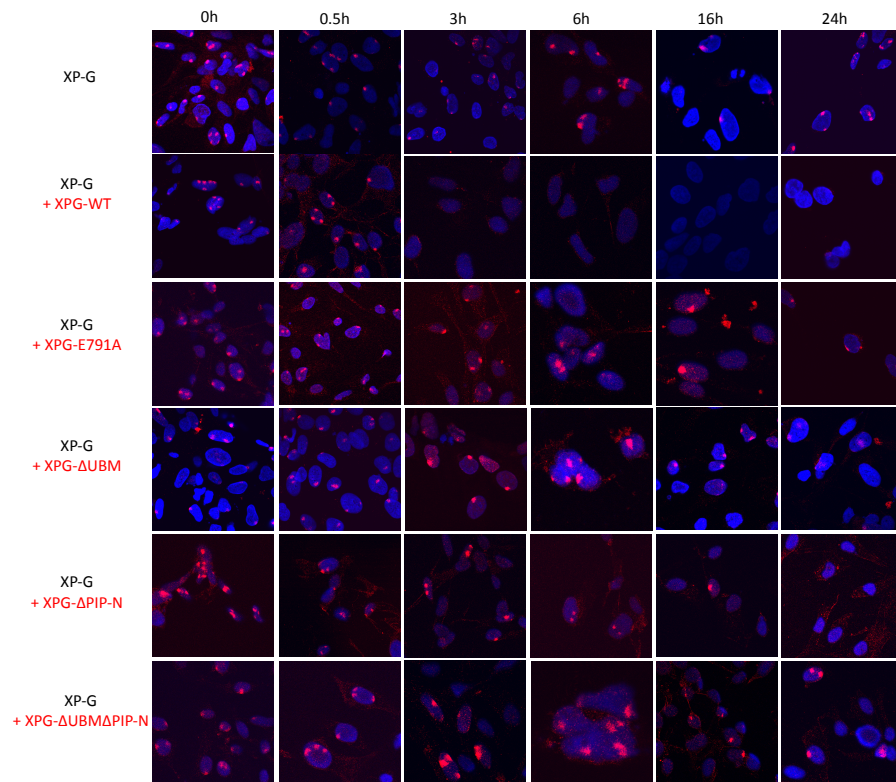


Figure 19: IF images of (6-4)PP foci in mutants at all time-points analyzed. Images of the UV irradiated cells at different time-points following irradiation, (see Figure 18) with (6-4)PP foci shown in red, and DAPI staining in blue.

The PIP-N but not PIP-C domain is required for the association of PCNA with (6-4)PPs.

Next we analyzed the localization of PCNA to damage regions by probing for PCNA along with the NER factor ERCC1 at various time points following UV-irradiation. We have previously shown that PCNA is recruited to damage regions in the XPG-E791A mutant, despite its inability to carry out incision, suggesting that the presence, but not catalytic activity of XPG

is required for the recruitment of PCNA to LUDs (Chapter 2 and [33]). We observed the same results in a quantitative manner, with PCNA foci visible in XPG^{E791A} cells as early as 0.5h following UV-irradiation, the same as is seen in XPG^{WT} cells. The XPG^{ΔUBM} and XPG^{ΔPIP-C} mutant cell-lines also supported normal recruitment of PCNA at the earliest time-point (Figures 20 and 21), demonstrating that the PIP-C domain was not required for the recruitment of PCNA. Interestingly however, mutations in putative PIP domain, ΔPIP-N, led to abolished PCNA recruitment to LUDs at 0.5h (Figures 20 and 21), and only 5-10% colocalization PCNA of foci with (6-4)PPs was observed at 1h following UV irradiation (Figure 21). It is important to note that XP-G deficient cell-lines did not show any recruitment of PCNA at the early time-points tested. These results suggest that the PIP-N domain plays a role in PCNA recruitment to damage regions, or at least in maintaining its stable interaction with the DNA at damage regions.

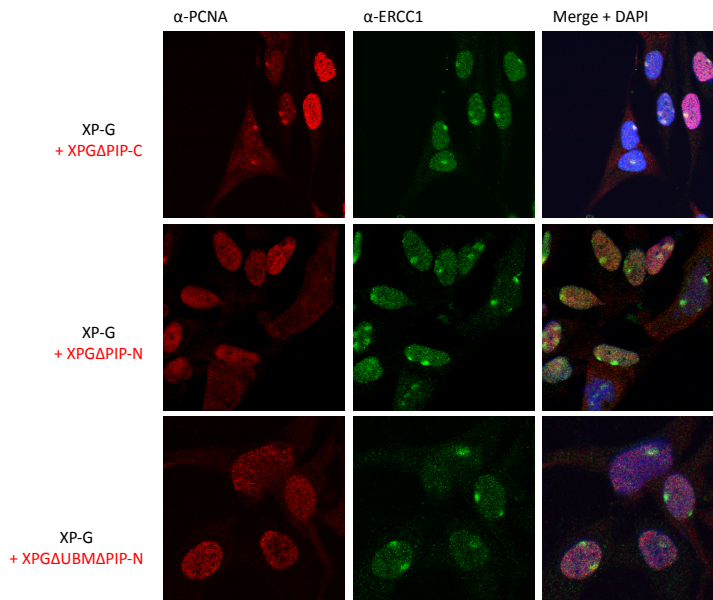


Figure 20: PCNA recruitment in the PIP mutants. XP-G cells transduced with either wild-type or mutant XPG were UV-irradiated, returned to culture, and fixed and stained for PCNA at the indicated times following irradiation. Images of the PIP mutants $XPG^{\Delta PIP-C}$, $XPG^{\Delta PIP-N}$ and $XPG^{\Delta UBM \Delta PIP-N}$ at 0.5h after UV irradiation showing PCNA foci (red) and ERCC1 foci (green). No PCNA foci are visible in $XPG^{\Delta PIP-N}$, and $XPG^{\Delta UBM \Delta PIP-N}$ mutants while PCNA foci are clearly visible in the $XPG^{\Delta PIP-C}$ mutant.

PCNA persists at sites of damage in active site and ΔUBM mutants

At the later time-points we observed some interesting results. In XPG^{WT} cells, PCNA disappears from damage regions by 16h with only a very small fraction (~5%) still visible at 6h following UV damage. The $\Delta PIP-C$ mutant once again behaved similar to XPG^{WT} with respect to PCNA kinetics further suggesting that this mutation does not affect NER. However in the XPG^{E791A} , $XPG^{\Delta UBM}$, and $XPG^{\Delta UBM \Delta PIP-C}$ expressing cells, PCNA foci persisted, with ~15-25% PCNA foci remaining in these cells at 24h after UV-irradiation (Figure 21). These results suggest that, as would

be expected in XPG-E791A, PCNA is recruited normally and stably to the DNA, where it initiates, but is unable to complete its function in repair synthesis, possibly because it is blocked by inactive XPG. Persistence of PCNA foci in XPG^{ΔUBM}, and XPG^{ΔUBMΔPIP-C} also supports such an explanation. However PCNA behaved distinctly in XPG^{ΔPIP-N} and XPG^{ΔUBMΔPIP-N} cells. In those mutants, PCNA levels remained low (<10%) at all time points examined (Figure 21). At 16h, and 24h following UV-irradiation, PCNA foci dropped to 0-5% in both mutants, although the XPG^{ΔPIP-N} mutant contained ~10-15% of the other NER factor ERCC1 at the same time-points (Figure 22) suggesting that this mutant specifically affects the association of PCNA with LUDs (for images of PCNA and ERCC1 foci colocalized in cells at all time-points examined see Figures 27-31 in the Appendix).

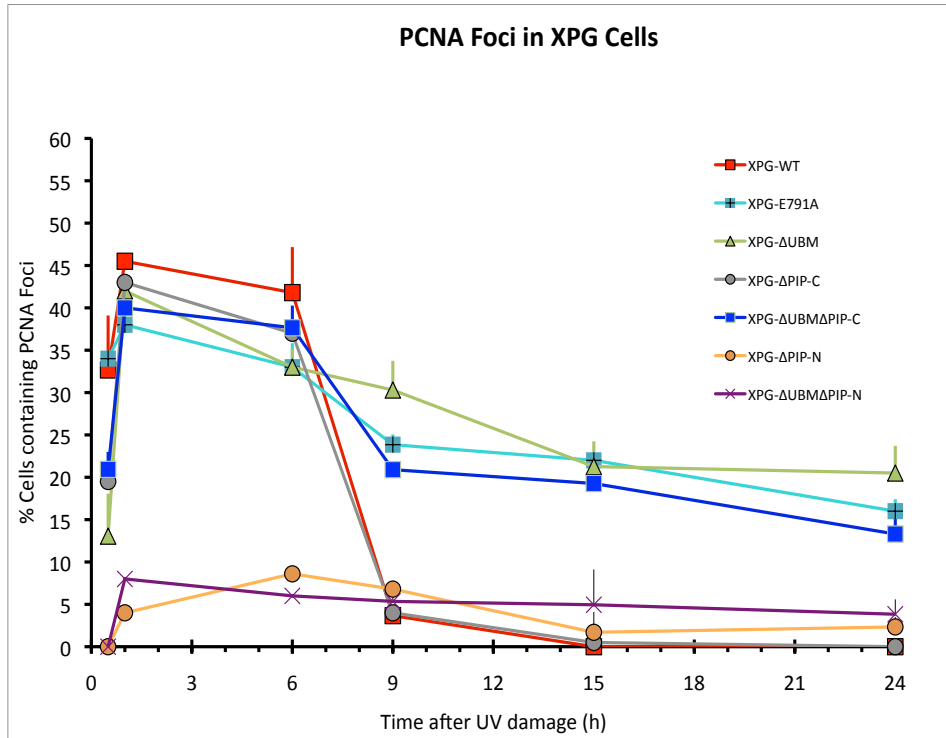


Figure 21: PCNA association with damaged regions is impaired in PIP-N mutants, while its dissociation is impaired in UBM and E791A mutants. A graphical representation of the percentage of cells containing PCNA foci at various time-points after UV. PCNA foci accumulate within 0.5h in XPG-WT, XPG-E791A, XPG^{ΔUBM}, XPG^{ΔPIP-C}, and XPG^{ΔUBMΔPIP-C}, but not in XPG^{ΔPIP-N}, or XPG^{ΔUBMΔPIP-N} indicating impairment of PCNA recruitment as a result of the PIP-N mutation. PCNA foci persist up to 24h in XPG^{ΔUBM}, XPG^{ΔUBMΔPIP-C}, and XPG-E791A mutants indicating inability of the replication factor to dissociate from repair factories in these mutants.

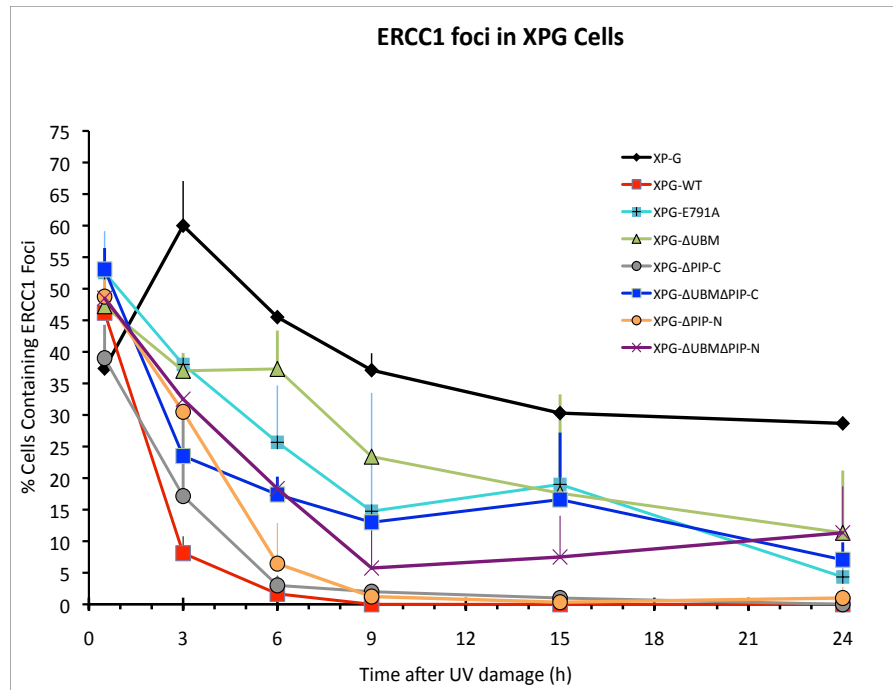


Figure 22: ERCC1 remains associated with damaged regions in E791A and UBM mutants up to 24h. A graphical representation of the percentage of cells containing ERCC1 foci at various time-points after UV.

XPG foci persist in XPG-E791A, ΔUBM, and ΔPIP-N mutants to different extents.

We analyzed the levels of association of XPG with (6-4)PPs in our XPG-mutant cell-lines. XPG was recruited to LUDs with similar dynamics in all of our cell lines, with significant foci levels seen at 0.5h following UV irradiation. In XPG^{WT} and $XPG^{\Delta PIP-C}$, XPG levels at LUDs dropped dramatically by 3h, with only <5% XPG foci present (Figures 23 and 24). However, the XPG-E791A mutant retained ~30-35% XPG foci at 3h, while the $XPG^{\Delta UBM}$, $XPG^{\Delta PIP-N}$, and $XPG^{\Delta UBM\Delta PIP-N}$ mutants retained 10-15% XPG foci levels at the same time point (Figures 23 and 24).

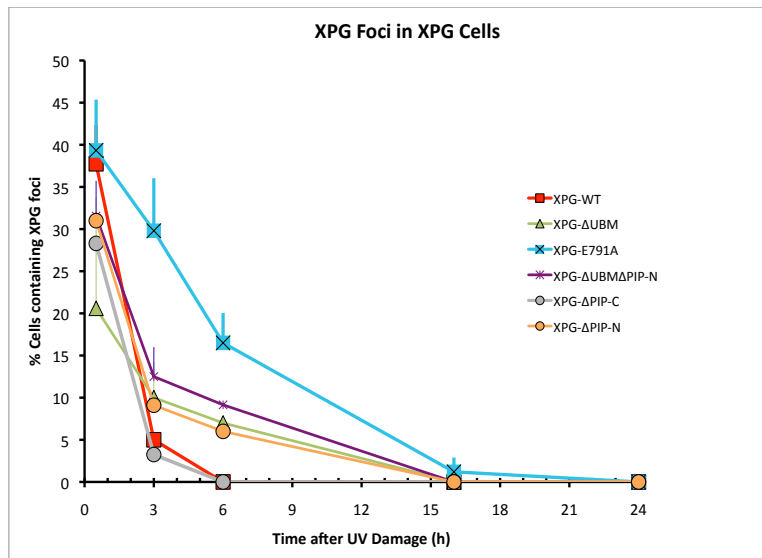


Figure 23: XPG remains associated with damaged regions for longer periods in the E791A, UBM and PIP-N mutants than the wildtype. XP-G deficient cells and those transduced with either wild-type or mutant XPG were UV-irradiated, returned to culture, and fixed and stained for the HA-tag on XPG constructs and (6-4)PP at the indicated times following irradiation. A graphical representation of the cells with persistent XPG foci at different time-points after irradiation. Compare XPG-WT to the E791A, Δ UBM, and Δ PIP-N mutants at 3h and 6h after UV irradiation. XPG does not appear to persist until 16h and 24h in any of the mutants in the conditions tested.

Likewise, at 6h following UV, whereas the XPG^{WT} and $XPG^{\Delta PIP-C}$ were no longer visible at LUDs, XPG^{E791A} , $XPG^{\Delta PIP-N}$, $XPG^{\Delta UBM}$, and $XPG^{\Delta UBM\Delta PIP-N}$ were found at LUDs in 20, 10, 6, ~6% of the cells (Figure 23). At the later time-points of 16h and 24h, no XPG was visible at LUDs in any of the cell-lines used in our experiments, which was surprising as XPG-E791A mutants have previously been shown to exhibit the maintenance of XPG foci even up until 24h after UV irradiation [46]. Figure 24 shows images of XPG foci co-localized with (6-4)PP in the different cell-lines at 0.5h and 3h following UV irradiation.

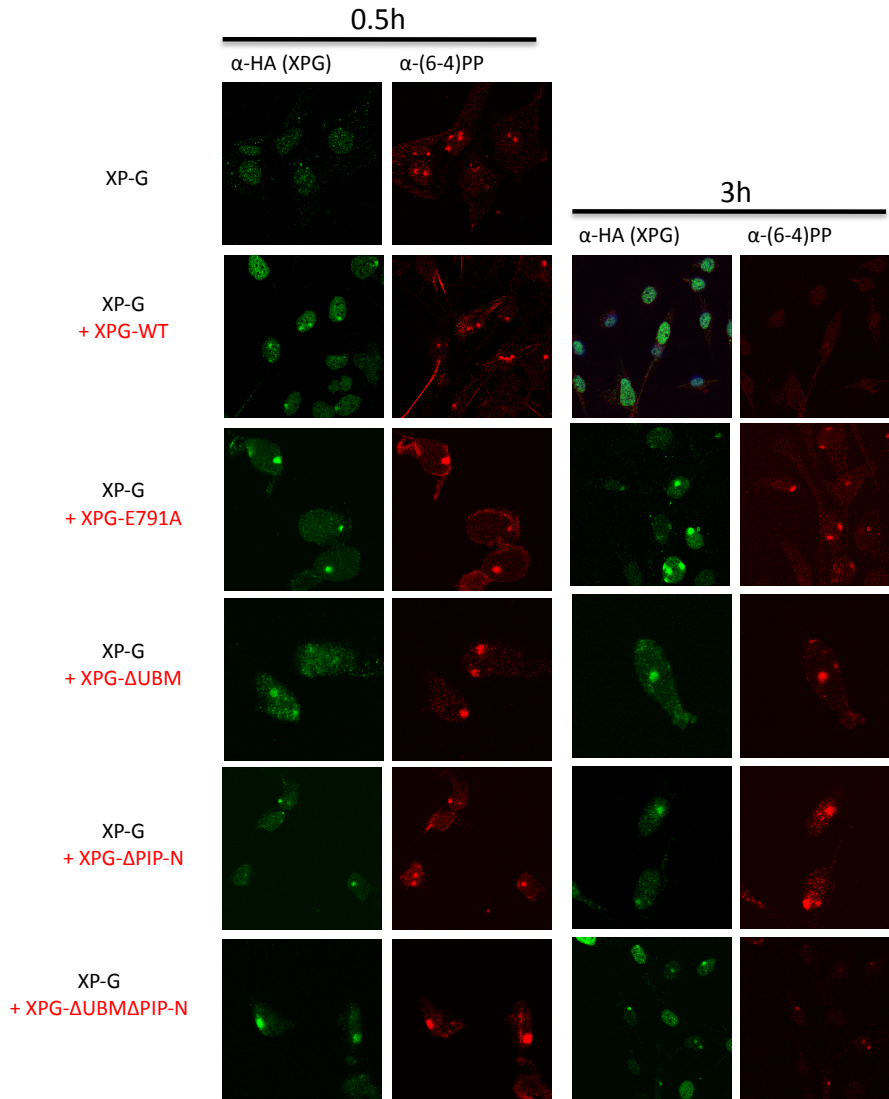


Figure 24: IF images of cells showing co-localization of XPG with (6-4)PP foci at 0.5h and 3h after UV irradiation. XP-G deficient cells and those transduced with either wild-type or mutant XPG were UV-irradiated as described, returned to culture, and fixed and stained for the HA-tag on XPG constructs (green) and (6-4)PP (red) at the indicated times following irradiation. These are images of the cells at 0.5h and 3h after UV showing XPG foci (green) and (6-4)PP foci (red).

The association and dissociation of the damage recognition factor XPC-RAD23B with (6-4)PPs is not affected by mutations in XPG.

The damage recognition factor XPC-RAD23B is ubiquitylated in NER by the UVDDDB/CUL4A/RBX1 complex [143-146], and has been shown to depart from NER complexes upon, or possibly as a consequence of XPG arrival (Figures 2B-2C) [30-32]. This raised the possibility that the UBM domain in XPG is actually important for interacting with ubiquitylated XPC and facilitating the exchange of XPG with XPC in NER complexes. To address this issue, we probed for XPC-RAD23B in our assays using an antibody specific to XPC at various time-points following UV irradiation (Figure 25). We observed rapid accumulation of XPC at 0.5h, with >35%-50% XPC foci present in all cell-lines. While XPC persisted in XPG-deficient cells, it quickly disengaged in XPG^{WT} and all the mutants tested to ~20% and 2-10% at 1h and 3h, respectively (Figure 25). At the later time-points of 16h and 24h there were no XPC foci visible in any of the transduced cells, whereas XPG deficient cells maintained 20% and >10% foci respectively. These results strongly indicate that the UBM in XPG does not interact with ubiquitylated XPC, nor does it facilitate the exchange of XPG with XPC on the DNA (for images of XPC and ERCC1 colocalized in cells at all time-points analyzed see Figures 32-36 in the Appendix).

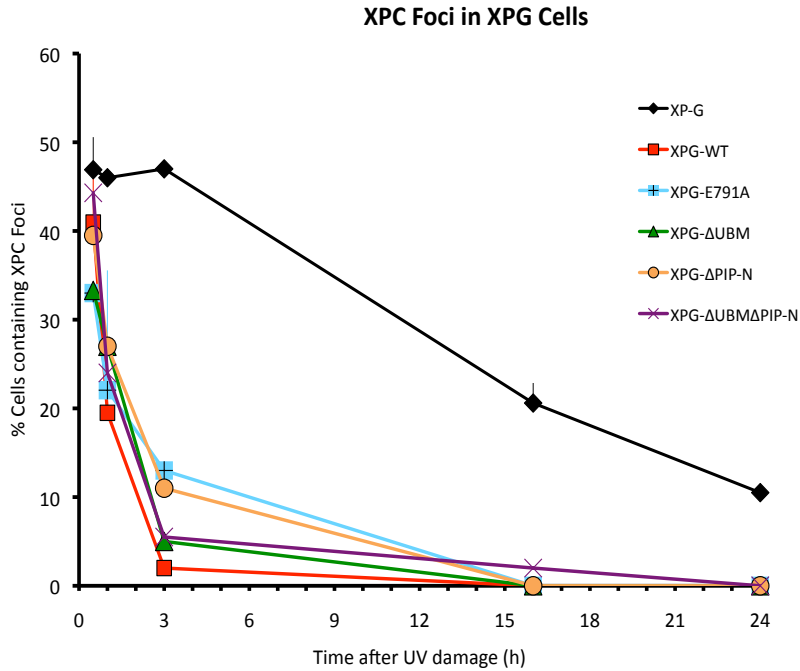


Figure 25: The damage recognition factor XPC-RAD23B behaves with similar kinetics in XPG-WT and all mutants tested. XP-G deficient cells (XPCS1RO) and those transduced with either wild-type or mutant XPG were UV-irradiated, returned to culture, and fixed and stained for XPC (red) and ERCC1 (green) at the indicated times following irradiation. The graph represents the percentage of cells containing XPC foci at the different time-points following UV irradiation. XPC foci are mostly gone from damage regions by 3h in XPG-WT and all mutants, whereas they persist in XP-G cells until 24h.

Discussion

An important unresolved issue in NER has been how the dual incision and repair synthesis steps are coordinated. XPG has long been suggested to play a role in this coordination, particularly because of known interaction with PCNA via its C-terminal PIP domain. To address this question further we have used local UV irradiation coupled with immunofluorescence to analyze XPG mutants impaired in nuclease activity, PCNA-binding via the PIP-C and PIP-N domains, and in ubiquitin-binding. The present study provides insights into how these XPG domains may regulate the transition from dual incision to repair synthesis, and suggest a mechanism by which a few subtle interactions between XPG, PCNA and ubiquitin could stabilize the NER complex and allow tight regulation of incisions.

Damage Removal

We examined the removal of (6-4)PP lesions in all the mutants and observed that the E791A, UBM, and PIP-N mutants are all impaired in damage removal although to different degrees (Figure 18). As expected, and as observed previously, the E791A mutant was significantly impaired in damage removal, however we were surprised to observe that the UBM mutant showed similar levels of impairment, although it appeared to function normally in *in vitro* repair assays. We also observed a weaker yet significant impairment in damage repair by the PIP-N mutant. The

difference in the *in vitro* versus *in vivo* repair ability of the UBM mutant can be attributed to a tendency for reactions to unnaturally go to completion *in vitro*, whereas *in vivo* certain conditions need to be met for the same reactions to occur. We have previously shown that the dual incisions in NER could be ordered with XPF first making the 5' incision, allowing initiation of repair synthesis, prior to the 3' incision by XPG [33]. If the ordered incisions were to take place *in vivo* as a mode of tighter regulation of the transition for incision to repair synthesis, then one could hypothesize that the interaction between XPG and PCNA could serve as a signal for XPG to make the 3' incision. These findings allow us to speculate that in certain instances, if the normal NER reaction is impaired from reaching completion, either due to structural DNA perturbations, or some other form of obstruction, the 5' cut could take place allowing initiation of repair synthesis, but leading to stalling of PCNA and the replication machinery. During replication, stalling of the replication machinery leads to ubiquitylation of PCNA which serves as a signal for the switch from replicative polymerases to TLS polymerases which are able to synthesize past the lesion, and allow replication to continue (Figure 14, left panel) [109, 147]. These take on added significance when considering the recent work of Ogi *et al.* involving the role of ubiquitylated PCNA and Polk in NER [36]. They showed that ubiquitylated PCNA along with Polk is involved in NER, and is involved in the completion of repair synthesis along with Pol δ in about 50% of the NER reactions. Therefore in NER, it is

possible that stalled PCNA becomes ubiquitylated and then interacts with XPG via its UBM, as an additional trigger to stimulate the nuclease function of the protein. One unresolved discrepancy exists between the model proposed here and the findings of Ogi *et al.* They show the ubiquitylation of PCNA regardless of whether NER reaches completion or not, observing ubiquitylated PCNA in XP cells, and suggest that ubiquitylated PCNA is loaded onto the DNA independently of NER. Regardless, it is still possible that an interaction between such ubiquitylated-PCNA and XPG serves as an additional trigger for the 3' incision. Clearly, the temporal and spatial kinetics of ubiquitylation of PCNA during NER warrant further investigation.

The PIP-N mutant shows a lower level of impaired damage removal that cannot be explained by the above phenomenon, however it is possible that the PCNA-XPG interaction, which also appears to be disrupted in this mutant is responsible for this impairment. Taken together it appears that XPG nuclease activity in NER may be regulated by its interaction with PCNA and ubiquitin.

Recruitment and Disassembly of NER Factors

We were also interested in observing the behavior of other NER factors in our different mutants following UV irradiation, and towards that end we observed the recruitment of the early damage recognition factor XPC, the dual incision factors ERCC1-XPF and XPG, and the repair

synthesis factor PCNA. Recruitment of all above factors proceeded normally in all our mutants, with presence detected at 0.5h. We were particularly interested in departure of XPC from damage regions, as XPC is also ubiquitylated during NER and it was a necessary question to consider whether the UBM in XPG actually interacts with ubiquitylated XPC rather than PCNA. We observed that unlike in the XP-G cells, XPC had mostly departed from LUDs within 3h in all our mutants, similar to its behavior in wildtype cells. The XPG-UBM mutant did not alter the XPC kinetics within the damage regions, showing that displacement of XPC by XPG was normal in these mutants (Figure 25). Importantly XPC departure was the same in XPG-E791A mutant, showing that the incision by XPG is not necessary for the departure of XPC from the damaged DNA, consistent with earlier *in vitro* experiments [32].

The dual incision factors behaved differently, and in some ways unexpectedly in our mutants. ERCC1-XPF appeared to remain bound to damage regions in XPG-E791A, and all mutants containing the Δ UBM mutation as well as in XP-G cells (Figure 22). This was unexpected, especially in XPG-E791A, as we have clearly previously demonstrated that this mutant supports 5' uncoupled incision and it seems counterintuitive that ERCC1-XPF would remain at damaged sites once PCNA has been recruited and repair synthesis initiated. Based on the expected loading of PCNA onto the free 3' OH made available following XPF incision, it is as yet unclear how both factors could remain stably

associated with the DNA for extended periods of time. It is worth noting that there were much greater margins of error when measuring ERCC1-XPF foci at the later time-points as compared with most other factors (Figure 22). XPG also gave some unexpected results. Based on the observation that damage repair was impaired in the E791A, Δ UBM and Δ PIP mutants, we expected a delay in XPG departure from damaged regions in these cell-lines. A previous report by Thorel *et al.* using XPG-E791A cells in a similar assay showed the clear presence of XPG foci in these cells along with the TFIIH factor XPB at 24h following UV irradiation [46]. In our hands, XPG^{E791A} persisted at damage sites at 3h and 6h when compared to XPG^{WT} cells, however by the later time-points of 16h and 24h, XPG foci were no longer visible in these cells even though damage foci were clearly still present (Figures 23 and 24). Likewise, XPG ^{Δ UBM} and XPG ^{Δ PIP-N} were present at LUDs at 3h and 6h although at lower levels than XPG^{E791A}. This discrepancy in XPG behavior in our mutants, especially as relates to the XPG^{E791A} mutant, could possibly be ascribed to the method used for detecting XPG in our assays. We detected XPG using an antibody specific to the C-terminal HA tag, rather than an XPG-specific antibody, as the HA antibody produced better, reproducible results. It is possible that the signal visible from the HA antibody is lost over time. Alternatively, a study by Essers *et al.* observing the behavior of a ubiquitylation mutant of PCNA, revealed that the residence time of this mutant (which is unable to participate in TLS) at UV damaged regions was

significantly shorter than that of wildtype PCNA [126]. Interestingly the GFP-hPCNA^{K164R} mutant had kinetics similar to wildtype PCNA in DNA replication foci. It is therefore possible that we are observing a similar phenomenon in our mutants, in that the XPG protein, although impaired in its function in NER, does not remain attached to the damaged regions. Although PCNA remains attached to the DNA, it is possible that the interaction between such ubiquitylated PCNA and XPG is necessary for the completion of dual incision, and PCNA is delayed at the DNA while XPG eventually dissociates after a slight delay (Figure 23). Furthermore, recent studies have reported a connection between NER and damage signaling. Studies by Marteijn *et al.* showed activation of ATR signaling following NER, with later recruitment of DSB repair factors 53BP1 and BRCA1 to LUD regions [148]. Subsequently it was shown that ssDNA intermediates generated by NER are processed by Exo1 endonuclease, generating much larger single-stranded regions, which then trigger the damage response [111]. The absence of XPG at damage regions at later time points could be due to its displacement by other factors resulting from damage signaling.

The transition from dual incision to repair synthesis

XPG has long been suggested to play additional roles in NER other than just performing the 3' incision [6]. The observation that XPG binds PCNA via a PIP domain in XPG [55], along with the delayed residence time of XPG at sites of incised DNA [32] encouraged the idea of XPG

involvement in coordinating the transition from dual incision to repair synthesis. This hypothesis is corroborated by recent observations by Mocquet *et al.* that the presence of XPG along with RPA at the damaged DNA is necessary for initiation of repair synthesis [104], as well as our findings that the XPG-E791A mutant supports uncoupled 5' incision, recruitment of replication factors, and partial repair synthesis (Chapter 2 and [33]). The observed function of ubiquitylated PCNA in NER [36] and the presence of a UBM in XPG [110] necessitated the next question of whether an interaction of XPG with ubiquitylated PCNA during NER is important for its role for the transition from dual incision to repair synthesis. This work shows that the UBM domain of XPG is indeed important for its role in NER, and suggests that this function is mediated by an interaction between XPG and ubiquitylated PCNA. The Δ UBM mutant, although impaired in repair, supports recruitment of all NER factors tested for, and like XPG-E791A, maintains the delay of PCNA at damaged regions within the cell. This impairment of PCNA signifies an inability of the complex to complete NER, and likely indicates that the replication machinery is blocked by the presence of XPG. Alternatively, PCNA ubiquitylation could be a mechanism that comes into play when repair synthesis is impaired, possibly due to irregularities in the DNA or other problems, and in this case, would be the alternative method for stimulating XPG activity.

The normal departure of the earlier factor XPC strongly suggests that the earlier steps in NER occur with normal dynamics. A new putative PIP domain in XPG (PIP-N) also impaired damage removal and XPG^{ΔPIP-N} mutant did not allow stable recruitment of PCNA to damage regions, either at early or late time-points following UV damage. Although the PIP-N is non-canonical (Figure 16B), it appears to be important for NER function of XPG, and other factors possess non-canonical PIPs, such as chromatin assembly factor 1 (CAF-1), which contains two distinct PIPs that differ in the strength of their interaction with PCNA, yet contribute to CAF-1 function in replication [142].

It appears that the relationship between XPG and PCNA is an important and dynamic one, possibly mediated by several, subtle interactions that have different roles with regards to recruitment of PCNA and its eventual departure from NER regions. Although a lot remains to be understood about the process, the work described here highlights the intricacy of the mechanism that drives NER from damage removal to repair synthesis.

Materials and Methods

Cell Culture Conditions

SV40-transformed XPG deficient human fibroblast cells XPCS1RO [136] were cultured in Dulbecco's Modified Eagle's Medium (DMEM) supplemented with 10% fetal bovine serum, 2mM L-glutamine, 100 U/ml penicillin, and 0.1 mg/ml streptomycin at 37°C in the presence of 5% CO₂.

Lentiviral Cell Transduction

The cDNA of XPG wildtype, XPG-E791A, XPG-UBM, XPG-PIP-N, XPG-PIP-C, XPG-UBMPIP-N, and XPG-UBMPIP-C were cloned into the pWPXL lentiviral vector with a C-terminal his₆HA tag using *Xma*I and *Mlu*I restriction sites and thereby replacing the GFP cDNA. Each lentiviral construct was co-transfected into 293T cells along with the packaging plasmid psPAX2, and the envelope plasmid pMD2G. Production of high titer viruses was achieved as described on the LentiWeb website <http://lentiweb.com/>. SV40 immortalized XP-G/CS (94RD27, patient XPCS1RO) fibroblasts [136] at 50% confluency were infected with the recombinant XPG viral particles to generate stably transduced XPG-mutant cell-lines. The transduced cells were maintained in cell culture as described above. Transduction efficiency was assessed by immunofluorescence.

Local UV Irradiation and Immunofluorescence

Cells were seeded and cultured on glass coverslips and processed as described previously [57]. Cells were briefly covered with a polycarbonate filter containing 5 μm pores (Millipore) and irradiated at 150 J/m^2 using a UV-C lamp (EL series, UVP, model UVLS-28). Following UV-irradiation cells were returned to culture for appropriate recovery times. Subsequently, cells were washed with PBS, then with PBS containing 0.05% Triton X-100 prior to fixation with 3% paraformaldehyde in PBS containing 0.1% Triton X-100 for 15 min. (for PCNA staining, upon recovery from UV irradiation cells were washed with PBS, and immediately fixed in ice-cold methanol at 4°C for 15 min). Then the cells were permeabilized by washing 5 times with PBS containing 0.1%-0.2% Triton X-100. To detect (6-4)PP, cells were treated with 0.07M NaOH for 5 min to denature the DNA, and the cells were again washed 5 times with PBS + 0.1% Triton X100. Cells were blocked in PBS+ (PBS containing 0.15% glycine and 0.5% bovine serum albumin) for a minimum of 30 min and then incubated with primary antibody diluted in PBS+ at room temperature in dark, humid conditions for 2 h. Subsequently the cells were washed 5 times with PBS + 0.1% Triton, washed briefly with PBS+, and incubated with secondary antibody diluted in PBS+ at room temperature in dark, humid conditions for 1 h. The cells were washed 5 times in PBS + 0.1% Triton X-100, and once in PBS, and finally the coverslips were mounted on vectashield mounting medium (Vector Laboratories)

containing 4'-6'diamino-2-phenylindole (DAPI) at a concentration of 0.1 mg/ml.

For quantification, at least 100 cells were counted in different fields per experiment, and three independent experiments were performed to generate standard error.

Primary antibodies used are as follows: to detect XPG, mouse monoclonal anti-XPG [8H7] (abcam, ab46), 1:2000, or rabbit polyclonal anti-HA (abcam, ab91110), 1:2000; to detect PCNA, mouse monoclonal anti-PCNA (DakoCytomation, clone PC10), 1:1000; to detect XPC, mouse monoclonal anti-XPC (abcam, ab6264), 1:1000; to detect ERCC1, rabbit polyclonal anti-ERCC1 (Santa Cruz, sc-10785), 1:100; and to detect (6-4)PPs, mouse monoclonal anti-(6-4)PPs (Cosmo Bio, clone 64M-2), 1:400.

Confocal Microscopy

Confocal images of the cells were captured using a Zeiss LSM 510 microscope equipped with a 25 mW Ar laser at 488 nm, a He/Ne 543 nm laser, and a 40 × 1.3 NA oil immersion lens. Alexa 488 was detected using a dichroic beam splitter (HFT 488), and an additional 505- to 530-nm bandpass emission filter. Cy3 was detected using a dichroic beam splitter (HFT 488/543) and a 560- to 615-nm bandpass emission filter.

Western Blotting

Western blotting was performed as described in [109].

Protein Expression and Purification

Wild-type XPG, XPG Δ UBM^{LP-AA}, and XPG Δ UBM^{Domain} proteins were expressed in Sf9 cells and purified as described previously [51]. Typically 0.2-0.5 mg of protein was obtained at concentrations of 0.2-0.3 mg/ml.

Acknowledgements

Marzena Bienko in the laboratory of Dr. Ivan Dikic performed the experiment described in Figure 17 and Lidija Staresincic purified the proteins used in the same experiment.

Conclusions
And
Future Directions

The aim of this thesis was to explore the role of the 3' structure-specific endonuclease XPG in regulating the late steps of NER. To this end we first investigated the *in vitro* and *in vivo* function of the nuclease dead mutant XPG-E791A. We describe in Chapter 2 how this mutant is able to support uncoupled 5' incision and partial repair synthesis. XPG-E791A enables recruitment of the replication machinery, which is not recruited in the absence of XPG protein. The corresponding structure-specific endonuclease that makes the 5' cut in NER, ERCC1-XPF, was also tested in a similar manner in our assays. The nuclease dead ERCC1-XPF-D676A was unable to support any incision (5' or 3'), and did not allow any recruitment of downstream replicative factors [33]. These findings strongly suggest that the XPF incision occurs first and that XPG has a special role in coordinating the transition from dual incision to repair synthesis.

An interaction between XPG and the sliding clamp PCNA had previously been shown [55], and we were interested in testing whether the interaction of these two proteins was important for the late steps of NER. The discovery of a UBM (ubiquitin-binding domain) in XPG [110], coupled with the recent report indicating that ubiquitylated PCNA functions during NER [36] encouraged us to study the function of this UBM in NER. We also discovered a second putative PIP domain in XPG and considered whether there was some cooperation (or alternatively redundancy)

between two or more of these domains in mediating the XPG-PCNA interaction. Such synergistic relationships have been shown with relation to the PIPs and UBMs in the TLS polymerases [109], or the two PIPs in proteins such as CAF-1 [142]. To this end we generated mutant XPG cell-lines stably expressing mutations of either of these three domains alone or in combinations. We tested these cells along with XP-G deficient, XPG-WT, and the nuclease dead XPG-E791A cell-lines in immunofluorescence assays [57]. We generated local damage to the DNA in the cells by UV irradiation, and observed the kinetics of removal of damage, and of the recruitment and disassembly of several NER factors, to give us a better understanding of how these mutations affect various stages of the NER process. We observed that the E791A, UBM, and PIP-N mutants all exhibited impaired damage removal while the PIP-C mutant, like XPG-WT cells, did not. We also observed that the mutants behaved differently with regards to the kinetics of PCNA. The UBM and E791A mutant cells allowed normal recruitment of PCNA, but did not permit its normal disassembly and subsequent recycling, whereas the PIP-N mutants did not support the stable association of PCNA to damage regions.

The conclusions from our findings are that the XPG-PCNA interaction is indeed important for the smooth transition from dual incision to repair synthesis. It appears that XPG mediates the interaction by at least two different domains with differing affinities for PCNA, and possibly also interacts with the modified version of the protein by interacting with

ubiquitin on its surface. A closer look at these mutations by *in vitro* methods would give a good understanding of their role. The different mutants will be tested in pull-down assays utilizing PCNA and ubiquitylated PCNA to test how they affect the PCNA-XPG interaction directly. They will also be tested in *in vitro* repair synthesis assays to detect whether any repair synthesis is initiated as was seen with XPG-E791A. Such a finding would reiterate the idea that at least in certain conditions, the 5' incision occurs prior to the 3' incision, and, as we have observed in our immunofluorescence assays, that the UBM mutant behaves in a manner similar to XPG-E791A.

A closer examination of the role of ubiquitylated PCNA in the later steps of NER would be of importance. It would be relevant to detect NER-dependent ubiquitylation of PCNA possibly by UV irradiation followed by western blotting to detect modified and unmodified versions of PCNA. PCNA is typically ubiquitylated on its K164 residue by the Rad6-Rad18 E3 ubiquitin ligase [147, 149, 150].

Recent reports have linked NER to ATM and ATR signaling, an important finding as no such connection was previously known. One such study showed that single-stranded intermediates generated during NER (products of incision, particularly upon inhibition repair synthesis) led to recruitment of RPA, which in turn resulted in ATR activation [151]. Subsequently a different study showed that damage-signaling factors such as RNF8, MDC1, and 53BP1, which are typically active during DSB repair

were also activated in an NER-dependent fashion [148]. It has been shown, at least in *S. cerevisiae*, that the Exo1 nuclease, which has been shown to function in MMR and homologous recombination, processes NER intermediates to generate longer ssDNA regions that activate downstream signaling [111]. Some of the mutants described in this thesis would be relevant for testing this hitherto unresolved connection between the different damage pathways. The XPG-E791A mutant would be an interesting model for testing the possible up-regulation of Exo1, or RNF8, as 5' uncoupled incision would mimic inhibition of repair synthesis. The UBM and PIP-N mutants would also be of interest with this regard.

In conclusion, the findings described in this thesis add to the understanding of NER, particularly in how the late steps of the pathway proceed. It would be beneficial to further explore the dynamics of the interactions described here and possibly link the previously parallel damage repair responses, NER and damage signaling, more clearly.

References

1. Lindahl, T., *Instability and decay of the primary structure of DNA*. Nature, 1993. **362**(6422): p. 709-15.
2. Cadet, J., M. Berger, T. Douki, and J.L. Ravanat, *Oxidative damage to DNA: formation, measurement, and biological significance*. Rev Physiol Biochem Pharmacol, 1997. **131**: p. 1-87.
3. Hoeijmakers, J.H., *Genome maintenance mechanisms for preventing cancer*. Nature, 2001. **411**(6835): p. 366-74.
4. Scharer, O.D., *Chemistry and biology of DNA repair*. Angew Chem Int Ed Engl, 2003. **42**(26): p. 2946-74.
5. Lindahl, T. and R.D. Wood, *Quality control by DNA repair*. Science, 1999. **286**(5446): p. 1897-905.
6. Gillet, L.C. and O.D. Scharer, *Molecular mechanisms of mammalian global genome nucleotide excision repair*. Chem Rev, 2006. **106**(2): p. 253-76.
7. Friedberg, E.C., G.C. Walker, W. Siede, R.D. Wood, R.A. Schultz, and T. Ellenberger, *DNA Repair and Mutagenesis*. 2nd edition ed2005, Washington DC: ASM Press.
8. Lehmann, A.R., *DNA repair-deficient diseases, xeroderma pigmentosum, Cockayne syndrome and trichothiodystrophy*. Biochimie, 2003. **85**(11): p. 1101-11.
9. Nospikel, T., *Nucleotide excision repair and neurological diseases*. DNA Repair (Amst), 2008. **7**(7): p. 1155-67.
10. *Xeroderma Pigmentosum*. Genetic People Website 2011; Available from: <http://geneticpeople.com/?p==1806>.
11. *Xeroderma Pigmentosum*. Holding on to Hope Website 2011; Available from: <http://dream92.tripod.com/hope/id9.html>.
12. de Laat, W.L., N.G. Jaspers, and J.H. Hoeijmakers, *Molecular mechanism of nucleotide excision repair*. Genes Dev, 1999. **13**(7): p. 768-85.
13. Hanawalt, P.C. and G. Spivak, *Transcription-coupled DNA repair: two decades of progress and surprises*. Nat Rev Mol Cell Biol, 2008. **9**(12): p. 958-70.

14. Min, J.H. and N.P. Pavletich, *Recognition of DNA damage by the Rad4 nucleotide excision repair protein*. Nature, 2007. **449**(7162): p. 570-5.
15. Scharer, O.D., *Achieving broad substrate specificity in damage recognition by binding accessible nondamaged DNA*. Mol Cell, 2007. **28**(2): p. 184-6.
16. Maillard, O., S. Solyom, and H. Naegeli, *An aromatic sensor with aversion to damaged strands confers versatility to DNA repair*. PLoS Biol, 2007. **5**(4): p. e79.
17. Coin, F., V. Oksenysh, and J.M. Egly, *Distinct Roles for the XPB/p52 and XPD/p44 Subcomplexes of TFIIH in Damaged DNA Opening during Nucleotide Excision Repair*. Mol Cell, 2007. **26**(2): p. 245-56.
18. Sugasawa, K., J. Akagi, R. Nishi, S. Iwai, and F. Hanaoka, *Two-step recognition of DNA damage for mammalian nucleotide excision repair: Directional binding of the XPC complex and DNA strand scanning*. Mol Cell, 2009. **36**(4): p. 642-53.
19. Mathieu, N., N. Kaczmarek, and H. Naegeli, *Strand- and site-specific DNA lesion demarcation by the xeroderma pigmentosum group D helicase*. Proc Natl Acad Sci U S A, 2010. **107**(41): p. 17545-50.
20. Evans, E., J. Fellows, A. Coffey, and R.D. Wood, *Open complex formation around a lesion during nucleotide excision repair provides a structure for cleavage by human XPG protein*. Embo J, 1997. **16**(3): p. 625-38.
21. Tapias, A., J. Auriol, D. Forget, J.H. Enzlin, O.D. Scharer, F. Coin, . . . J.M. Egly, *Ordered conformational changes in damaged DNA induced by nucleotide excision repair factors*. J Biol Chem, 2004. **279**(18): p. 19074-83.
22. Missura, M., T. Buterin, R. Hindges, U. Hubscher, J. Kasparkova, V. Brabec, and H. Naegeli, *Double-check probing of DNA bending and unwinding by XPA-RPA: an architectural function in DNA repair*. Embo J, 2001. **20**(13): p. 3554-64.
23. Camenisch, U., R. Dip, S.B. Schumacher, B. Schuler, and H. Naegeli, *Recognition of helical kinks by xeroderma pigmentosum group A protein triggers DNA excision repair*. Nat Struct Mol Biol, 2006. **13**(3): p. 278-84.

24. Matsuda, T., M. Saijo, I. Kuraoka, T. Kobayashi, Y. Nakatsu, A. Nagai, . . . et al., *DNA repair protein XPA binds replication protein A (RPA)*. J Biol Chem, 1995. **270**(8): p. 4152-7.
25. Li, R.Y., P. Calsou, C.J. Jones, and B. Salles, *Interactions of the transcription/DNA repair factor TFIIH and XP repair proteins with DNA lesions in a cell-free repair assay*. J Mol Biol, 1998. **281**(2): p. 211-8.
26. Park, C.H., D. Mu, J.T. Reardon, and A. Sancar, *The general transcription-repair factor TFIIH is recruited to the excision repair complex by the XPA protein independent of the TFIIIE transcription factor*. J Biol Chem, 1995. **270**(9): p. 4896-902.
27. Li, L., S.J. Elledge, C.A. Peterson, E.S. Bales, and R.J. Legerski, *Specific association between the human DNA repair proteins XPA and ERCC1*. Proc Natl Acad Sci U S A, 1994. **91**(11): p. 5012-6.
28. Tsodikov, O.V., D. Ivanov, B. Orelli, L. Staresincic, I. Shoshani, R. Oberman, . . . T. Ellenberger, *Structural basis for the recruitment of ERCC1-XPF to nucleotide excision repair complexes by XPA*. Embo J, 2007. **26**(22): p. 4768-76.
29. Wold, M.S., *Replication protein A: a heterotrimeric, single-stranded DNA-binding protein required for eukaryotic DNA metabolism*. Annu Rev Biochem, 1997. **66**: p. 61-92.
30. Wakasugi, M. and A. Sancar, *Assembly, subunit composition, and footprint of human DNA repair excision nuclease*. Proc Natl Acad Sci U S A, 1998. **95**(12): p. 6669-74.
31. Araujo, S.J., E.A. Nigg, and R.D. Wood, *Strong functional interactions of TFIIH with XPC and XPG in human DNA nucleotide excision repair, without a preassembled repairosome*. Mol Cell Biol, 2001. **21**(7): p. 2281-91.
32. Riedl, T., F. Hanaoka, and J.M. Egly, *The comings and goings of nucleotide excision repair factors on damaged DNA*. Embo J, 2003. **22**(19): p. 5293-303.
33. Staresincic, L., A.F. Fagbemi, J.H. Enzlin, A.M. Gourdin, N. Wijgers, I. Dunand-Sauthier, . . . O.D. Scharer, *Coordination of dual incision and repair synthesis in human nucleotide excision repair*. Embo J, 2009.
34. Evans, E., J.G. Moggs, J.R. Hwang, J.M. Egly, and R.D. Wood, *Mechanism of open complex and dual incision formation by human*

- nucleotide excision repair factors*. *Embo J*, 1997. **16**(21): p. 6559-73.
35. Orelli, B., T.B. McClendon, O.V. Tsodikov, T. Ellenberger, L.J. Niedernhofer, and O.D. Scharer, *The XPA-binding domain of ERCC1 is required for nucleotide excision repair but not other DNA repair pathways*. *J Biol Chem*, 2010. **285**(6): p. 3705-12.
 36. Ogi, T., S. Limsirichaikul, R.M. Overmeer, M. Volker, K. Takenaka, R. Cloney, . . . A.R. Lehmann, *Three DNA polymerases, recruited by different mechanisms, carry out NER repair synthesis in human cells*. *Mol Cell*, 2010. **37**(5): p. 714-27.
 37. Moser, J., H. Kool, I. Giakzidis, K. Caldecott, L.H. Mullenders, and M.I. Fousteri, *Sealing of chromosomal DNA nicks during nucleotide excision repair requires XRCC1 and DNA ligase III alpha in a cell-cycle-specific manner*. *Mol Cell*, 2007. **27**(2): p. 311-23.
 38. Mueser, T.C., N.G. Nossal, and C.C. Hyde, *Structure of bacteriophage T4 RNase H, a 5' to 3' RNA-DNA and DNA-DNA exonuclease with sequence similarity to the RAD2 family of eukaryotic proteins*. *Cell*, 1996. **85**(7): p. 1101-12.
 39. Ceska, T.A., J.R. Sayers, G. Stier, and D. Suck, *A helical arch allowing single-stranded DNA to thread through T5 5'-exonuclease*. *Nature*, 1996. **382**(6586): p. 90-3.
 40. Hwang, K.Y., K. Baek, H.Y. Kim, and Y. Cho, *The crystal structure of flap endonuclease-1 from Methanococcus jannaschii*. *Nat Struct Biol*, 1998. **5**(8): p. 707-13.
 41. Hosfield, D.J., D.S. Daniels, C.D. Mol, C.D. Putnam, S.S. Parikh, and J.A. Tainer, *DNA damage recognition and repair pathway coordination revealed by the structural biochemistry of DNA repair enzymes*. *Prog Nucleic Acid Res Mol Biol*, 2001. **68**: p. 315-47.
 42. Constantinou, A., D. Gunz, E. Evans, P. Lalle, P.A. Bates, R.D. Wood, and S.G. Clarkson, *Conserved residues of human XPG protein important for nuclease activity and function in nucleotide excision repair*. *J Biol Chem*, 1999. **274**(9): p. 5637-48.
 43. Wakasugi, M., J.T. Reardon, and A. Sancar, *The non-catalytic function of XPG protein during dual incision in human nucleotide excision repair*. *J Biol Chem*, 1997. **272**(25): p. 16030-4.
 44. Scherly, D., T. Nospikel, J. Corlet, C. Ucla, A. Bairoch, and S.G. Clarkson, *Complementation of the DNA repair defect in xeroderma*

- pigmentosum* group G cells by a human cDNA related to yeast RAD2. *Nature*, 1993. **363**(6425): p. 182-5.
45. Iyer, N., M.S. Reagan, K.J. Wu, B. Canagarajah, and E.C. Friedberg, *Interactions involving the human RNA polymerase II transcription/nucleotide excision repair complex TFIIH, the nucleotide excision repair protein XPG, and Cockayne syndrome group B (CSB) protein*. *Biochemistry*, 1996. **35**(7): p. 2157-67.
 46. Thorel, F., A. Constantinou, I. Dunand-Sauthier, T. Nospikel, P. Lalle, A. Raams, . . . S.G. Clarkson, *Definition of a short region of XPG necessary for TFIIH interaction and stable recruitment to sites of UV damage*. *Mol Cell Biol*, 2004. **24**(24): p. 10670-80.
 47. He, Z., L.A. Henricksen, M.S. Wold, and C.J. Ingles, *RPA involvement in the damage-recognition and incision steps of nucleotide excision repair*. *Nature*, 1995. **374**(6522): p. 566-9.
 48. Dunand-Sauthier, I., M. Hohl, F. Thorel, P. Jaquier-Gubler, S.G. Clarkson, and O.D. Scharer, *The spacer region of XPG mediates recruitment to nucleotide excision repair complexes and determines substrate specificity*. *J Biol Chem*, 2005. **280**(8): p. 7030-7.
 49. Kim, C.Y., M.S. Park, and R.B. Dyer, *Human flap endonuclease-1: conformational change upon binding to the flap DNA substrate and location of the Mg²⁺ binding site*. *Biochemistry*, 2001. **40**(10): p. 3208-14.
 50. Storici, F., G. Henneke, E. Ferrari, D.A. Gordenin, U. Hubscher, and M.A. Resnick, *The flexible loop of human FEN1 endonuclease is required for flap cleavage during DNA replication and repair*. *Embo J*, 2002. **21**(21): p. 5930-42.
 51. Hohl, M., F. Thorel, S.G. Clarkson, and O.D. Scharer, *Structural determinants for substrate binding and catalysis by the structure-specific endonuclease XPG*. *J Biol Chem*, 2003. **278**(21): p. 19500-8.
 52. Hohl, M., I. Dunand-Sauthier, L. Staresincic, P. Jaquier-Gubler, F. Thorel, M. Modesti, . . . O.D. Scharer, *Domain swapping between FEN-1 and XPG defines regions in XPG that mediate nucleotide excision repair activity and substrate specificity*. *Nucleic Acids Res*, 2007. **35**(9): p. 3053-63.
 53. Sarker, A.H., S.E. Tsutakawa, S. Kostek, C. Ng, D.S. Shin, M. Peris, . . . P.K. Cooper, *Recognition of RNA polymerase II and transcription bubbles by XPG, CSB, and TFIIH: insights for*

- transcription-coupled repair and Cockayne Syndrome*. Mol Cell, 2005. **20**(2): p. 187-98.
54. Matsunaga, T., C.H. Park, T. Bessho, D. Mu, and A. Sancar, *Replication protein A confers structure-specific endonuclease activities to the XPF-ERCC1 and XPG subunits of human DNA repair excision nuclease*. J Biol Chem, 1996. **271**(19): p. 11047-50.
 55. Gary, R., D.L. Ludwig, H.L. Cornelius, M.A. MacInnes, and M.S. Park, *The DNA repair endonuclease XPG binds to proliferating cell nuclear antigen (PCNA) and shares sequence elements with the PCNA-binding regions of FEN-1 and cyclin-dependent kinase inhibitor p21*. J Biol Chem, 1997. **272**(39): p. 24522-9.
 56. Zotter, A., M.S. Luijsterburg, D.O. Warmerdam, S. Ibrahim, A. Nigg, W.A. van Cappellen, . . . A.B. Houtsmuller, *Recruitment of the nucleotide excision repair endonuclease XPG to sites of UV-induced dna damage depends on functional TFIIH*. Mol Cell Biol, 2006. **26**(23): p. 8868-79.
 57. Volker, M., M.J. Mone, P. Karmakar, A. van Hoffen, W. Schul, W. Vermeulen, . . . L.H. Mullenders, *Sequential assembly of the nucleotide excision repair factors in vivo*. Mol Cell, 2001. **8**(1): p. 213-24.
 58. Nospikel, T., P. Lalle, S.A. Leadon, P.K. Cooper, and S.G. Clarkson, *A common mutational pattern in Cockayne syndrome patients from xeroderma pigmentosum group G: implications for a second XPG function*. Proc Natl Acad Sci U S A, 1997. **94**(7): p. 3116-21.
 59. Scharer, O.D., *XPG: its products and biological roles*. Adv Exp Med Biol, 2008. **637**: p. 83-92.
 60. Ito, S., I. Kuraoka, P. Chymkowitch, E. Compe, A. Takedachi, C. Ishigami, . . . K. Tanaka, *XPG Stabilizes TFIIH, Allowing Transactivation of Nuclear Receptors: Implications for Cockayne Syndrome in XP-G/CS Patients*. Mol Cell, 2007. **26**(2): p. 231-43.
 61. Scharer, O.D., *Hot topics in DNA repair: the molecular basis for different disease states caused by mutations in TFIIH and XPG*. DNA Repair (Amst), 2008. **7**(2): p. 339-44.
 62. Lee, S.K., S.L. Yu, L. Prakash, and S. Prakash, *Requirement of yeast RAD2, a homolog of human XPG gene, for efficient RNA polymerase II transcription. implications for Cockayne syndrome*. Cell, 2002. **109**(7): p. 823-34.

63. Fousteri, M., W. Vermeulen, A.A. van Zeeland, and L.H. Mullenders, *Cockayne syndrome A and B proteins differentially regulate recruitment of chromatin remodeling and repair factors to stalled RNA polymerase II in vivo*. Mol Cell, 2006. **23**(4): p. 471-82.
64. Laine, J.P. and J.M. Egly, *Initiation of DNA repair mediated by a stalled RNA polymerase II*. Embo J, 2006. **25**(2): p. 387-97.
65. Sarasin, A. and A. Stary, *New insights for understanding the transcription-coupled repair pathway*. DNA Repair (Amst), 2007. **6**(2): p. 265-9.
66. Klungland, A., M. Hoss, D. Gunz, A. Constantinou, S.G. Clarkson, P.W. Doetsch, . . . T. Lindahl, *Base excision repair of oxidative DNA damage activated by XPG protein*. Mol Cell, 1999. **3**(1): p. 33-42.
67. Bessho, T., *Nucleotide excision repair 3' endonuclease XPG stimulates the activity of base excision repair enzyme thymine glycol DNA glycosylase*. Nucleic Acids Res, 1999. **27**(4): p. 979-83.
68. Clarkson, S.G., *The XPG story*. Biochimie, 2003. **85**(11): p. 1113-21.
69. O'Donovan, A., A.A. Davies, J.G. Moggs, S.C. West, and R.D. Wood, *XPG endonuclease makes the 3' incision in human DNA nucleotide excision repair*. Nature, 1994. **371**(6496): p. 432-5.
70. Sijbers, A.M., W.L. de Laat, R.R. Ariza, M. Biggerstaff, Y.F. Wei, J.G. Moggs, . . . R.D. Wood, *Xeroderma pigmentosum group F caused by a defect in a structure-specific DNA repair endonuclease*. Cell, 1996. **86**(5): p. 811-22.
71. Biggerstaff, M., D.E. Szymkowski, and R.D. Wood, *Co-correction of the ERCC1, ERCC4 and xeroderma pigmentosum group F DNA repair defects in vitro*. Embo J, 1993. **12**(9): p. 3685-92.
72. van Vuuren, A.J., E. Appeldoorn, H. Odijk, A. Yasui, N.G. Jaspers, D. Bootsma, and J.H. Hoeijmakers, *Evidence for a repair enzyme complex involving ERCC1 and complementing activities of ERCC4, ERCC11 and xeroderma pigmentosum group F*. Embo J, 1993. **12**(9): p. 3693-701.
73. Westerveld, A., J.H. Hoeijmakers, M. van Duin, J. de Wit, H. Odijk, A. Pastink, . . . D. Bootsma, *Molecular cloning of a human DNA repair gene*. Nature, 1984. **310**(5976): p. 425-9.

74. Brookman, K.W., J.E. Lamerdin, M.P. Thelen, M. Hwang, J.T. Reardon, A. Sancar, . . . L.H. Thompson, *ERCC4 (XPF) encodes a human nucleotide excision repair protein with eukaryotic recombination homologs*. Mol Cell Biol, 1996. **16**(11): p. 6553-62.
75. Gaillard, P.H. and R.D. Wood, *Activity of individual ERCC1 and XPF subunits in DNA nucleotide excision repair*. Nucleic Acids Res, 2001. **29**(4): p. 872-9.
76. de Laat, W.L., E. Appeldoorn, N.G. Jaspers, and J.H. Hoeijmakers, *DNA structural elements required for ERCC1-XPF endonuclease activity*. J Biol Chem, 1998. **273**(14): p. 7835-42.
77. Tsodikov, O.V., J.H. Enzlin, O.D. Scharer, and T. Ellenberger, *Crystal structure and DNA binding functions of ERCC1, a subunit of the DNA structure-specific endonuclease XPF-ERCC1*. Proc Natl Acad Sci U S A, 2005. **102**(32): p. 11236-41.
78. Tripsianes, K., G. Folkers, E. Ab, D. Das, H. Odijk, N.G. Jaspers, . . . R. Boelens, *The structure of the human ERCC1/XPF interaction domains reveals a complementary role for the two proteins in nucleotide excision repair*. Structure, 2005. **13**(12): p. 1849-58.
79. Nishino, T., K. Komori, Y. Ishino, and K. Morikawa, *Structural and Functional Analyses of an Archaeal XPF/Rad1/Mus81 Nuclease: Asymmetric DNA Binding and Cleavage Mechanisms*. Structure (Camb), 2005. **13**(8): p. 1183-92.
80. Newman, M., J. Murray-Rust, J. Lally, J. Rudolf, A. Fadden, P.P. Knowles, . . . N.Q. McDonald, *Structure of an XPF endonuclease with and without DNA suggests a model for substrate recognition*. Embo J, 2005. **24**(5): p. 895-905.
81. Sgouros, J., P.H. Gaillard, and R.D. Wood, *A relationship between a DNA-repair/recombination nuclease family and archaeal helicases*. Trends Biochem Sci, 1999. **24**(3): p. 95-7.
82. Nishino, T., K. Komori, D. Tsuchiya, Y. Ishino, and K. Morikawa, *Crystal structure and functional implications of Pyrococcus furiosus hef helicase domain involved in branched DNA processing*. Structure (Camb), 2005. **13**(1): p. 143-53.
83. Bardwell, A.J., L. Bardwell, A.E. Tomkinson, and E.C. Friedberg, *Specific cleavage of model recombination and repair intermediates by the yeast Rad1-Rad10 DNA endonuclease*. Science, 1994. **265**(5181): p. 2082-5.

84. Bessho, T., A. Sancar, L.H. Thompson, and M.P. Thelen, *Reconstitution of human excision nuclease with recombinant XPF-ERCC1 complex*. J Biol Chem, 1997. **272**(6): p. 3833-7.
85. Aravind, L., D.R. Walker, and E.V. Koonin, *Conserved domains in DNA repair proteins and evolution of repair systems*. Nucleic Acids Res, 1999. **27**(5): p. 1223-42.
86. Enzlin, J.H. and O.D. Scharer, *The active site of the DNA repair endonuclease XPF-ERCC1 forms a highly conserved nuclease motif*. Embo J, 2002. **21**(8): p. 2045-53.
87. Nishino, T., K. Komori, Y. Ishino, and K. Morikawa, *X-ray and biochemical anatomy of an archaeal XPF/Rad1/Mus81 family nuclease: similarity between its endonuclease domain and restriction enzymes*. Structure (Camb), 2003. **11**(4): p. 445-57.
88. Li, L., C.A. Peterson, X. Lu, and R.J. Legerski, *Mutations in XPA that prevent association with ERCC1 are defective in nucleotide excision repair*. Mol Cell Biol, 1995. **15**(4): p. 1993-8.
89. Bhagwat, N., A.L. Olsen, A.T. Wang, K. Hanada, P. Stuckert, R. Kanaar, . . . P.J. McHugh, *XPF-ERCC1 participates in the Fanconi anemia pathway of cross-link repair*. Mol Cell Biol, 2009. **29**(24): p. 6427-37.
90. Niedernhofer, L.J., G.A. Garinis, A. Raams, A.S. Lalai, A.R. Robinson, E. Appeldoorn, . . . J.H. Hoeijmakers, *A new progeroid syndrome reveals that genotoxic stress suppresses the somatotroph axis*. Nature, 2006. **444**(7122): p. 1038-43.
91. Andersen, S.L., D.T. Bergstralh, K.P. Kohl, J.R. LaRocque, C.B. Moore, and J. Sekelsky, *Drosophila MUS312 and the vertebrate ortholog BTBD12 interact with DNA structure-specific endonucleases in DNA repair and recombination*. Mol Cell, 2009. **35**(1): p. 128-35.
92. Fekairi, S., S. Scaglione, C. Chahwan, E.R. Taylor, A. Tissier, S. Coulon, . . . P.H. Gaillard, *Human SLX4 is a Holliday junction resolvase subunit that binds multiple DNA repair/recombination endonucleases*. Cell, 2009. **138**(1): p. 78-89.
93. Munoz, I.M., K. Hain, A.C. Declais, M. Gardiner, G.W. Toh, L. Sanchez-Pulido, . . . J. Rouse, *Coordination of structure-specific nucleases by human SLX4/BTBD12 is required for DNA repair*. Mol Cell, 2009. **35**(1): p. 116-27.

94. Svendsen, J.M., A. Smogorzewska, M.E. Sowa, B.C. O'Connell, S.P. Gygi, S.J. Elledge, and J.W. Harper, *Mammalian BTBD12/SLX4 assembles a Holliday junction resolvase and is required for DNA repair*. Cell, 2009. **138**(1): p. 63-77.
95. Ahmad, A., A.R. Robinson, A. Duensing, E. van Drunen, H.B. Beverloo, D.B. Weisberg, . . . L.J. Niedernhofer, *ERCC1-XPF endonuclease facilitates DNA double-strand break repair*. Mol Cell Biol, 2008. **28**(16): p. 5082-92.
96. Li, F., J. Dong, X. Pan, J.H. Oum, J.D. Boeke, and S.E. Lee, *Microarray-based genetic screen defines SAW1, a gene required for Rad1/Rad10-dependent processing of recombination intermediates*. Mol Cell, 2008. **30**(3): p. 325-35.
97. Toh, G.W., N. Sugawara, J. Dong, R. Toth, S.E. Lee, J.E. Haber, and J. Rouse, *Mec1/Tel1-dependent phosphorylation of Six4 stimulates Rad1-Rad10-dependent cleavage of non-homologous DNA tails*. DNA Repair (Amst), 2010. **9**(6): p. 718-26.
98. Munoz, P., R. Blanco, J.M. Flores, and M.A. Blasco, *XPF nuclease-dependent telomere loss and increased DNA damage in mice overexpressing TRF2 result in premature aging and cancer*. Nat Genet, 2005. **37**(10): p. 1063-71.
99. Wu, Y., N.J. Zacal, A.J. Rainbow, and X.D. Zhu, *XPF with mutations in its conserved nuclease domain is defective in DNA repair but functions in TRF2-mediated telomere shortening*. DNA Repair (Amst), 2007. **6**(2): p. 157-66.
100. Zhu, X.D., L. Niedernhofer, B. Kuster, M. Mann, J.H. Hoeijmakers, and T. de Lange, *ERCC1/XPF removes the 3' overhang from uncapped telomeres and represses formation of telomeric DNA-containing double minute chromosomes*. Mol Cell, 2003. **12**(6): p. 1489-98.
101. Lazzaro, F., M. Giannattasio, F. Puddu, M. Granata, A. Pelliccioli, P. Plevani, and M. Muzi-Falconi, *Checkpoint mechanisms at the intersection between DNA damage and repair*. DNA Repair (Amst), 2009. **8**(9): p. 1055-67.
102. Mu, D., D.S. Hsu, and A. Sancar, *Reaction mechanism of human DNA repair excision nuclease*. J Biol Chem, 1996. **271**(14): p. 8285-94.
103. Matsunaga, T., D. Mu, C.H. Park, J.T. Reardon, and A. Sancar, *Human DNA repair excision nuclease. Analysis of the roles of the*

- subunits involved in dual incisions by using anti-XPG and anti-ERCC1 antibodies.* J Biol Chem, 1995. **270**(35): p. 20862-9.
104. Mocquet, V., J.P. Laine, T. Riedl, Z. Yajin, M.Y. Lee, and J.M. Egly, *Sequential recruitment of the repair factors during NER: the role of XPG in initiating the resynthesis step.* Embo J, 2008. **27**(1): p. 155-67.
 105. Overmeer, R.M., J. Moser, M. Volker, H. Kool, A.E. Tomkinson, A.A. van Zeeland, . . . M. Fousteri, *Replication protein A safeguards genome integrity by controlling NER incision events.* J Cell Biol, 2011.
 106. Liu, Y., H.I. Kao, and R.A. Bambara, *Flap endonuclease 1: a central component of DNA metabolism.* Annu Rev Biochem, 2004. **73**: p. 589-615.
 107. Chapados, B.R., D.J. Hosfield, S. Han, J. Qiu, B. Yelent, B. Shen, and J.A. Tainer, *Structural basis for FEN-1 substrate specificity and PCNA-mediated activation in DNA replication and repair.* Cell, 2004. **116**(1): p. 39-50.
 108. Kannouche, P.L. and A.R. Lehmann, *Ubiquitination of PCNA and the polymerase switch in human cells.* Cell Cycle, 2004. **3**(8): p. 1011-3.
 109. Bienko, M., C.M. Green, N. Crosetto, F. Rudolf, G. Zapart, B. Coull, . . . I. Dikic, *Ubiquitin-binding domains in Y-family polymerases regulate translesion synthesis.* Science, 2005. **310**(5755): p. 1821-4.
 110. Hofmann, K., *Ubiquitin-binding domains and their role in the DNA damage response.* DNA Repair (Amst), 2009. **8**(4): p. 544-56.
 111. Giannattasio, M., C. Follonier, H. Tourriere, F. Puddu, F. Lazzaro, P. Pasero, . . . M. Muzi-Falconi, *Exo1 competes with repair synthesis, converts NER intermediates to long ssDNA gaps, and promotes checkpoint activation.* Mol Cell, 2010. **40**(1): p. 50-62.
 112. Hanawalt, P.C., *Subpathways of nucleotide excision repair and their regulation.* Oncogene, 2002. **21**(58): p. 8949-56.
 113. Svejstrup, J.Q., *Mechanisms of transcription-coupled DNA repair.* Nat Rev Mol Cell Biol, 2002. **3**(1): p. 21-9.
 114. Sugasawa, K., J.M. Ng, C. Masutani, S. Iwai, P.J. van der Spek, A.P. Eker, . . . J.H. Hoeijmakers, *Xeroderma pigmentosum group C*

protein complex is the initiator of global genome nucleotide excision repair. Mol Cell, 1998. **2**(2): p. 223-32.

115. Sugasawa, K., T. Okamoto, Y. Shimizu, C. Masutani, S. Iwai, and F. Hanaoka, *A multistep damage recognition mechanism for global genomic nucleotide excision repair.* Genes Dev, 2001. **15**(5): p. 507-21.
116. Tirode, F., D. Busso, F. Coin, and J.M. Egly, *Reconstitution of the transcription factor TFIIH: assignment of functions for the three enzymatic subunits, XPB, XPD, and cdk7.* Mol Cell, 1999. **3**(1): p. 87-95.
117. Mu, D., M. Wakasugi, D.S. Hsu, and A. Sancar, *Characterization of reaction intermediates of human excision repair nuclease.* J Biol Chem, 1997. **272**(46): p. 28971-9.
118. Ogi, T. and A.R. Lehmann, *The Y-family DNA polymerase kappa (pol kappa) functions in mammalian nucleotide-excision repair.* Nat Cell Biol, 2006. **8**(6): p. 640-2.
119. Shivji, M.K., V.N. Podust, U. Hubscher, and R.D. Wood, *Nucleotide excision repair DNA synthesis by DNA polymerase epsilon in the presence of PCNA, RFC, and RPA.* Biochemistry, 1995. **34**(15): p. 5011-7.
120. Green, C.M. and G. Almouzni, *Local action of the chromatin assembly factor CAF-1 at sites of nucleotide excision repair in vivo.* Embo J, 2003. **22**(19): p. 5163-74.
121. Shechter, D., V. Costanzo, and J. Gautier, *Regulation of DNA replication by ATR: signaling in response to DNA intermediates.* DNA Repair (Amst), 2004. **3**(8-9): p. 901-8.
122. Berneburg, M., J.E. Lowe, T. Nardo, S. Araujo, M.I. Fousteri, M.H. Green, . . . A.R. Lehmann, *UV damage causes uncontrolled DNA breakage in cells from patients with combined features of XP-D and Cockayne syndrome.* Embo J, 2000. **19**(5): p. 1157-66.
123. Theron, T., M.I. Fousteri, M. Volker, L.W. Harries, E. Botta, M. Stefanini, . . . A.R. Lehmann, *Transcription-associated breaks in xeroderma pigmentosum group D cells from patients with combined features of xeroderma pigmentosum and Cockayne syndrome.* Mol Cell Biol, 2005. **25**(18): p. 8368-78.
124. Moggs, J.G., K.J. Yarema, J.M. Essigmann, and R.D. Wood, *Analysis of incision sites produced by human cell extracts and purified proteins during nucleotide excision repair of a 1,3-*

- intrastrand d(GpTpG)-cisplatin adduct*. J Biol Chem, 1996. **271**(12): p. 7177-86.
125. Hansson, J., M. Munn, W.D. Rupp, R. Kahn, and R.D. Wood, *Localization of DNA repair synthesis by human cell extracts to a short region at the site of a lesion*. J Biol Chem, 1989. **264**(36): p. 21788-92.
 126. Essers, J., A.F. Theil, C. Baldeyron, W.A. van Cappellen, A.B. Houtsmuller, R. Kanaar, and W. Vermeulen, *Nuclear dynamics of PCNA in DNA replication and repair*. Mol Cell Biol, 2005. **25**(21): p. 9350-9.
 127. Hanawalt, P.C., *Repair replication in the bacterial genome*. Genetical aspects of radiosensitivity: mechanisms of repair, 1966. **24**: p. 97-104.
 128. Hanawalt, P.C. and R.H. Haynes, *The repair of DNA*. Sci Am, 1967. **216**(2): p. 36-43.
 129. Aboussekhra, A., M. Biggerstaff, M.K. Shivji, J.A. Vilpo, V. Moncollin, V.N. Podust, . . . R.D. Wood, *Mammalian DNA nucleotide excision repair reconstituted with purified protein components*. Cell, 1995. **80**(6): p. 859-68.
 130. Araujo, S.J., F. Tirode, F. Coin, H. Pospiech, J.E. Syvaoja, M. Stucki, . . . R.D. Wood, *Nucleotide excision repair of DNA with recombinant human proteins: definition of the minimal set of factors, active forms of TFIIH, and modulation by CAK*. Genes Dev, 2000. **14**(3): p. 349-59.
 131. Pascucci, B., M. Stucki, Z.O. Jonsson, E. Dogliotti, and U. Hubscher, *Long patch base excision repair with purified human proteins. DNA ligase I as patch size mediator for DNA polymerases delta and epsilon*. J Biol Chem, 1999. **274**(47): p. 33696-702.
 132. Matsumoto, Y., K. Kim, J. Hurwitz, R. Gary, D.S. Levin, A.E. Tomkinson, and M.S. Park, *Reconstitution of proliferating cell nuclear antigen-dependent repair of apurinic/apyrimidinic sites with purified human proteins*. J Biol Chem, 1999. **274**(47): p. 33703-8.
 133. Gary, R., K. Kim, H.L. Cornelius, M.S. Park, and Y. Matsumoto, *Proliferating cell nuclear antigen facilitates excision in long-patch base excision repair*. J Biol Chem, 1999. **274**(7): p. 4354-63.
 134. Nichols, A.F. and A. Sancar, *Purification of PCNA as a nucleotide excision repair protein*. Nucleic Acids Res, 1992. **20**(13): p. 2441-6.

135. Shivji, M.K., J.G. Moggs, I. Kuraoka, and R.D. Wood, *Dual-incision assays for nucleotide excision repair using DNA with a lesion at a specific site*. *Methods Mol Biol*, 1999. **113**: p. 373-92.
136. Ellison, A.R., T. Nospikel, N.G. Jaspers, S.G. Clarkson, and D.C. Gruenert, *Complementation of transformed fibroblasts from patients with combined xeroderma pigmentosum-Cockayne syndrome*. *Exp Cell Res*, 1998. **243**(1): p. 22-8.
137. Biggerstaff, M. and R.D. Wood, *Assay for nucleotide excision repair protein activity using fractionated cell extracts and UV-damaged plasmid DNA*. *Methods Mol Biol*, 1999. **113**: p. 357-72.
138. Mone, M.J., M. Volker, O. Nikaido, L.H. Mullenders, A.A. van Zeeland, P.J. Verschure, . . . R. van Driel, *Local UV-induced DNA damage in cell nuclei results in local transcription inhibition*. *EMBO Rep*, 2001. **2**(11): p. 1013-7.
139. Ng, J.M., W. Vermeulen, G.T. van der Horst, S. Bergink, K. Sugasawa, H. Vrieling, and J.H. Hoeijmakers, *A novel regulation mechanism of DNA repair by damage-induced and RAD23-dependent stabilization of xeroderma pigmentosum group C protein*. *Genes Dev*, 2003. **17**(13): p. 1630-45.
140. de Laat, W.L., E. Appeldoorn, K. Sugasawa, E. Weterings, N.G. Jaspers, and J.H. Hoeijmakers, *DNA-binding polarity of human replication protein A positions nucleases in nucleotide excision repair*. *Genes Dev*, 1998. **12**(16): p. 2598-609.
141. Lieber, M.R., *The FEN-1 family of structure-specific nucleases in eukaryotic DNA replication, recombination and repair*. *Bioessays*, 1997. **19**(3): p. 233-40.
142. Rolef Ben-Shahar, T., A.G. Castillo, M.J. Osborne, K.L. Borden, J. Kornblatt, and A. Verreault, *Two fundamentally distinct PCNA interaction peptides contribute to chromatin assembly factor 1 function*. *Mol Cell Biol*, 2009. **29**(24): p. 6353-65.
143. Sugasawa, K., Y. Okuda, M. Saijo, R. Nishi, N. Matsuda, G. Chu, . . . F. Hanaoka, *UV-induced ubiquitylation of XPC protein mediated by UV-DDB-ubiquitin ligase complex*. *Cell*, 2005. **121**(3): p. 387-400.
144. Sugasawa, K., *UV-induced ubiquitylation of XPC complex, the UV-DDB-ubiquitin ligase complex, and DNA repair*. *J Mol Histol*, 2006.
145. Wang, Q.E., Q. Zhu, G. Wani, M.A. El-Mahdy, J. Li, and A.A. Wani, *DNA repair factor XPC is modified by SUMO-1 and ubiquitin*

- following UV irradiation*. Nucleic Acids Res, 2005. **33**(13): p. 4023-34.
146. Huang, T.T. and A.D. D'Andrea, *Regulation of DNA repair by ubiquitylation*. Nat Rev Mol Cell Biol, 2006. **7**(5): p. 323-34.
147. Moldovan, G.L., B. Pfander, and S. Jentsch, *PCNA, the maestro of the replication fork*. Cell, 2007. **129**(4): p. 665-79.
148. Marteijn, J.A., S. Bekker-Jensen, N. Mailand, H. Lans, P. Schwertman, A.M. Gourdin, . . . W. Vermeulen, *Nucleotide excision repair-induced H2A ubiquitination is dependent on MDC1 and RNF8 and reveals a universal DNA damage response*. J Cell Biol, 2009. **186**(6): p. 835-47.
149. Nakajima, S., L. Lan, S. Kanno, N. Usami, K. Kobayashi, M. Mori, . . . A. Yasui, *Replication-dependent and -independent responses of RAD18 to DNA damage in human cells*. J Biol Chem, 2006. **281**(45): p. 34687-95.
150. Lee, K.Y. and K. Myung, *PCNA modifications for regulation of post-replication repair pathways*. Mol Cells, 2008. **26**(1): p. 5-11.
151. Hanasoge, S. and M. Ljungman, *H2AX phosphorylation after UV irradiation is triggered by DNA repair intermediates and is mediated by the ATR kinase*. Carcinogenesis, 2007. **28**(11): p. 2298-304.

APPENDIX

The appendix contains supplemental figures for Chapter 3 as indicated within the text. These figures are listed in the preliminary pages under “List of Figures”.

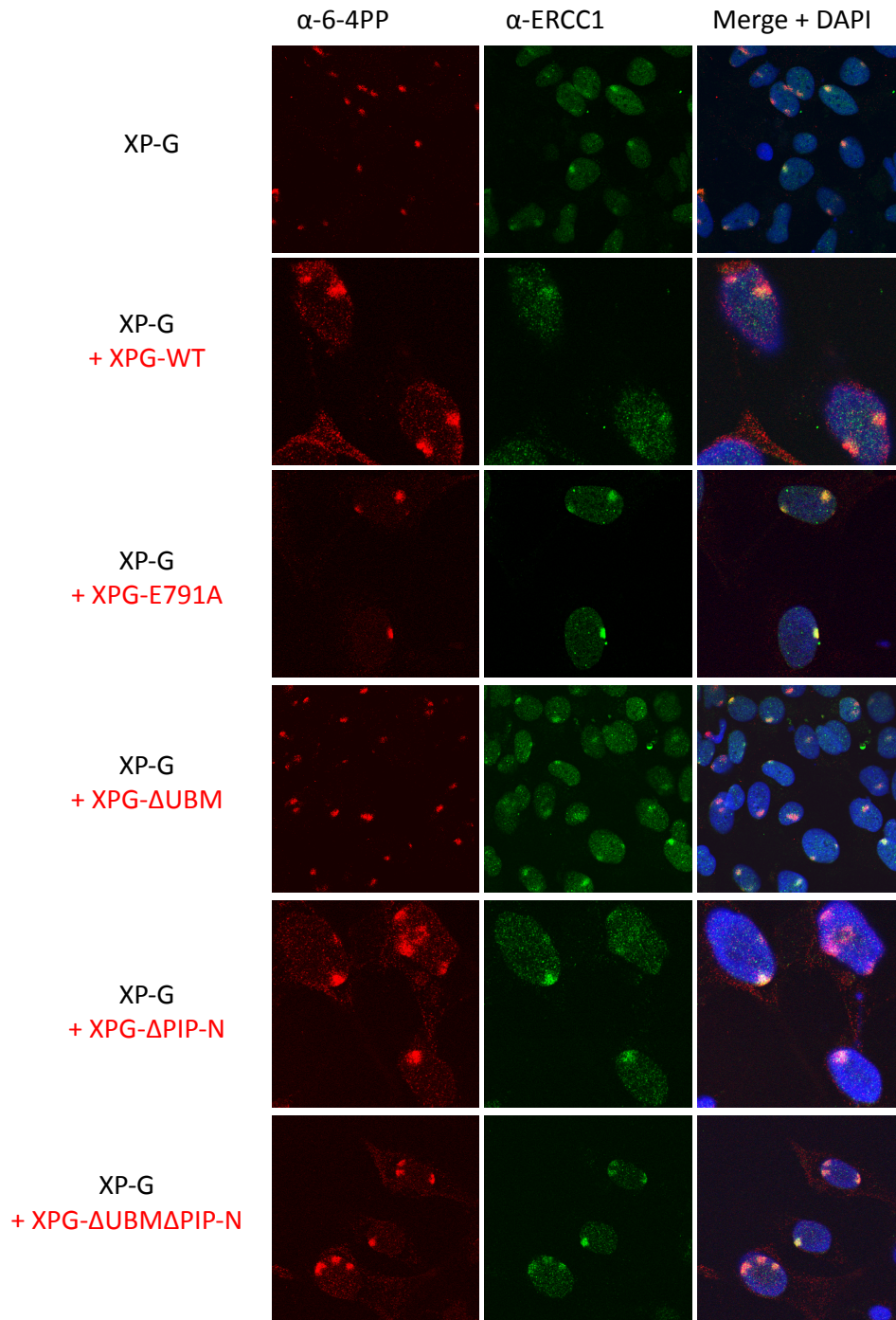


Figure 26: IF images of (6-4)PPs colocalized with ERCC1 foci in XPG cell-lines at 0.5h following UV irradiation. (6-4)PP foci are shown in red, ERCC1 foci in green and merged images with DAPI staining in blue to highlight the nucleus.

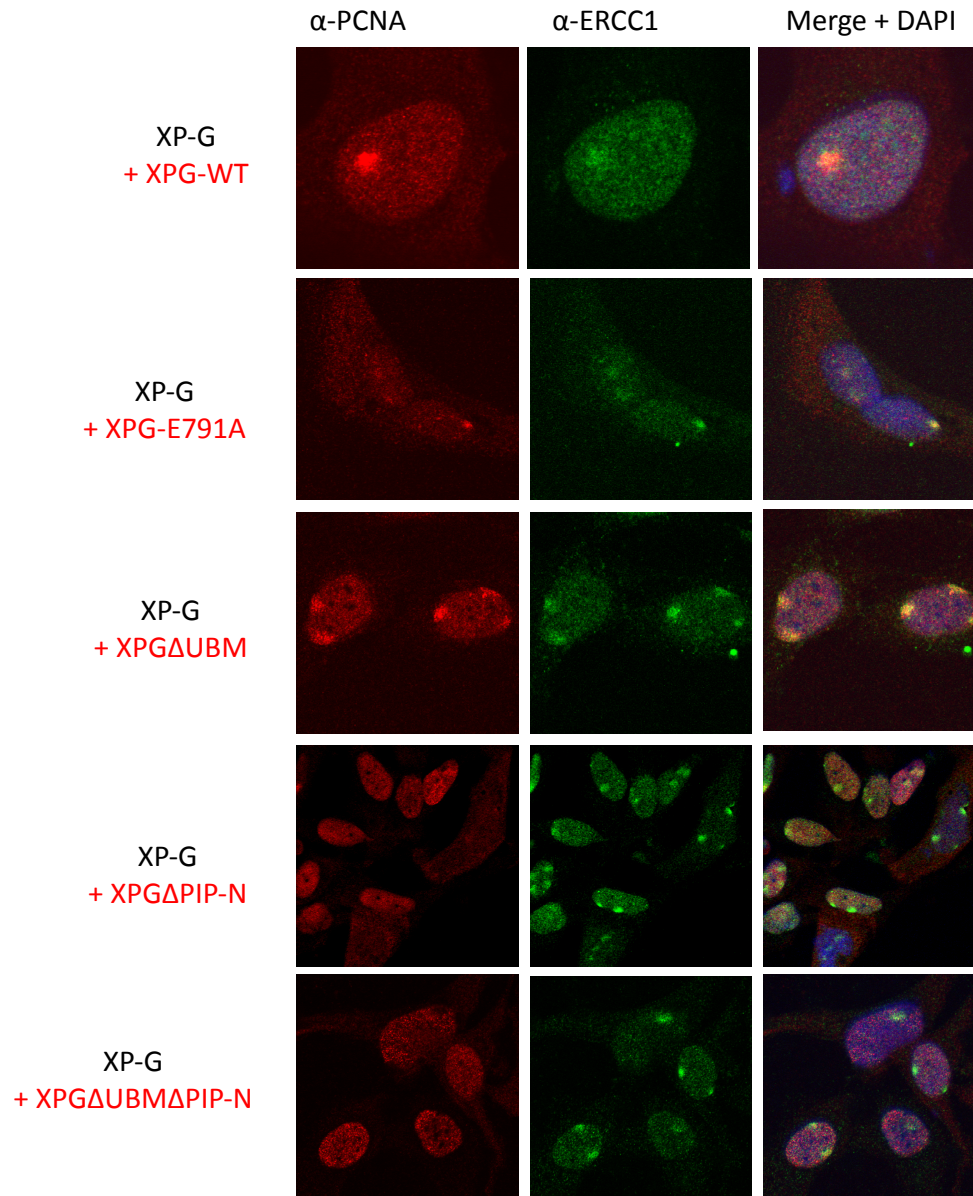


Figure 27: IF images of PCNA foci colocalized with ERCC1 foci in XPG cell-lines at 0.5h following UV irradiation. PCNA foci are shown in red, ERCC1 foci in green and merged images with DAPI staining in blue to highlight the nucleus.

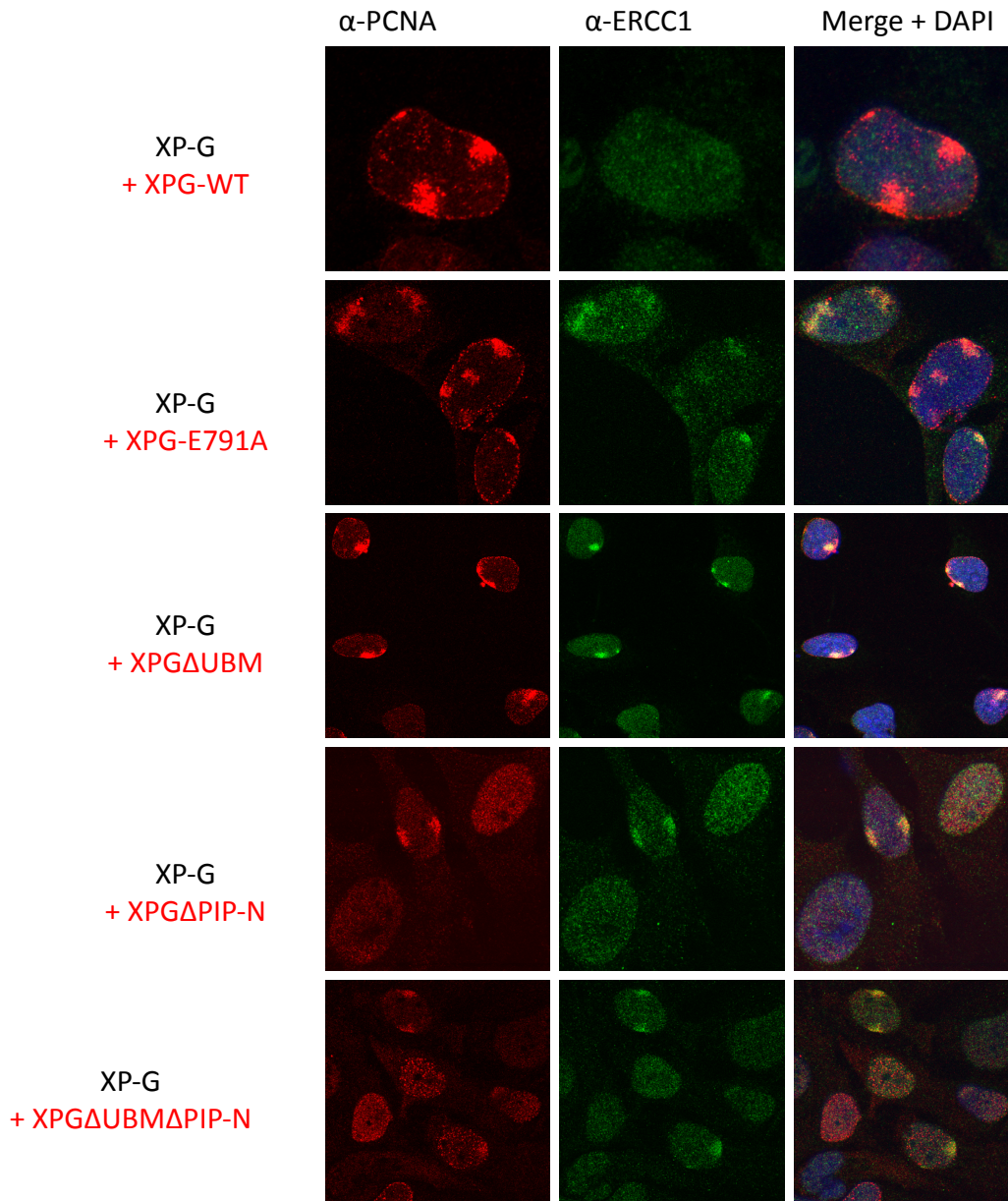


Figure 28: IF images of PCNA foci colocalized with ERCC1 foci in XPG cell-lines at 6h following UV irradiation. PCNA foci are shown in red, ERCC1 foci in green and merged images with DAPI staining in blue to highlight the nucleus.

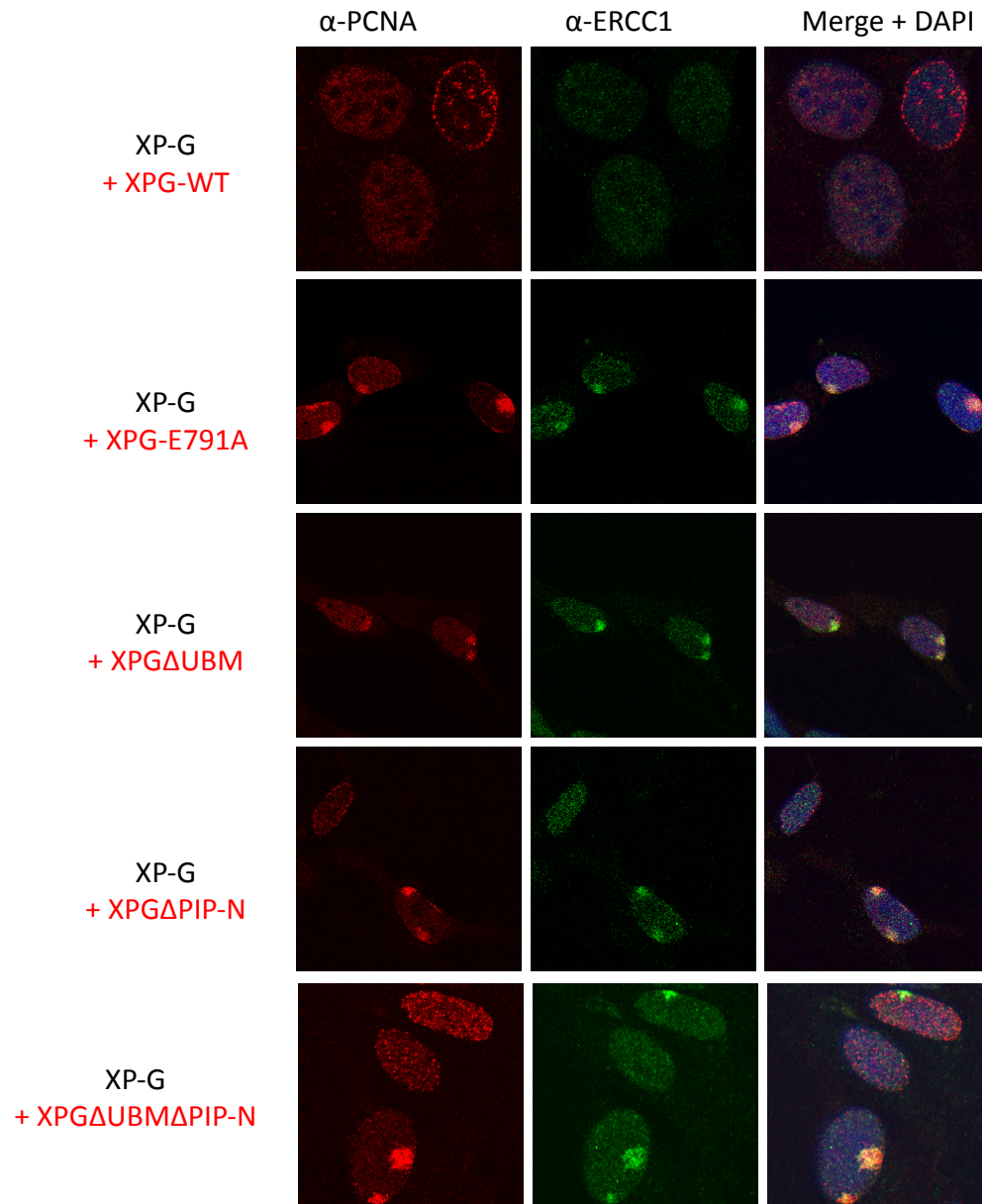


Figure 29: IF images of PCNA foci colocalized with ERCC1 foci in XPG cell-lines at 9h following UV irradiation. PCNA foci are shown in red, ERCC1 foci in green and merged images with DAPI staining in blue to highlight the nucleus.

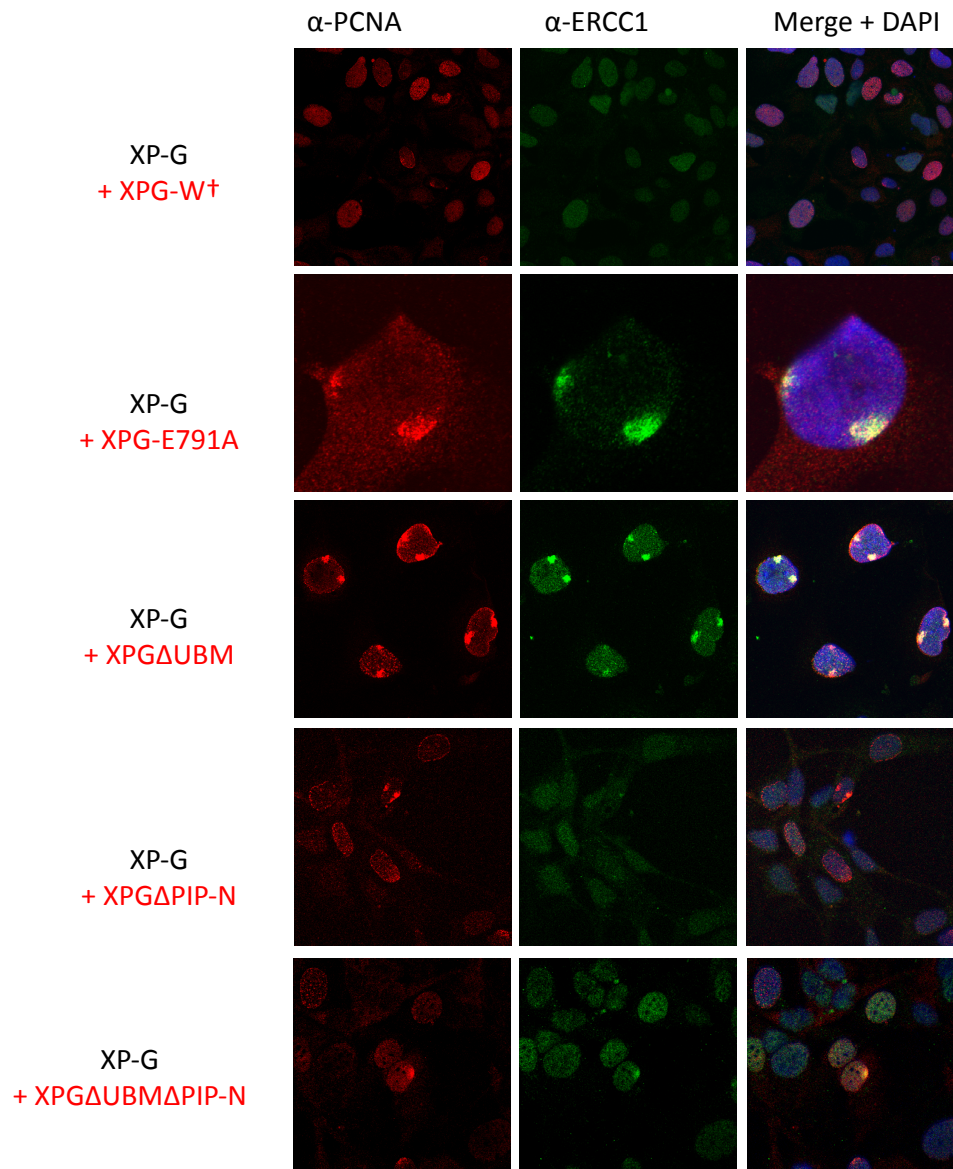


Figure 30: IF images of PCNA foci colocalized with ERCC1 foci in XPG cell-lines at 15h following UV irradiation. PCNA foci are shown in red, ERCC1 foci in green and merged images with DAPI staining in blue to highlight the nucleus.

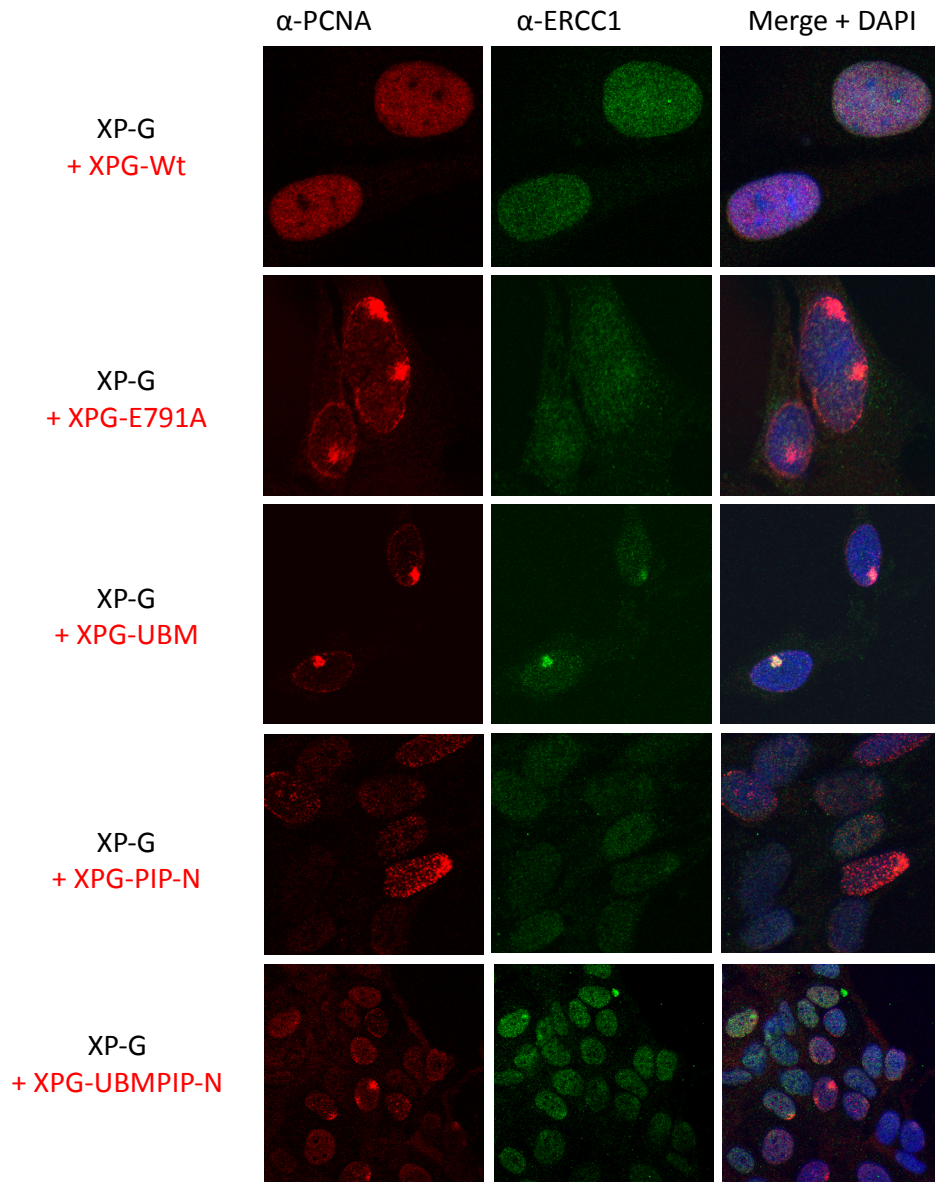


Figure 31: IF images of PCNA foci colocalized with ERCC1 foci in XPG cell-lines at 24h following UV irradiation. PCNA foci are shown in red, ERCC1 foci in green and merged images with DAPI staining in blue to highlight the nucleus.

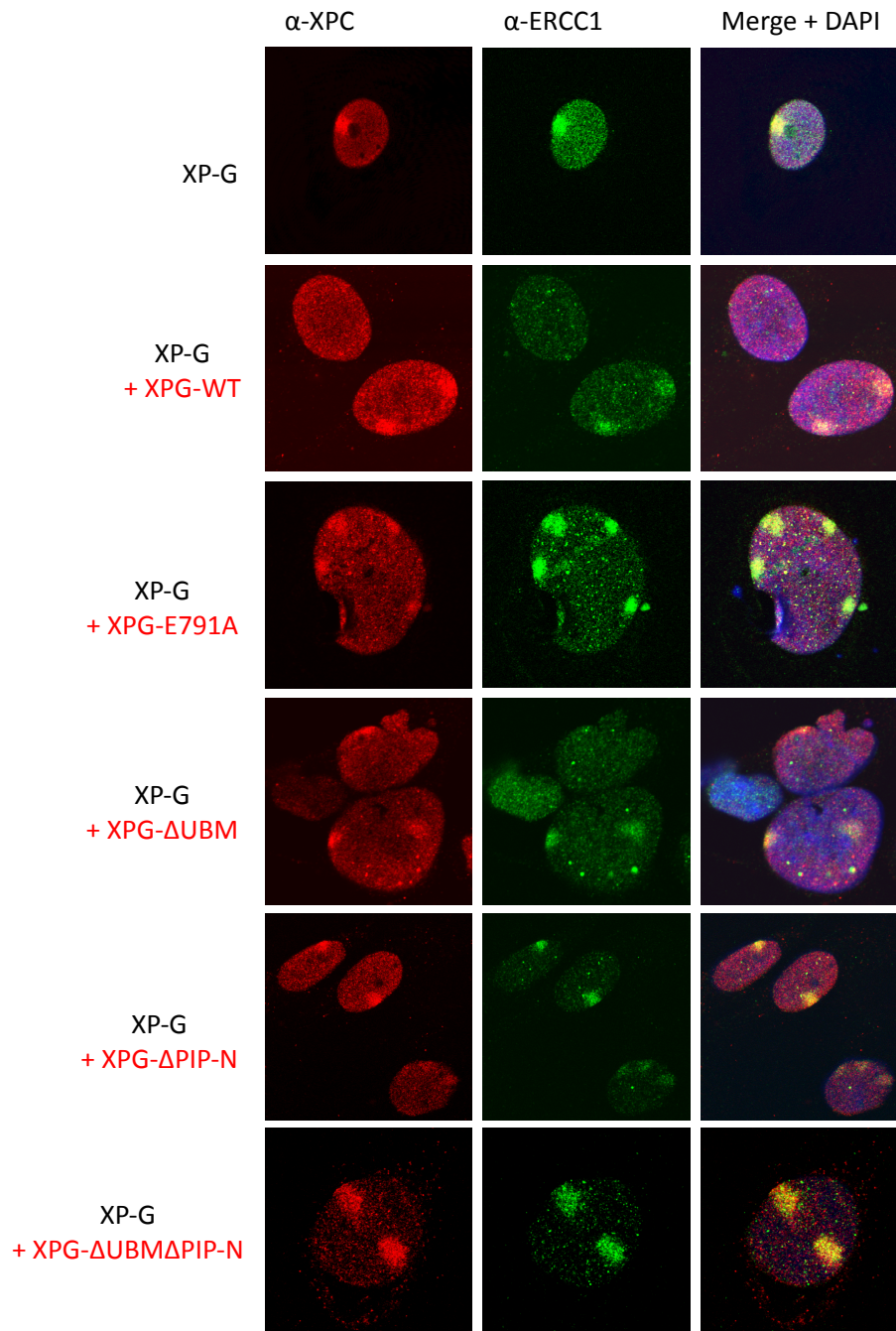


Figure 32: IF images of XPC foci colocalized with ERCC1 foci in XPG cell-lines at 0.5h following UV irradiation. XPC foci are shown in red, ERCC1 foci in green and merged images with DAPI staining in blue to highlight the nucleus.

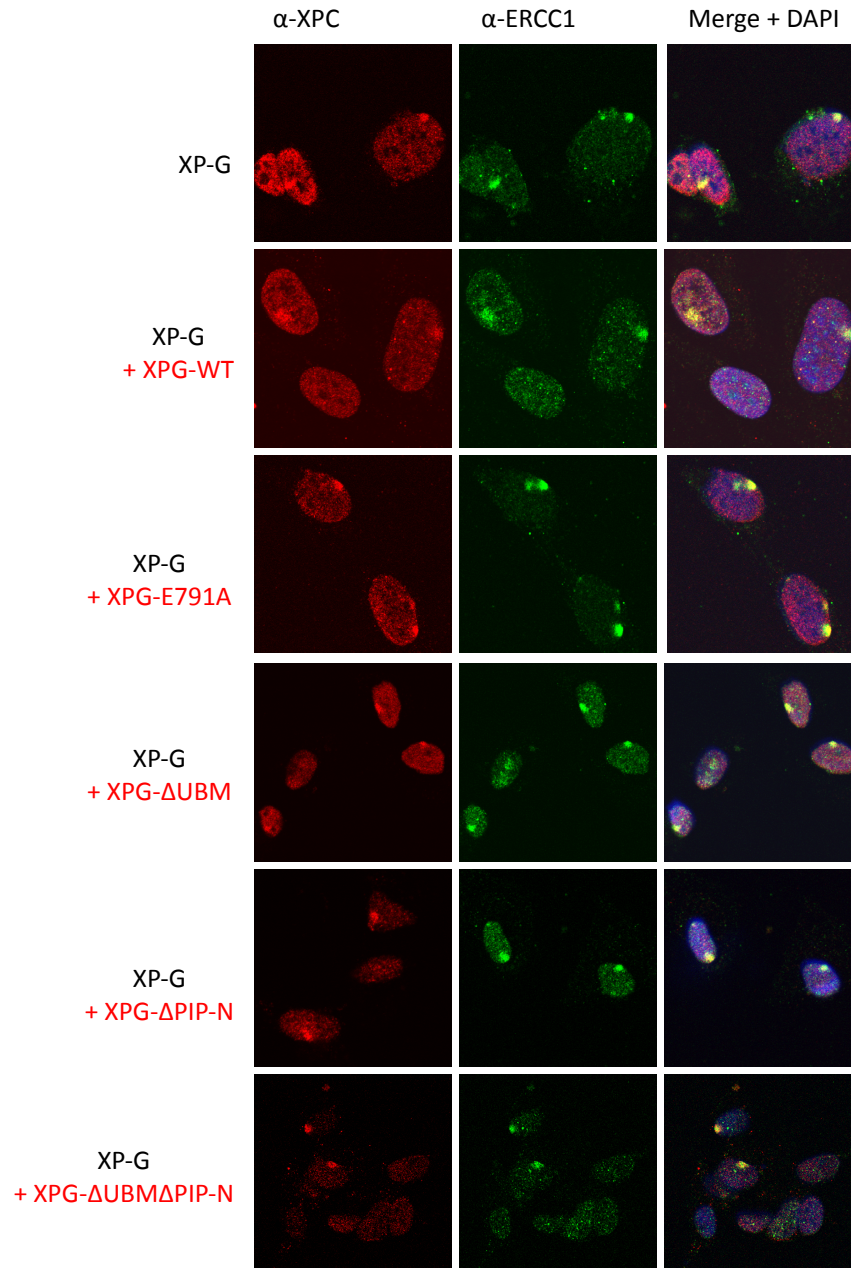


Figure 33: IF images of XPC foci colocalized with ERCC1 foci in XPG cell-lines at 1h following UV irradiation. XPC foci are shown in red, ERCC1 foci in green and merged images with DAPI staining in blue to highlight the nucleus.

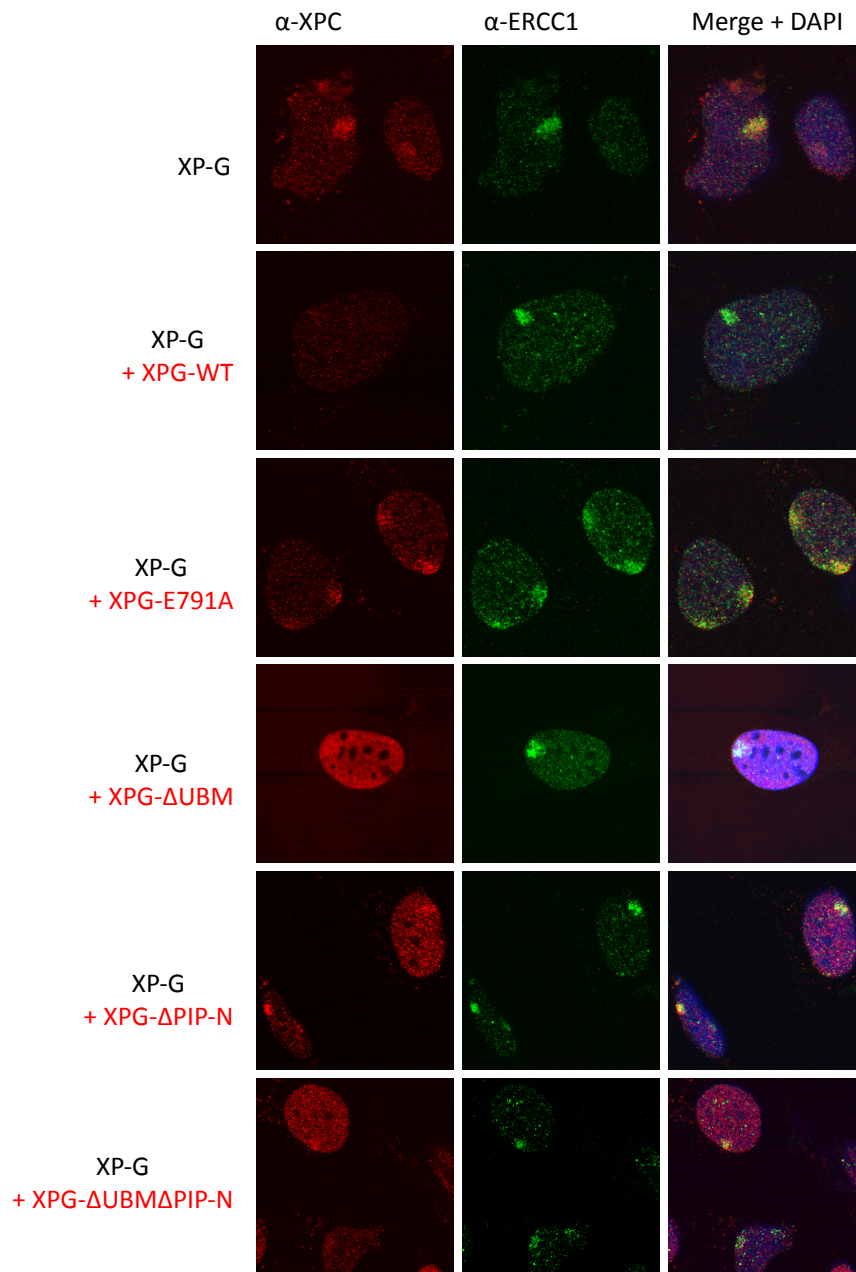


Figure 34: IF images of XPC foci colocalized with ERCC1 foci in XPG cell-lines at 3h following UV irradiation. XPC foci are shown in red, ERCC1 foci in green and merged images with DAPI staining in blue to highlight the nucleus.

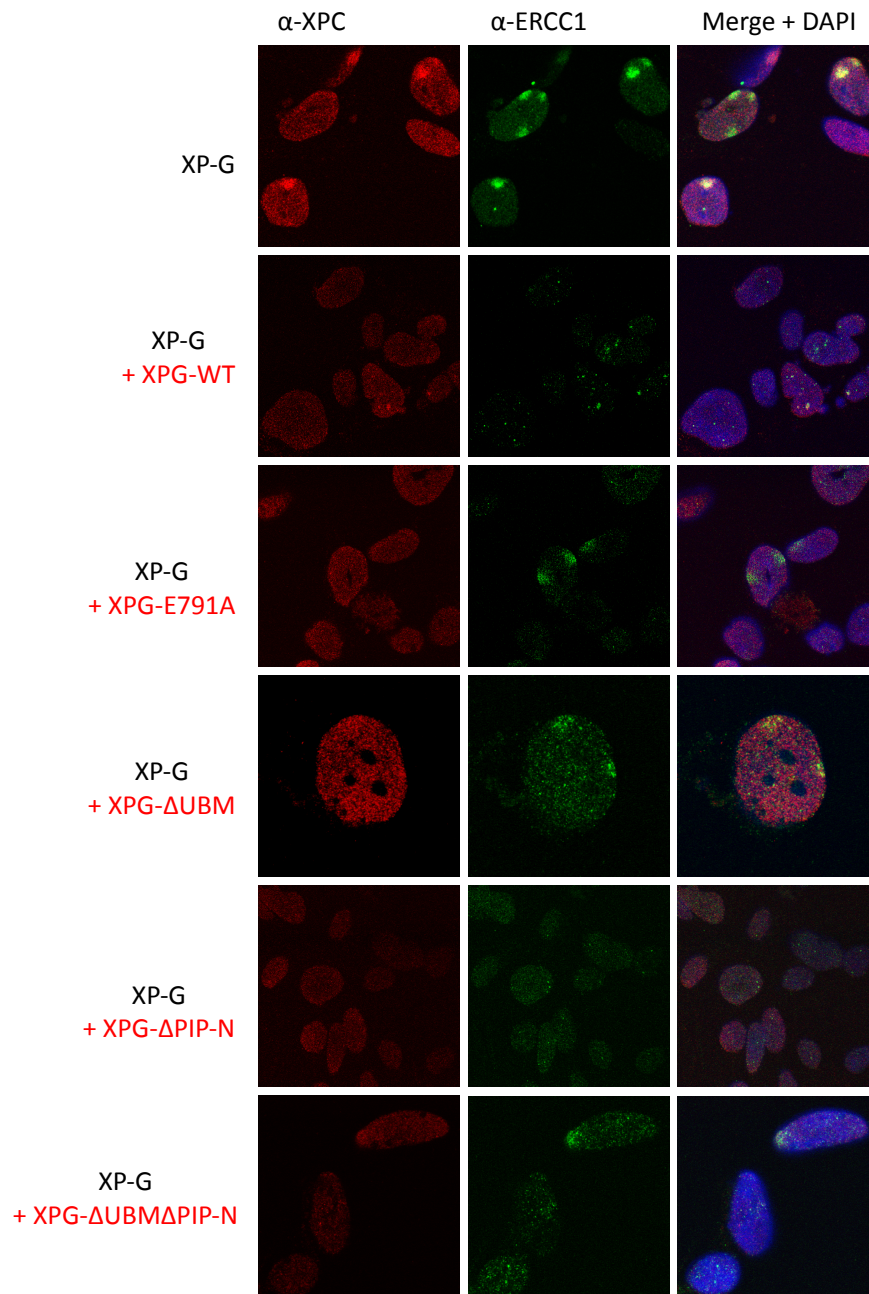


Figure 35: IF images of XPC foci colocalized with ERCC1 foci in XPG cell-lines at 16h following UV irradiation. XPC foci are shown in red, ERCC1 foci in green and merged images with DAPI staining in blue to highlight the nucleus.

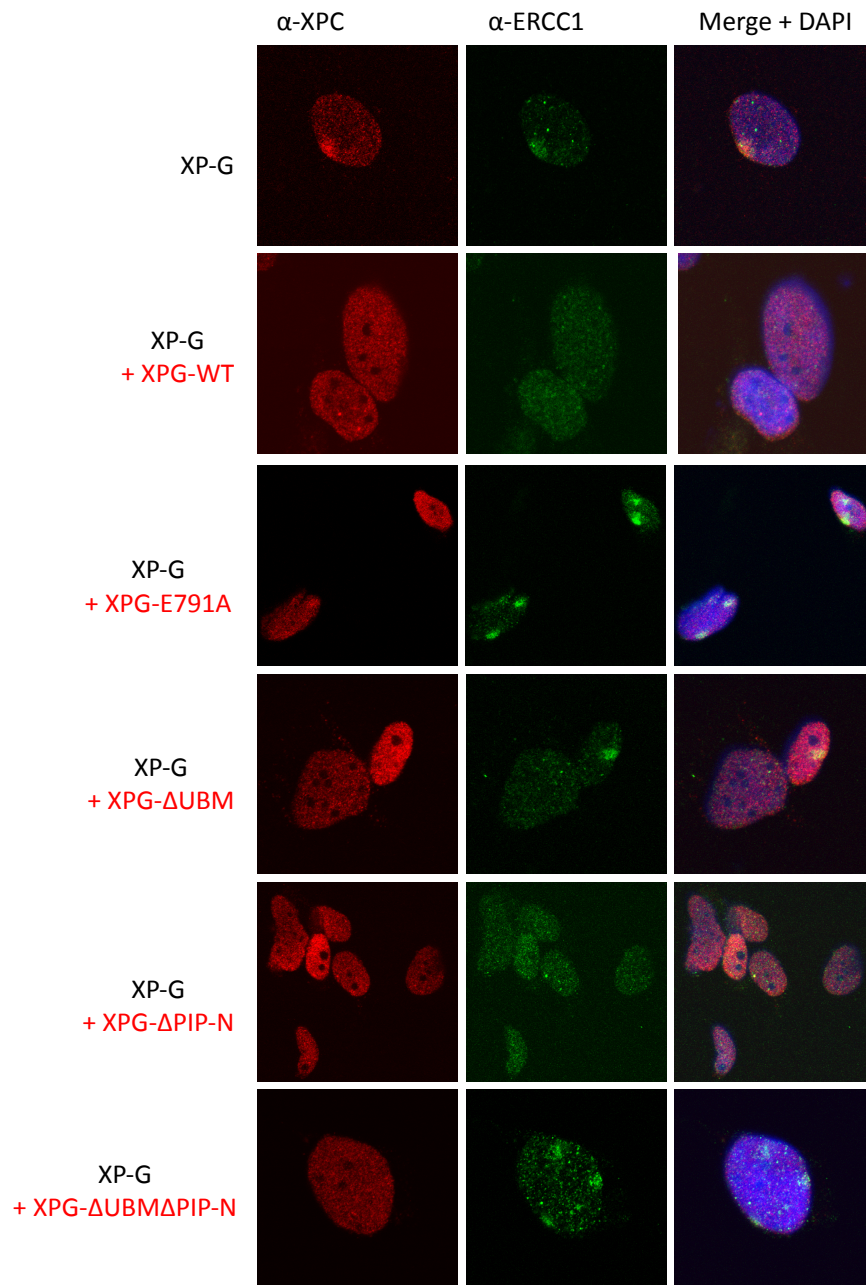


Figure 36: IF images of XPC foci colocalized with ERCC1 foci in XPG cell-lines at 24h following UV irradiation. XPC foci are shown in red, ERCC1 foci in green and merged images with DAPI staining in blue to highlight the nucleus.